CNS Remyelination and the Gut Microbiota

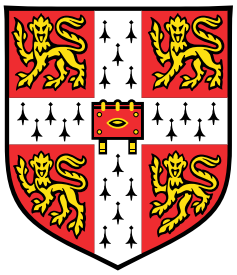

Christopher McMurran

Department of Clinical Neurosciences
University of Cambridge

This dissertation is submitted for the degree of
Doctor of Philosophy

Trinity College June 2018

Abstract

CNS Remyelination and the Gut Microbiota

Christopher McMurran

Remyelination describes the regeneration of myelin sheaths, and is considered one of the most promising strategies for improving the prognosis of demyelinating diseases such as multiple sclerosis. Data from animal models and human studies have shown that remyelination can occur extensively in the central nervous system (CNS), leading to functional recovery and axonal protection. However, remyelination does not always proceed to completion, and its failure is associated with progressive neurological disability. Thus, there is clinical need for interventions that can optimise the conditions for remyelination.

Recent advances in genomics and animal husbandry have kindled an interest in the microbiome as a means to influence processes throughout the body. Our commensal microbes communicate with host cells at epithelial barriers, stimulate neural and endocrine axes and directly produce a plethora of long-range signaling molecules. Critically, the development and maintenance of the immune system depend on signals from the microbiota, and we know that a well-coordinated immune response is a key determinant of the success of remyelination. This thesis explores how the microbiome can influence CNS remyelination.

To do so, I have studied remyelination in three murine models of microbiome alteration. Firstly, long-term oral administration of an antibiotic cocktail was used to deplete the microbiota of adult mice. Following focal demyelination, these mice had deficits in their inflammatory response, clearance of myelin debris and differentiation of new oligodendrocytes from oligodendrocyte progenitor cells (OPCs). Faecal microbial transplant was able to rescue aspects of the inflammatory response and phagocytosis, but not OPC differentiation.

Secondly, I looked at remyelination in germ-free (GF) mice following cuprizone-induced demyelination. As with the antibiotics-treated mice, there were deficits in inflammation following demyelination, which tended to peak later than in control mice.

Finally, I investigated the potential of a therapeutic probiotic (VSL#3) to improve remyelination in aged mice. In contrast to antibiotic treatment, probiotic administration caused a slight enhancement in the onset of inflammation following focal demyelination. However, there was no significant improvement in OPC differentiation or toluidine blue rank analysis, suggesting these changes in inflammation were not sufficient to positively modulate remyelination.

The results from these three studies introduce a significant but previously unconsidered environmental influence on remyelination in the CNS. Whilst the effects are subtle relative to more direct interventions, the microbiome can be manipulated simply and non-invasively, which may provide a useful adjunct to other strategies for optimising remyelination.

Declaration

I hereby declare that except where specific reference is made to the work of others, the contents of this dissertation are original and have not been submitted in whole or in part for consideration for any other degree or qualification in this, or any other university. This dissertation is my own work and contains nothing which is the outcome of work done in collaboration with others, except as specified in the text and Acknowledgements. This dissertation contains fewer than 60,000 words including appendices, bibliography, footnotes, tables and equations and has fewer than 150 figures.

Christopher McMurran
June 2018

Acknowledgements

I would like to thank everyone who helped me on my journey to submitting this thesis. Firstly, to Prof. Robin Franklin for the opportunity to carry out a PhD in his lab, the insight into his approach to biology and the freedom to pursue my own ideas and develop as a scientist. Secondly, I am immensely grateful to Dr. Alerie Guzman de la Fuente, my lab-mum, who has been a constant source of ideas, technical support and encouragement throughout my PhD.

Thank you to the other members of the Franklin Lab helped with the work included here – particularly Chao Zhao, Dan Ma, Björn Neumann, Ginez Gonzalez and Daniel Morrison, who have answered many a question over the last three years. And thanks to all the other #franklinlab friends I made along the way: my bench-buddy Ludo, fellow MB/PhD Natalia, Sarah, Roey, Myf, Mikey, Joe, Uncle Adam, Alisa, Zhaozong, Michal and many more.

I am grateful to the Cambridge MB/PhD programme for the flexibility and funding to embark on research at this stage of my medical career, and particularly to Lesley Flood for enabling the process to run so smoothly. Thank you to MedImmune for accepting me into their PhD programme, providing funding and for the support from my two supervisors there: Clare Jones and Claire Hollins. I am also thankful to the Jean Shanks Foundation, James Baird Fund, MS Society and British Trust for the Myelin project for financially supporting this work.

I would like to acknowledge the other scientists around the world that contributed to the project: Denise Fitzgerald (Belfast) and her lab (particularly Yvonne, Rosana, John), Ofra Zidon (Cambridge/Jerusalem), Andrew Goldson and Arlaine Brion (Norwich) Fynn Krause (Cambridge) and Markus Heimesaat (Berlin). Thanks also to Chris, Emma, Jon, Maria and Lewis at the Innes facility for their help and advice.

Finally, a huge thank you to all my family and friends for their part in this journey. I'm particularly grateful to my mum for teaching me to think like a biologist, my dad for teaching me to think like an engineer and Frederica for putting up with my erratic writing timetable and having a near-endless capacity to hear about oligodendrocytes.

Table of contents

List of figures

List of tables

Abbreviations

*Arg*1 arginase-1

BBB blood-brain barrier

CC corpus callosum

CFU colony-forming unit

CNS central nervous system

CSF cerebrospinal fluid

DAMP danger-associated molecular pattern

dMBP degenerated MBP

DNA deoxyribonucleic acid

dpl days post lesion

EAE experimental autoimmune encephalomyelitis

ECM extracellular matrix

EdU 5-ethynyl-2'-deoxyuridine

FMT faecal microbiota transplantation

GALT gut-associated lymphoid tissue

$GC-MS$ gas chromatography-mass spectrometry

GF germ-free

GFAP glial fibrillary acidic protein

GFP green fluorescent protein

GM grey matter

GPCR G-protein coupled receptor

HALF hibernate-A low fluorescence

HDAC histone-deacetylase

*Iba*1 ionized calcium-binding adapter molecule 1

iNOS inducible nitric oxide synthase

LPS lipopolysaccharide

MACS magnetic-activated cell sorting

MBP myelin basic protein

MHCII major histocompatibility complex class II

MLN mesenteric lymph node

MR mannose receptor

MS multiple sclerosis

MTR magnetisation transfer ratio

MWB modified Miltenyi wash buffer

NDS normal donkey serum

NO nitric oxide

OPC oligodendrocyte progenitor cell

PAMP pathogen-associated molecular pattern

PBS phosphate-buffered saline

PCA principal component analysis

PCR polymerase chain reaction

PET positron emission tomography

PFA positron emission tomography

PFC prefrontal cortex

PLP proteolipid protein

PMD Pelizaeus-Merzbacher disease

PNS peripheral nervous system

PP Peyer's patch

PRR pattern recognition receptor

px pixel

RNA ribonucleic acid

rpm rotations per minute

RT room temperature

RXR retinoid X receptor

SCFA short-chain fatty acid

SEM standard error of the mean

SFB segmented filamentous bacteria

SPF specific pathogen free

WM white matter

Chapter 1

Introduction

1.1 Remyelination

To begin my thesis, I will give an overview of how regeneration occurs in biology, before introducing remyelination: an example of regeneration that can be remarkably effective, despite occurring within the inhibitory environment of the mammalian central nervous system (CNS). I will discuss the clinical relevance of myelin diseases and some of the current treatments available and their limitations. Next, I will delineate the known roles of the immune system in coordinating remyelination, paying particular attention to toxin-based models for remyelination - in which many of these functions have been identified. I will then describe some of the ways the microbiota can in turn influence the immune system, with a focus on the CNS. Finally, I will bring these strands together to present my hypothesis.

1.1.1 Injury and regeneration

Life is full of danger. An animal fending for itself in the world faces the constant threat of injury by competitors, by a predator or simply by accident. A breath of air, or a mouthful of food may expose his organs to damaging toxins. Pathogens, looking to exploit a niche, will seize an opportunity to multiply at the expense of their host's tissue integrity, whilst the systems in place to prevent this can themselves malfunction in autoimmune disease. These dangers aside, for tissues that suffer constant wear and tear, including the skin or gut epithelium, continuous cell death is part and parcel of their physiological function.

However, an organism irreversibly damaged by its environment will have difficulty surviving to pass on its genes. This has produced an evolutionary drive for strategies to overcome the attrition of a dangerous environment. The gold standard for this is regeneration:

the replacement of lost or damaged tissue in a way that recreates its original architecture and function (Stocum, 2012, p.3).

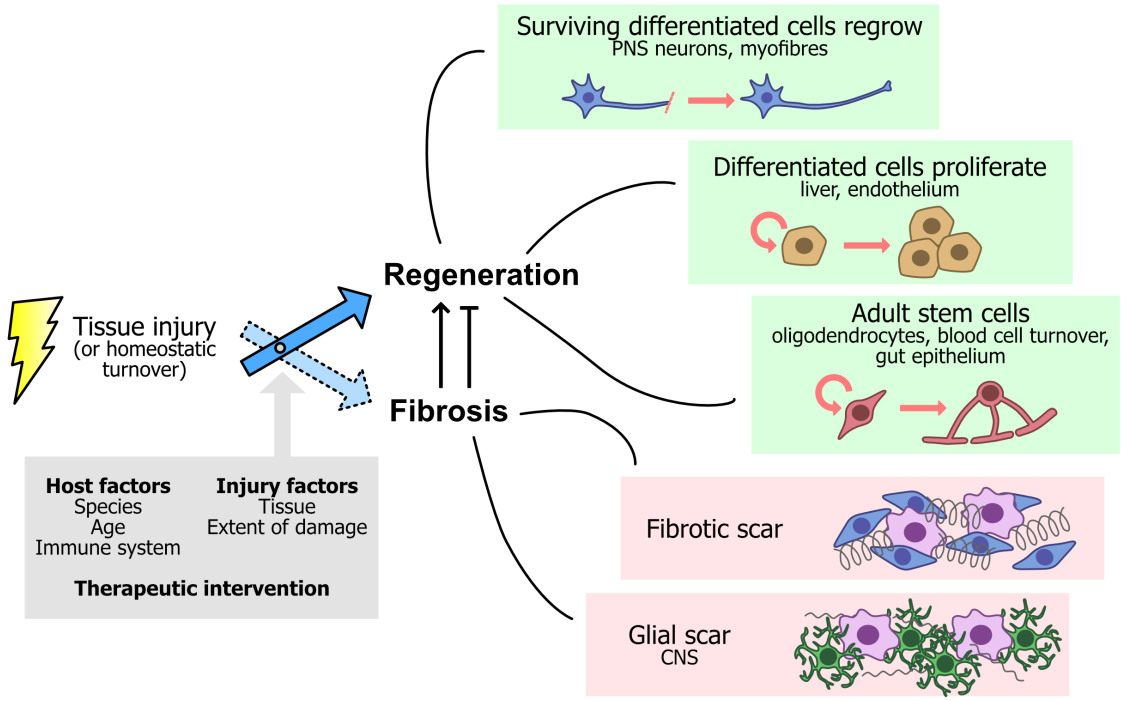

Fig. 1.1 **Outcomes of tissue injury in mammals.** Various factors can tip the balance between success and failure of regeneration. Regeneration can proceed by one of several mechanisms - or a combination of these. *Adapted from Stocum (2012).*

In mammals, tissue regeneration can be achieved by a number of strategies, depending on the location and the extent of damage (Fig. 1.1). In some cells with an elongated shape, such as skeletal myofibres or neurons of the peripheral nervous system, the cell body may be able to survive damage to a distant cytoplasmic region (McNeil and Steinhardt, 1997). In these examples, the tissue can be regenerated by cells resealing their membrane and regrowing damaged processes, providing the damage is not too extensive. In most cases, however, a damaged tissue will experience some degree of parenchymal cell death and part of the regenerative response will be the replacement of these cells. In the liver or the vascular endothelium, terminally differentiated cells can replicate in response to injury, balancing the deficit in cell number (Michalopoulos and DeFrances, 2007; Potente et al., 2011). Elsewhere, differentiated cells do not proliferate, with cells being replaced instead by asymmetric division from a pool of adult stem cells. This is the case in the regeneration or turnover of gut epithelium from stem cells in the intestinal crypts (Barker et al., 2007), and for the maintenance of blood cells by haematopoietic stem cells in bone marrow (Becker et al.,

1963; Till and McCulloch, 1961). It is also the mechanism at play in the CNS regenerative paradigm that I have studied for my thesis: multipotent oligodendrocyte progenitor cells (OPCs) are able to give rise to new oligodendrocytes, allowing myelin to be regenerated in the central nervous system.

Where none of these regenerative strategies can take place, the alternative tissue response is fibrosis. This is a reaction to tissue damage in which the cellular architecture is not restored, instead being replaced with dense connective tissue to form a scar (Stocum, 2012, p.21). In most sites of the human body, this connective tissue is comprised mainly of fibroblasts which proliferate and produce extracellular matrix (ECM) proteins such as collagen in response to chemical signals in the damaged tissue. In the CNS, a similar scar forms when reactive astrocytes hypertrophy and secrete ECM proteins. A compound glial/fibrotic scar can develop in CNS injury if blood-brain barrier disruption allows invasion of fibroblasts from the periphery (Silver and Miller, 2004). Whilst fibrosis does not restore the function of the damaged tissue, it protects the adjacent tissue by sealing off the wound, and can restore the structural integrity of an organ. Scar formation, particularly in the CNS, has traditionally been thought of as a physical and chemical barrier to regeneration of parenchymal tissue. This view has recently been challenged, as manipulations of the glial scar in spinal cord injury have convincingly demonstrated that elements of the scar also facilitate subsequent axonal regeneration through a lesion (Anderson et al., 2016). Whether the scar blocks regeneration or is an ineffective attempt to promote it, fibrosis is generally an undesirable outcome that occurs following more extensive damage, or in tissues with poor regenerative capacity (Stocum, 2012, p.21). The term “multiple sclerosis” refers to the sclerotic plaques that form where myelin is unable to regenerate and the damaged white matter instead develops into scar tissue (Charcot, 1868).

The ability of an injured tissue to achieve regeneration versus fibrosis depends on a range of factors. Firstly, there is a huge inter-species variation in regenerative capacity. Urodele amphibians are able to flawlessly regenerate full appendages, whilst some invertebrates such as planaria can regenerate an entire body from a tiny fragment of tissue. To do so, these animals can employ strategies that are not seen in mammalian regeneration. Urodeles can carry out dedifferentiation, converting mature cells into progenitor cells, which then expand and differentiate to regenerate limbs or other body parts (Lo et al., 1993). Planaria have a population of totipotent stem cells scattered throughout their body, as opposed to the relative lineage restriction found in mammalian adult stem cells (Aboobaker, 2011).

In mammals, different tissues have widely different regenerative capacity. Robust regeneration is essential in tissues with high exposure to environmental threats, including the epidermis, which acts as our barrier to the outside world, and the liver, which detoxifies

substances entering the circulation from the diet. In contrast, severed axons in the CNS are notoriously poor at regenerating. This is a reflection on both the regenerating cells themselves, and their environment: a phenomenon elegantly demonstrated using a peripheral nerve graft, through which rat CNS axons could regrow across a lesion (David and Aguayo, 1981). The type and extent of injury also guide subsequent regeneration: the liver will regenerate by compensatory hyperplasia after surgical ressection (Michalopoulos and DeFrances, 2007), but also has a pool of adult stem cells that are utilised if chemical damage makes hyperplasia impossible (Shafritz and Dabeva, 2002). However, even this highly regenerative organ can have its capacity exceded - as seen in patients with end-stage liver failure. Ageing is another important determinent of regenerative capacity: all regenerative processes decline in efficiency with age, with clear implications for chronic diseases of adulthood including multiple sclerosis (Franklin and Ffrench-Constant, 2008).

As we shall see, within an injured tissue is a complex network of cells and signalling molecules, some of which are endogenous whilst others enter from the circulation. Many of these cells and mediators are part of the immune system, which can play both positive and negative roles in resolving tissue damage and promoting regeneration. The basis of prospective therapies for regenerative medicine is to shift the balance away from fibrosis, towards the regeneration of functional tissue.

1.1.2 Remyelination: regeneration in the central nervous system

With mammals at the poorer end of the regenerative spectrum, and the CNS a particularly complex and inhibitory setting, the prognosis of neurological injury can be bleak. Endogenous regeneration of neurons and their axons is extremely limited in diseases such as stroke, spinal cord injury or neurodegenerative disease, with devastating consequences for a patient's quality of life (Kordower and Tuszynski, 2011). There is some optimism to be seen in neuronal plasticity: the rewiring of surviving neurons to allow some functional recovery without true regeneration. A promising avenue for treatment is to facilitate these plasticity mechanisms in combination with targeted rehabilitation to guide the formation of useful new synapses (Fawcett, 2009).

However, there is one *bona fide* example of CNS regeneration that can be extensive, even in the context of human disease. This is remyelination: the regeneration of myelin sheaths. Myelin consists of layers of lipid-rich dielectric membrane and is found throughout nervous system, wrapped around many of our axons. This membrane is produced by specialised glial cells: oligodendrocytes in the CNS, or Schwann cells in the peripheral nervous system (PNS). The myelin sheath electrically insulates segments of axons between unmyelinated nodes of Ranvier, and this allows action potentials to propagate faster and more efficiently

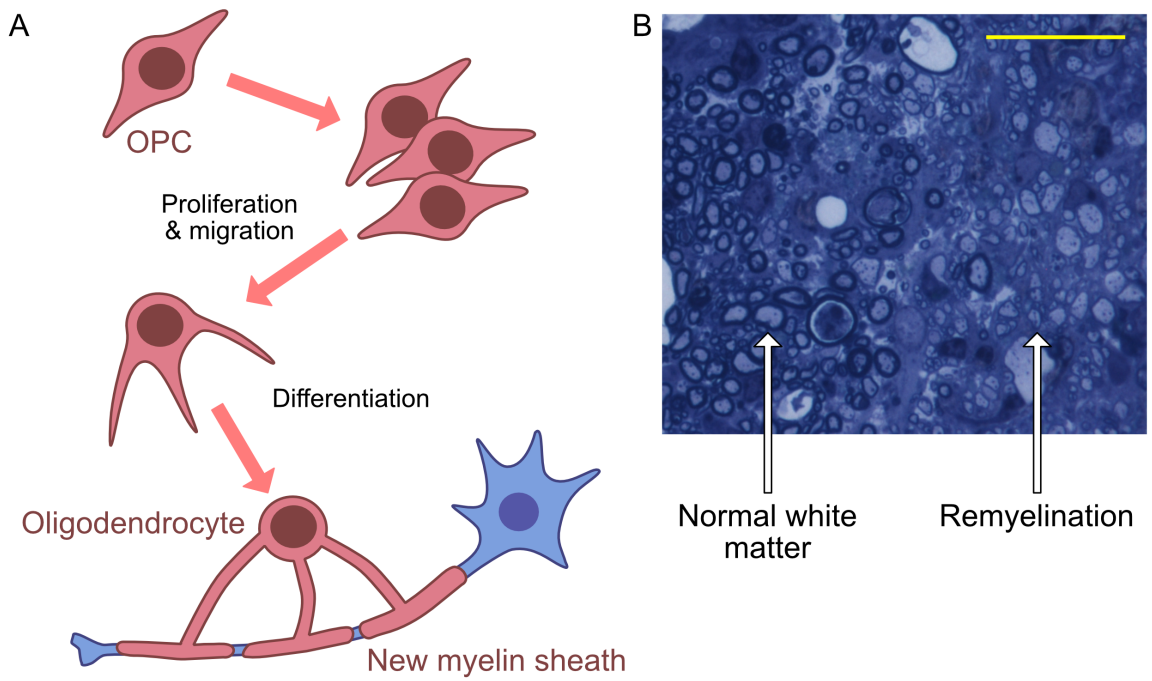

Fig. 1.2 **The OPC response to demyelination.** (A) Following a primary demyelinating injury, OPCs proliferate, migrate and differentiate into oligodendrocytes, restoring the myelin sheaths of denuded axons. (B) Toluidine blue-stained transverse section of a lysolecithin lesion in mouse spinal cord, demonstrating regions of normal white matter and remyelination. Note the thinner sheaths surrounding the remyelinated axons. Scale bar: B = 25 µm.

by saltatory conduction (Nave and Werner, 2014; Tasaki, 1939). Besides their roles in electrical conduction, oligodendrocytes are in fact essential for axonal survival, as evidenced by axonal degeneration when oligodendrocytes are selectively ablated by diphtheria toxin (Pohl et al., 2011). Part of this support role depends upon myelin proteins such as proteolipid protein (PLP) (Griffiths et al., 1998), though a myelin-independent aspect involves the flux of metabolites from oligodendrocyte to axon (Lee et al., 2012).

The loss of myelin sheaths is known as demyelination, and can be either a primary pathology or secondary to axonal loss as a component of Wallerian degeneration. Remyelination involves the reinstatement of myelin around intact axons that have lost their sheaths by primary demyelination (Franklin and Ffrench-Constant, 2017). This process is performed by newly generated oligodendrocytes that derive from a pool of oligodendrocyte progenitor cells (OPCs) following a demyelinating insult. OPCs are present throughout both grey and white matter in the CNS and exhibit features typical of adult stem cells such as multipotency and self-renewal. In response to demyelination, OPCs proliferate and migrate to the lesion site (Crawford et al., 2014; Di Bello et al., 1999) where they differentiate to mature oligodendro-

cytes, extending processes to remyelinate denuded axons (Fig. 1.2A). Consequently, saltatory conduction and function are restored (Duncan et al., 2009; Smith et al., 1979) and axons are protected from degeneration (Irvine and Blakemore, 2008). The regenerated sheaths do not reach the full thickness of those in unlesioned white matter, which a helpful feature for identifying remyelination histologically (Fig. 1.2B). This has expected implications for axonal velocity, though whether this limits the function of neuronal circuits is still unclear. Myelin sheaths generated in adulthood outside an injury context have a similar morphology to remyelination (Young et al., 2013), and this could depend in part on the dynamics of the axon being (re)myelinated (Franklin and Ffrench-Constant, 2017).

1.1.3 Clinical myelin disease

A principal reason for investigating the biology of remyelination is that a range of clinical diseases cause primary demyelination. Some of these result from extrinsic pathologies that damage previously healthy myelin, whilst others are the result of intrinsic deficits in the oligodendrocyte-myelin unit (Fig. 1.3). These exhibit wide heterogeneity in their outcomes – from complete recovery to rapid progression, secondary axonal loss and disability or death. Though it is difficult to prove causation in human disease, an extensive evidence base from post-mortem studies and medical imaging, combined with insights from animal models, suggests that the success or failure of remyelination plays an important role in the prognosis. Thus, if we can develop therapies to facilitate remyelination where it would otherwise fail, this could dramatically improve the quality of life of afflicted individuals.

Extrinsic aetiologies

The most prevalent causes of demyelination are autoimmune – notably multiple sclerosis (MS), which has a lifetime risk of approximately 1/200 for women and 1/400 for men (Alonso et al., 2007). In affected patients, autoreactive T cells recognising myelin antigens escape tolerance mechanisms and recruit microglia, macrophages and neutrophils to initiate an inflammatory response in the CNS (reviewed: Dendrou et al. (2015)). In combination, these cells release oligodendrocyte-toxic factors and strip the myelin from axons to cause demyelination. This occurs in discrete lesions throughout the CNS, with the anatomical location accounting for the patient's associated symptoms and clinical signs – often affecting motor systems, sensation, coordination or cognition.

MS can follow different clinical courses, but 85-90% of patients present with relapsing/remitting disease (Kumar and Clark, 2012, p.1124), in which there is functional recovery between clinical episodes. As axonal regeneration is poor within the CNS, recovery will

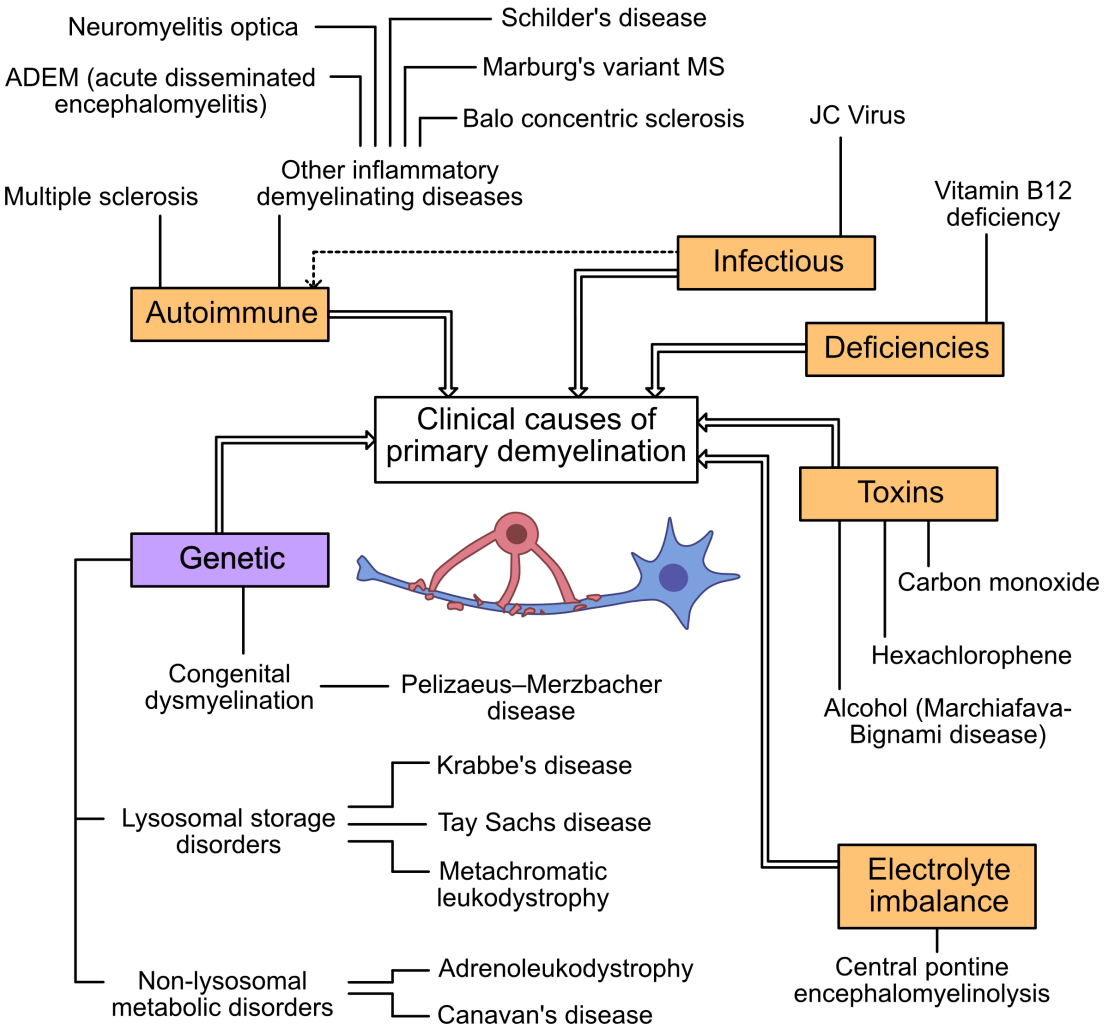

Fig. 1.3 **Clinical causes of primary demyelination.** A range of clinical aetiologies can lead to primary demyelination in humans. Processes extrinsic to oligodendrocytes are shown in orange, whilst those originating intrinsically are purple.

only be possible where axons survive the demyelination and inflammation of the lesion environment. Surviving axons can regain normal conduction as the inflammation resolves, and associated conduction-inhibitory molecules such as nitric oxide diminish (Redford et al., 1997). Restored conduction in surviving axons corresponds with remission of the disease (Waxman, 2006), whilst axonal degeneration is a strong correlate with persistent functional deficit (Trapp and Nave, 2008). Remyelination can be extensive in MS (Patrikios et al., 2006) and is thought to be vital for restoring the trophic support to axons to ensure their long-term survival. Whilst axons in lesions that remain chronically demyelinated continue to degenerate, they are spared in lesions where remyelination has taken place (Kornek et al., 2000), though interpretation is difficult as it may instead be that remyelination cannot occur where axons have already begun to degenerate. A relapsing-remitting pattern is common early in the disease, but many of these patients enter a secondary progressive phase in which functional deficits persist and accumulate. Post-mortem tissue has shown that remyelination becomes less extensive later in the disease (Goldschmidt et al., 2009) and the failure in myelin regeneration, with its associated axonal degeneration, are thought to be central to this unfortunate outcome that many MS patients experience (Franklin, 2002).

Multiple sclerosis is a heterogeneous condition, and there is debate as to whether a number of similar diseases represent separate entities or should be considered within an MS spectrum of disorders (Simon and Kleinschmidt-DeMasters, 2005). These are all autoimmune demyelinating disorders but differ in their clinical course, pathology and anatomical involvement. However, a common feature with MS is that axonal preservation is a strong prognostic indicator. In neuromyelitis optica, for example, lesions occur preferentially in the optic nerve and spinal cord, and often with more extensive axonal injury than relapsing remitting MS, manifesting as generally more permanent deficits (Trebst et al., 2014). Even more extreme, Marburg's variant MS progresses rapidly, with widespread demyelination and axonal damage that completely overwhelm the CNS's capacity to regenerate myelin (Simon and Kleinschmidt-DeMasters, 2005). The peculiarities of these rarer MS-like diseases can give us insight into why remyelination fails and in turn they may eventually benefit from remyelination-enhancing therapies.

Besides these autoimmune disorders, a number of other pathological states can damage myelin. Electrolyte disturbances can cause central pontine myelinolysis, classically with an iatrogenic cause due to rapid correction of hyponatraemia. Oligodendrocytes in the pons appear particularly vulnerable to the resultant changes in cell volume, which trigger apoptosis (Martin, 2004). This is an unusual example of demyelination occurring in the relative absence of an inflammatory infiltrate, and again shows a wide range of prognostic outcomes, which can be difficult to predict. Exposure to various toxins can also cause clinical

demyelination, presumably by selective toxicity to oligodendrocytes. This includes carbon-monoxide which is thought to kill oligodendrocytes by hypoxia and damage myelin through lipid peroxidation (Parkinson et al., 2002). The disinfectant hexachlorophene, once widely used, became heavily regulated in the 1970s after being shown to alter the ultrastructure of myelin and cause demyelination (Cammer et al., 1975). Dietary deficiency can also lead to CNS demyelination, for example of vitamin B12, which is an essential cofactor for maintaining a myelin sheath (Miller et al., 2005). The JC virus is a direct infective cause of multifocal primary demyelination (Ferenczy et al., 2012), whilst several other pathogens are likely triggers for autoimmune demyelination through molecular mimicry (Steelman, 2015).

As less is known about these rarer causes of demyelination, we lack large-scale studies into the extent of remyelination and how this correlates with clinical progression. However, as for MS, severe and permanent disability is associated with axonal damage rather than demyelination in isolation (Medana and Esiri, 2003). Thus there is reason to believe that enhancing remyelination to improve survival of vulnerable, denuded axons in the lesion environment could also be beneficial here.

Intrinsic aetiologies

Whilst all of the above conditions involve the degeneration of healthy myelin by external factors, primary demyelination can also result from genetic disorders that compromise the integrity of oligodendrocytes or the myelin they lay down. Some of these directly affect proteins components of the myelin sheath, for example Pelizaeus-Merzbacher disease (PMD), which is caused by a mutant form of the myelin constituent proteolipid protein (PLP) (Koeppen et al., 1987). Other mutations perturb cellular lipid turnover, which tends to affect oligodendrocytes due to the careful coordination required in these metabolic pathways to produce and maintain a myelin sheath (Chrast et al., 2011). Examples include the lysosomal storage disorders (including Krabbe's disease, Tay-Sachs disease and metachromatic leukodystrophy) as well as extra-lysosomal errors in lipid metabolism (such as adrenoleukodystrophy and Canavan's disease) (Franklin and Goldman, 2015). These generally present in childhood, as myelination is defective throughout development. As in the diseases where demyelination occurs later in life, the absence of a functional myelin sheath will provoke axonal degeneration, correlating with neurological signs (Garbern et al., 2002).

As the machinery for producing new myelin is defective in these examples of intrinsic pathology of the oligodendrocyte-myelin unit, enhancing endogenous remyelination is considered less of a therapeutic goal in these diseases. Instead, a cell replacement approach would likely be more beneficial, where genetically functional cells are introduced into the CNS to form new oligodendrocytes and healthy myelin sheaths. Conversely, where demyelination is

caused by external factors, transplanting exogenous oligodendrocyte-forming cells may be a fruitless exercise without first confronting the environmental drivers of demyelination and blockades to remyelination (Franklin and Goldman, 2015).

1.1.4 Current therapies for myelin disease

Supportive therapies can bring about great improvements in quality of life for a patient suffering from a demyelinating disease. These might include, for example, managing pain and urinary symptoms as well as providing appropriate physiotherapy, occupational therapy and social support. However, these measures do nothing to alter the course of the disease, prolong life and prevent further disability. Having established that axonal preservation is vital for a good prognosis, a disease-modifying treatment for demyelinating disease could act through any of the following mechanisms:

- inhibit the pathological processes causing myelin damage
- enhance remyelination to prevent axonal degeneration by either:
  - promoting endogenous remyelination
  - introducing exogenous remyelinating cells
- promote axonal survival by other means

In the past few decades, we have witnessed major advancements in addressing the first of these points. A range of drugs have now shown efficacy in reducing demyelination in relapsing-remitting MS. These include interferon-β therapies (PRISMS Study Group, 1998) and glatiramer acetate (Comi et al., 2001), which can reduce relapse rate and the development of new lesions in relapsing-remitting MS. More aggressive biological agents have higher efficacy at reducing relapse rate and accumulation of disability, though with associated side-effects. These include alemtuzumab, which blocks CD52 to deplete T cells (Coles et al., 2012), and natalizumab, which blocks the α-4 integrin necessary for T cell entry to the CNS (Polman et al., 2006). As for osmotic demyelination syndrome, the careful management and slow correction of hyponatraemia can prevent central pontine myelinolysis from developing iatrogenically. In the paediatric cases where demyelination arises from intrinsic oligodendrocyte deficits, the possibility of reducing myelin damage is very limited, but may eventually be possible using gene therapy to correct genomic mutations.

However effective some of these treatments are, there are also plenty of limitations. Notably, once the damage to myelin has been done, they cannot alter the subsequent neurological outcomes of demyelination that result from axonal degeneration in the absence

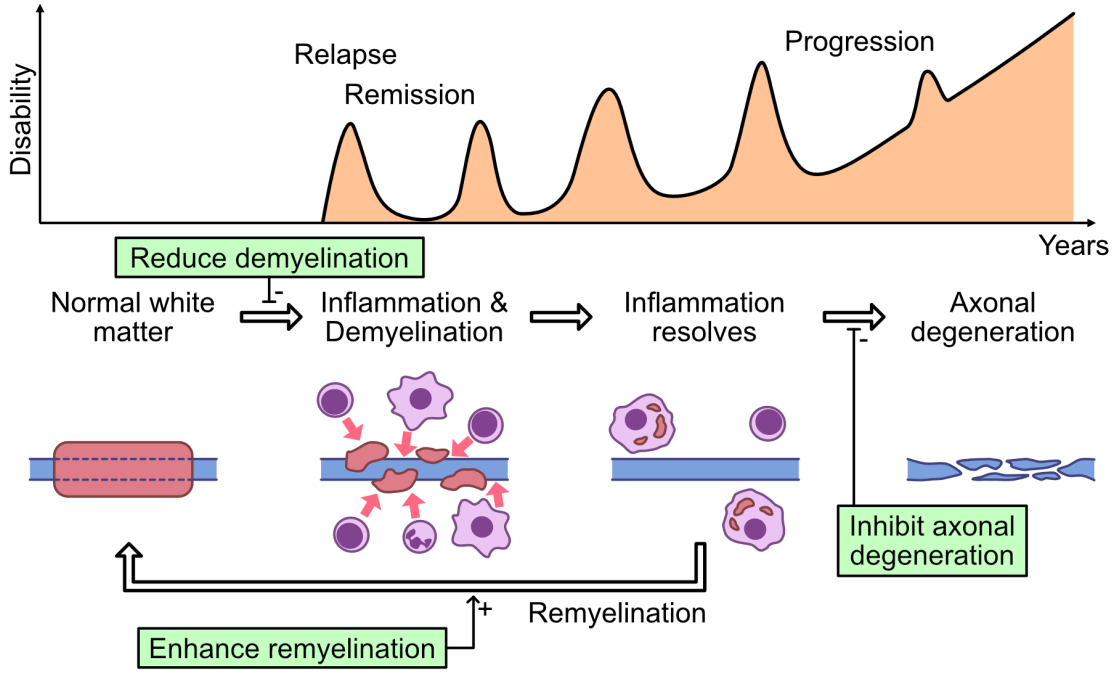

Fig. 1.4 **A model for the progression of multiple sclerosis.** Inflammation upsets axonal conduction through destruction of the myelin sheath, and production of inhibitory mediators such as nitric oxide. As inflammation resolves the effects of these mediators reduce allowing some functional improvement. However, without remyelination axons will degenerate, causing irreversible disability. Prospective routes to disrupt this process are (1) reducing demyelination, (2) enhancing remyelination and (3) protecting axons by alternative pathways.

of a myelin sheath. Whilst current MS therapies can successfully reduce relapses and even delay conversion to secondary progressive MS (Brown et al., 2017), little can be done once the progressive phase is reached. Thus, these therapies would ideally be combined with approaches that protect demyelinated axons, preventing entry into a progressive phase in which demyelination-inhibiting drugs become ineffective (Fig. 1.4).

The mechanisms by which axons become damaged following demyelination are poorly understood (Lee et al., 2014), but likely involve a combination of increased energy demands in the absence of saltatory conduction (Kiryu-Seo et al., 2010), redistribution of ion-channels resulting in neurotoxic levels of calcium (Craner et al., 2004) and impaired oligodendrocyte-axonal shuttling of metabolites such as lactate (Fünfschilling et al., 2012; Lee et al., 2012). Given that we have a built in mechanism to regenerate myelin and address the root cause of these changes, enhancing this process seems the most obvious approach to maximise axonal survival. Remyelination is the default response to demyelination (Franklin and Ffrench-

Constant, 2017), so discovering what causes it to fail and how to overcome these constraints are key to this line of enquiry.

One of the strongest brakes on remyelination is ageing - a common feature of regenerative responses throughout the body. Ageing brings about changes in OPCs (Shen et al., 2008) and their environmental signals (Zhao et al., 2006), both of which negatively impact remyelination. Clinical data has shown that regardless of the initial presentation of MS, each disability milestone is reached at a consistent age, suggesting an age-dependent process is driving progression of the disease (Confavreux and Vukusic, 2006). As most situations where we want to enhance endogenous remyelination occur in the adult (and often ageing) CNS, remyelination is likely to be sub-optimal with considerable scope for improvement.

Various drugs have been shown to enhance remyelination in animal models (Franklin and Ffrench-Constant, 2017). Of these, opicinumab, a humanised monoclonal antibody targeting the LINGO-1 protein, has generated the most information in phase II clinical trials. Preliminary results suggest some clinical efficacy in acute optic neuritis (ClinicalTrials.gov Identifier: NCT01721161) but the end points have been missed in the SYNERGY trial for patients with relapsing-remitting MS (ClinicalTrials.gov Identifier: NCT01864148). Other candidates in phase II clinical trials are clemastine, an over-the-counter antihistamine (ClinicalTrials.gov Identifier: NCT02040298) and bexarotene, a retinoid X receptor agonist previously licensed for T cell lymphoma (ISRCTN 14265371). Clemastine has likewise shown an increase in the measured optic nerve conduction for MS patients, though without a significant improvement in vision (Green et al., 2016), whilst the bexarotene study is ongoing. Whilst these trials have shown some promise, no drug has yet been demonstrated to promote functionally important remyelination in humans, and there is a tight bottleneck in translating candidates from success in animal models into clinical settings.

There is therefore much clinical need for therapies to enhance remyelination. In this thesis, I investigate the potential of the microbiota as a novel route to influence remyelination in the mammalian CNS. The immune system is a likely mediator of any such effect, as it is a central force in shaping the lesion environment (Miron and Franklin, 2014), and is itself tuned by exposure to commensal microbes (Belkaid and Hand, 2014). In the next two sections, I elaborate on the mechanisms underlying each of these processes.

1.2 The immune system in remyelination

1.2.1 Inflammation is a prominent feature of injury

Active MS lesions are characterised by an inflammatory infiltrate containing activated macrophages and microglia, CD8+ T cells and in lower numbers CD4+ T cells, B cells and plasma cells (Popescu et al. (2013), Fig. 1.5A). This is consistent with an autoimmune insult, in which microglia and macrophages are stimulated by autoreactive T cells. However, even in sterile, toxin-mediated models of demyelination, activated microglia and macrophages are highly abundant at the site of injury (Fig. 1.5B, C), demonstrating that, as well as driving demyelination in certain circumstances, these cells can also become activated as a response to myelin damage. The sheer number of these cells, combined with their well-established phagocytic and secretory functions, points towards a profound influence of the immune system on the lesion environment in which the OPCs reside.

Inflammation is a common feature of other injury paradigms, spanning a diverse array of tissues and species. The immune system of vertebrates can be broadly divided into an innate and an adaptive branch, with much crosstalk between them. Following any variety of injury, the innate immune system responds rapidly and relatively non-specifically to environmental signs of tissue damage, using pattern recognition receptors (PRRs). If infection is present, these receptors recognise pathogen-associated molecular patterns (PAMPs), such as bacterial lipopolysaccharide (LPS) or peptidoglycan. In sterile injury, different PRRs will recognise host-derived damage-associated molecular patterns (DAMPs) including exposed DNA or leaked intracellular proteins. Cells expressing these PRRs include mast cells, dendritic cells and neutrophils as well as macrophages and their native CNS counterparts, microglia. Together, these cells mediate an inflammatory response to injury, which can influence the lesion environment in a variety of ways:

- fight infection where epithelial barriers are compromised
- activate / sensitise nociceptors to create awareness of injury (pain)
- clear debris arising from dead cells
- remodel the ECM by secreting proteases
- secrete cytokines and other factors to influence other cells in the lesion
- stimulate angiogenesis, to deliver further resources
- recruit reactive astrocytes (CNS) or myofibroblasts (elsewhere) when a tissue's regenerative capacity is exceeded, leading to fibrosis

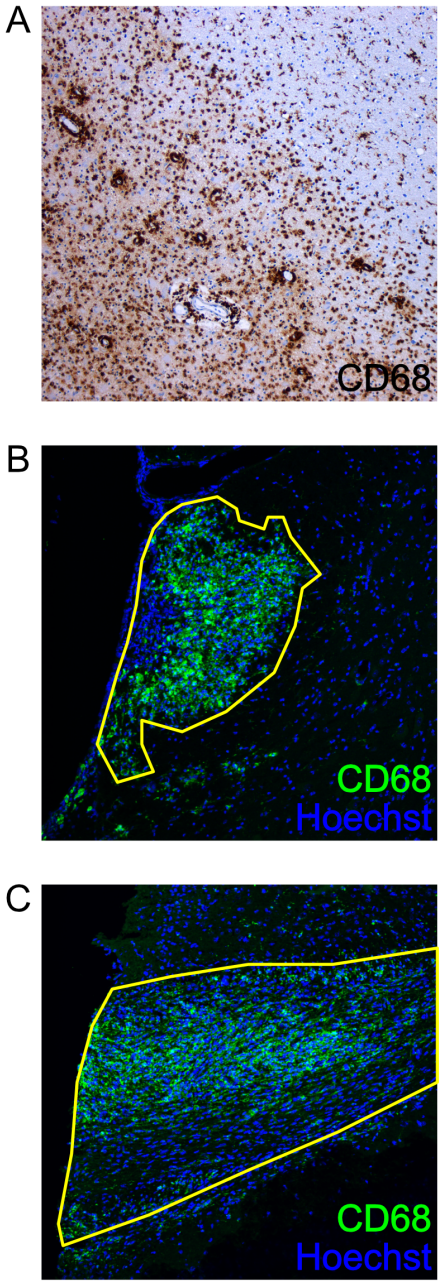

Fig. 1.5 **Extensive inflammation is seen in different demyelination paradigms.** (A) Photomicrograph of an MS lesion immunostained for CD68. The lesion environment on the left shows numerous activated, amoeboid microglia/macrophages compared to the ramified microglia present in normal white matter on the right[1]. (B) Demyelinated lesion in the spinal cord ventral white matter of a mouse caused by focal injection of lysolecithin. Abundant green CD68+ cells are visible within the lesion boundary (yellow line), with Hoechst-stained nuclei in blue. (C) Corpus callosum (yellow line) of a mouse after 5 weeks of dietary cuprizone administration to cause demyelination. Again, green CD68+ cells are a prominent feature of the injured white matter. [1]*Image in (A) from https://commons.wikimedia.org File:MS Demyelinisation CD68 10xv2.jpg*

These innate immune-driven processes may help regeneration depending on the species, tissue, injury, age and other factors.

1.2.2 Macrophages and microglia

However, persistent or dysregulated macrophage activity can itself be detrimental to regeneration. These opposing influences on regenerative outcome were demonstrated in the liver by altering the timing of macrophage depletion with a CD11b-driven diphtheria toxin receptor (Duffield et al., 2005). Depleting macrophages during ongoing toxin-mediated injury was a successful means to reduce fibrosis, but depletion during the repair phase gave a worse regenerative outcome. *In vitro* studies have supported this concept of macrophage populations with conflicting effects on regeneration. Macrophages are highly plastic cells, and adopt different phenotypes in response to different extracellular cues (Edwards et al., 2006). These are often termed "M1" (pro-inflammatory) or "M2" (anti-inflammatory / pro-regenerative) polarisation for convenience, though *in vivo* represent a spectrum with a broad degree of plasticity, which is likely to underpin their divergent influences on regeneration (Murray et al., 2014). With this caveat, I shall use the terms "M1" and "M2" throughout this thesis to describe microglial/macrophage phenotypes *in vivo* with similarities at the protein level to their respective *in vitro* paradigms. In mammals, macrophages have been linked to both positive *and* negative roles during regeneration in liver, heart, skeletal muscle and the CNS, amongst other organs (Wynn and Vannella, 2016). Finding ways to promote the pro-regenerative functions of macrophages, whilst limiting their contributions to damage is an important goal of regenerative medicine.

Part of this functional heterogeneity may arise from the fact that a regenerating tissue contains macrophages from two different sources: tissue-resident macrophages that activate in response to DAMPs, and monocyte-derived macrophages that infiltrate from the periphery. Tissues throughout the body have their own populations of resident macrophages, which are essential for normal development (Dai et al., 2002; Gouon-Evans et al., 2000) and throughout adulthood have important homeostatic roles in metabolism (Nathan et al., 2013) and cellular turnover (Arandjelovic and Ravichandran, 2015). At times of injury, these are supplemented by a pool of circulating blood monocytes, which are recruited to the site of damage and differentiate into macrophages. In the mammalian CNS, the resident macrophages are called microglia and enter the parenchyma from the yolk sac prior to formation of the blood brain barrier (Ginhoux et al., 2010). Throughout life, they participate in clearance of senescent cells (Ferrer et al., 1990) and synaptic plasticity (Paolicelli et al., 2011), all the time using their dynamic processes to patrol the environment for DAMPs or PAMPs (Nimmerjahn et al., 2005). If a danger cue is detected microglia become activated, adopting an amoeboid

morphology and drastically altering their transcriptome (Bodea et al., 2014). Meanwhile, monocytes extravasate and cross the blood-brain barrier, honing towards PAMPs, DAMPs and locally-produced cytokines (Fig. 1.6). These two macrophage populations constitute the majority of immune cells in many lesions of the CNS.

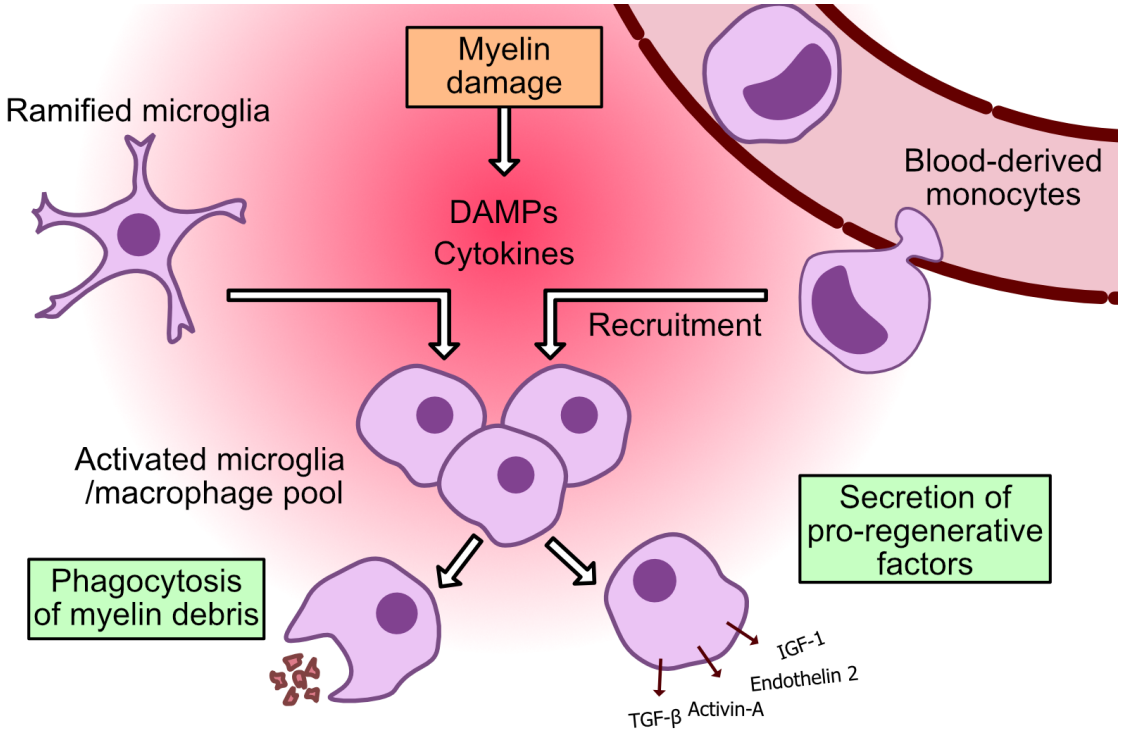

Fig. 1.6 **The contribution of microglia and infiltrating macrophages to remyelination.** Following both myelin damage, the presence of DAMPs and locally-produced cytokines activate resident microglia to adopt an amoeboid morphology and recruits monocytes from the periphery. This combined macrophage pool can phagocytose myelin debris and produce pro-regenerative factors to create an environment that promotes remyelination.

1.2.3 Inflammation is an important orchestrator of remyelination

The role of inflammation in myelin injury is particularly complex, given that the most common causes of demyelination are autoimmune (Fig. 1.3). In MS, macrophages and microglia are recruited by myelin-reactive T cells to attack the myelin sheath by release of toxic inflammatory mediators, and the majority of genetic risk factors involve the major histocompatibility complex and other immune-related loci (Beecham et al., 2013; Jersild et al., 1972). In fact, for a long time the pathogenesis of MS masked important beneficial roles of inflammation in tissue repair.

Toxin	Delivery	Mechanism	Principal uses
Lysolecithin	Focal injection (commonly spinal cord ventral white matter)	Detergent effect on oligodendrocytes, also activates immune cells directly	• most commonly used focal model, with well-defined kinetics
Cuprizone	Administration in diet over 4-6 weeks	Disturbs copper homeostasis causing metabolic stress, to which oligodendrocytes are particularly vulnerable and undergo apoptosis	• no surgery required • model for remyelination with an intact blood-brain barrier • similarities with pattern III lesions in MS [a]

Table 1.1 **Two commonly used toxin-induced models of demyelination.**

[a] Similarly to cuprizone, pattern III lesions are diffuse with ill-defined borders, and have a histological appearance that suggests metabolic dysfunction in oligodendrocytes is an early event in lesion development (Gudi et al., 2014; Lucchinetti et al., 2000).

By administering oligodendrocyte-toxic compounds, demyelination can be induced independently of an autoimmune process (Table 1.1). Once these autoimmune elements of demyelination are removed, it becomes clear that inflammation is in fact one of the principal drivers of remyelination. This was first demonstrated by depleting circulating monocytes in rats using clodronate liposomes, which are toxic to cells that phagocytose them (Kotter et al., 2001). Following demyelination with by lysolecithin, clodronate-treated rats had reduced macrophage infiltration and reduced remyelination. Conversely, by promoting inflammation it is possible to increase the efficiency of myelin formation. The Toll-Like Receptor 2 agonist zymosan was able to increase inflammation and myelination by OPCs transplanted into the retina (Setzu et al., 2006). The link between inflammation and successful remyelination in toxin-based models has since been verified in a variety of other "loss of function" and "gain of function" experiments (Doring et al., 2015; Lampron et al., 2015; Miron et al., 2013; Natrajan et al., 2015; Ruckh et al., 2012).

Furthermore, the decline in remyelination with ageing occurs in part at the level of the innate immune system. In a heterochronic parabiosis model, in which mice of different ages were connected via their circulatory system, it was shown that exposure to a young circulation could rejuvenate remyelination in old mice (Ruckh et al., 2012). The effect was abrogated by knocking out CCR2, a receptor needed for monocyte extravasation, in the younger partner. Thus, young monocyte-derived macrophages must contribute to the lesion environment in a way that promotes differentiation of aged OPCs. Aged animals also show an impaired ability to shift their microglia/macrophages from an M1 to M2 phenotype following demyelination, and this too is reversed by heterochronic parabiosis (Miron et al., 2013).

1.2.4 Phagocytosis and mediator section by macrophages in the lesion environment

There are two principal mechanisms by which microglia/macrophages can fashion a remyelination-promoting environment: (1) phagocytosis of myelin debris and (2) secretion of pro-regenerative factors. As a myelin sheath disintegrates, fragments of myelin debris persist in the environment. This debris is known to inhibit OPC differentiation *in vitro* (Robinson and Miller, 1999) and *in vivo* it was shown that remyelination is impaired if a lesion is supplemented with additional myelin debris (Kotter et al., 2006). Thus it would appear that clearance of the myelin debris is a necessary step towards forming new oligodendrocytes. More recent work has shown an impairment in remyelination when phagocytosis is specifically impaired in either microglia (CX3CR1 knockout, Lampron et al. (2015)) or in infiltrating macrophages (LysM-specific RXR knockout, Natrajan et al. (2015)).

Inflammation also promotes remyelination in a model where OPCs are transplanted into the retina – a site that was not previously myelinated (Setzu et al., 2006). This suggests that there are important contributions of inflammation besides clearance of myelin debris. Microglia/macrophages also secrete a range of molecular signals into the lesion environment, and this is disturbed with ageing (Hinks and Franklin, 2000; Zhao et al., 2006). Experiments using microglia-conditioned media have shown that these secreted factors can modulate the OPC response, and this depends on the phenotype of the conditioning microglia (Miron et al., 2013). Some of these molecules are classical growth factors, including insulin-like growth factor (IGF-1) and transforming growth factor- (TGF-β). Both have long been known to promote OPC differentiation in vitro (McKinnon et al., 1993; McMorris and Dubois-Dalcq, 1988) and their expression is delayed in the slow remyelination of old rats (Hinks and Franklin, 2000). More recently, transcriptional profiling of the OPC retinal transplant model identified endothelin-2 as a factor promoting remyelination (Yuen et al., 2013), and activin-A was found to be essential for the pro-differentiation effects of microglia-conditioned media (Miron et al., 2013).

These two key functions of phagocytosis and mediator secretion can be carried out by both resident microglia and infiltrating macrophages, which are often discussed as a single functional population (Fig. 1.6). There is indeed much overlap in their roles – for example, using a GFP+ bone-marrow chimera, it was shown that both microglia and infiltrating macrophages undergo a similar M1 to M2 transition following demyelination (Miron et al., 2013). In rats depleted of peripheral monocytes, microglia numbers in the lesion increase to compensate (Kotter et al., 2005).

However, as our models of remyelination and the tools to probe them become more sophisticated, differences between these two pools of innate immune cells are emerging. For

example, in demyelination induced by dietary cuprizone, microglia are more important than infiltrating macrophages as blocking monocyte entry by CCR2 knockout had no effect on remyelination (Lampron et al., 2015). This was in contrast to the importance of monocytes following a stereotactic lysolecithin injection (Ruckh et al., 2012), and the difference might involve the blood brain barrier, which remains intact in the cuprizone model (Bakker and Ludwin, 1987). The identification of stable molecular signatures such as P2ry12, FCRLS (Butovsky et al., 2014) and Tmem119 (Bennett et al., 2016) should help us resolve the similarities and differences between these two populations going forwards. However, the techniques to distinguish these cells using immunohistochemistry are still in their infancy, and I will generally refer to the microglial/macrophage population as a whole during my analysis.

Whilst I focus here on microglia and infiltrating macrophages, other cells of the immune system can also be found in a demyelinated lesion. In particular, regulatory T (T_{reg}) cells have recently been shown to have a beneficial effect on remyelination by signalling directly to OPCs (Dombrowski et al., 2017). As for the innate immune system, neutrophils (Liu et al., 2010), mast cells (Letourneau et al., 2003), dendritic cells (Karni et al., 2006) and natural killer cells (Maghazachi, 2012) can all contribute to demyelination, but there is currently little evidence to suggest a role for these cells in remyelination. Due to their abundance and well-established role in remyelination (Miron and Franklin, 2014), and their substantial modulation by the microbiota (Erny et al., 2015; Möhle et al., 2016), I have focused my experiments on microglia and monocyte-derived macrophages.

1.2.5 Multiple sclerosis and the opposing roles of the immune system

Whilst a large body of evidence now links inflammation to remyelination in toxin-mediated models, it is important to establish whether these findings are of relevance to diseases like MS, where the pathology itself is immune-mediated. Our best models for the immunogenic features of MS involve inoculating animals with myelin constituents to trigger the expansion and dysregulation of myelin-reactive T cells (Robinson et al., 2014). These models are known collectively as experimental autoimmune encephalomyelitis (EAE) and, as in MS, both microglia and infiltrating monocytes are implicated in demyelination (Ajami et al., 2011; Fife et al., 2000; Heppner et al., 2005).

However, evidence suggests that even on this backdrop of inflammatory damage, a subset of the inflammatory cells can play beneficial roles in limiting damage and promoting remyelination. A shift toward the anti-inflammatory M2 phenotype is associated with a milder clinical picture in EAE (Mikita et al., 2011), and administration of M2-polarized monocytes to animals with EAE can enhance differentiation of oligodendrocytes and improve

symptoms (Butovsky et al., 2006). These results have much in common with the beneficial roles of M2 macrophages in toxin-mediated demyelination (Miron et al., 2013).

In fact, autoimmune demyelination may be a context in which the heterogeneity between resident microglia and infiltrating monocytes becomes very important. When EAE was induced in transgenic mice with green CX3CR1+ microglia and red CCR2+ macrophages (Yamasaki et al., 2014), highly activated monocyte-derived macrophages appeared to initiate demyelination, whilst microglia had more beneficial roles in clearing debris. However, this result contrasts with an earlier study, in which selective microglial inhibition was shown to be beneficial (Heppner et al., 2005). Thus, we still have much to learn about the intricacies of these two populations and their roles in damage and repair.

As for human disease, whilst inflammation is clearly linked to demyelination, post-mortem histology of MS lesions shows a correlation between the density of macrophages and the density of OPCs within a lesion (Wolswijk, 2002). "Active" lesions, characterised by ongoing inflammation, have more OPC recruitment and remyelination than chronic inactive plaques (Clemente et al., 2013). Whilst immunosuppression is our best means to prevent demyelination, maintaining a well-tuned inflammatory response in MS lesions may be a route to achieve remyelination where it would otherwise fail (Franklin and Ffrench-Constant, 2017).

1.3 The microbiota as immune modulators

1.3.1 The microbiota in health and disease

And how might we tune this inflammatory response? In recent years our commensal microbes have emerged as one of the principal environmental determinants of immune function throughout development and adult life, in health and disease (Belkaid and Hand, 2014). The term "microbiota" refers to all the microorganisms that inhabit a host. In humans, this encompasses communities of bacteria, fungi, archaea, protists and viruses living on the skin, and in the gut, oral cavity, vagina, lungs and various other mucosal surfaces. The "microbiome" refers to the collective genomes of the microbiota. Whilst important roles for other microbes are emerging, bacteria are by far the most abundant at the genetic level (Qin et al., 2010) and the multitude of bacterial cells in fact outnumbers the (much larger) host cells of the human body (Sender et al., 2016). Much attention is focused on the gut microbiota as, with a surface area of 30-40 m^2 (Helander and Fändriks, 2014) and a conveyer belt of nutrients supporting 10^{13} microorganisms (Sears, 2005), the human gastrointestinal tract represents a hugely important interface between host and microbes. After billions of

years of evolution in the presence of these microbes, it is not surprising that some of their functionality has been integrated into our own development and physiology, not least in the immune and nervous systems.

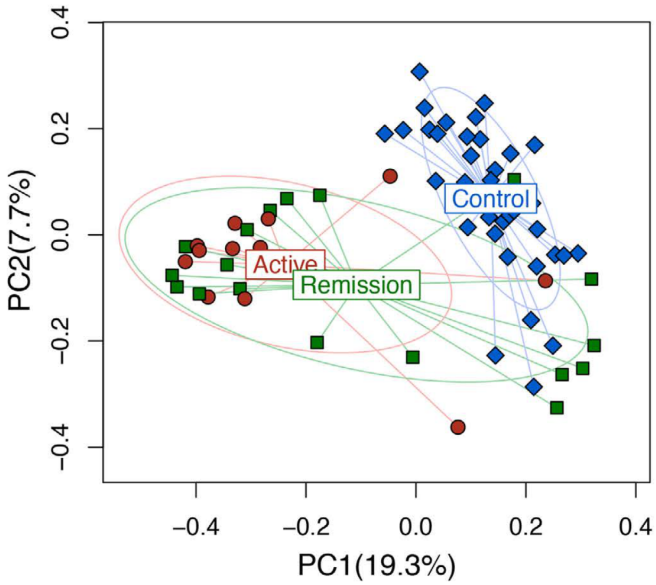

Fig. 1.7 **Patients with relapsing-remitting MS have a distinct microbiome.** Principal coordinate plot demonstrating how the microbiome of MS patients with an active relapse (red) clusters apart from healthy controls (blue). Patients currently in remission (green) have a more heterogeneous microbiome that shows similarities with both groups. *Adapted from Chen et al., 2016.*

Two lines of technological advancement have been particularly useful in developing our understanding of these interactions. Firstly, the advent of "-omics" techniques and related bioinformatic pipelines have revolutionised our ability to observe and characterise the microbiota (van Baarlen et al., 2013). Whereas our knowledge was previously limited to microbes that could be cultured and how they behaved outside the body, sequencing our commensal "metagenome" has revealed the true diversity and complexity of the microbiota (Eckburg et al., 2005). Such approaches have shown us that the microbiome can change substantially in disease. Various studies have shown that MS patients have a distinct microbiome compared to healthy controls (Fig. 1.7), for example they show reduced levels of certain *Firmicutes* species and other butyrate-producing organisms (Chen et al., 2016; Jhangi et al., 2014; Mowry et al., 2012). Interestingly, patients in remission appear to form a heterogeneous group, with patients' microbiomes showing similarities to either active disease states or healthy controls (Fig. 1.7, Chen et al. (2016)). Whether this reflects a gradual return to normal following a previous relapse, or a prodromal change preceding a future

episode is not clear from the current literature. As such, longitudinal studies following the microbiomes of a patient cohort through relapses and remissions would be informative as to the potential for using the microbiota as a biomarker for early detection of relapses. The microbiome also changes with ageing, and the abundance of different microbes can be used as predictors of health within an elderly population (Claesson et al., 2012). However, whilst these technologies flag up interesting correlations, they cannot resolve whether changes on the microbiota are a cause or a symptom of disease in the host.

To investigate causation, another technology has been incredibly useful: gnotobiotic models. These are model organisms in which we know the exact composition of their microbiota. The "blank-canvas" is a fully germ-free organism, first conceptualised by Louis Pasteur in the 1880s, which allows studies of development, physiology and disease in the absence of microbes. Mammalian germ-free (GF) colonies are derived from a sterile caesarean section followed by careful husbandry in a sterile isolator, and the most widely studied are mice and rats (Bibiloni, 2012). On top of a GF background, an artificial microbiota can be introduced, as a reductionist means to look at causative roles of individual microbes. Whilst they have taught us much, gnotobiotic models have their limitations – for example the lack of microbes during development may lead to long-lasting changes which are not representative of human diseases of adulthood (Bibiloni, 2012). Thus, experiments are often contextualised with other, more translatable, methods of microbial manipulation – for example antibiotic treatment or administration of probiotics to conventional animals.

In combination, the advent of "big-data" observational techniques and animal models to investigate causation have revealed a multitude of host functions that depend on the microbiota. These include many aspects of the host immune system (Belkaid and Hand, 2014), metabolism (Boulangé et al., 2016) and behaviour (Mayer et al., 2014). Fascinating as this is from a pure biological perspective, the microbiota also offer an attractive therapeutic target. Our gut microbiome is easily accessible and can be effectively modulated using probiotics, which contain live microbial organisms, as well as prebiotics and antibiotics, which respectively promote and inhibit the growth of certain microbes (Scott et al., 2015). Probiotics have been used successfully to treat patients with irritable bowel syndrome (Moayyedi et al., 2010). Moreover, faecal microbiota transplantation (FMT) is now a commonplace treatment for *Clostridium difficile* infection (Aas et al., 2003). Experimental FMT has been shown capable of transferring systemic phenotypes between mice including obesity (Ridaura et al., 2013), anxiety (Collins et al., 2013) and indeed patterns of myelination (Gacias et al., 2016). Thus, the microbiota offer a relatively non-invasive route to influence diverse processes throughout the body.

1.3.2 The microbiota in CNS inflammation

There is now a well-established link between the microbiota and autoimmune demyelination in rodent models. Mice treated with oral, but not intraperitoneal antibiotics are resistant to developing EAE (Ochoa-Reparaz et al., 2009), as are GF mice (Berer et al., 2011; Lee et al., 2011). This is largely attributed to changes in the adaptive immune system, which is underdeveloped in GF mice (Belkaid and Hand, 2014). In particular, Th17 dysregulation is implicated in many autoimmune diseases, and this population is induced by the presence of segmented filamentous bacteria (SFB) in the gut (Ivanov et al., 2009). Colonisation of GF mice with SFB alone is permissive for the development of EAE (Lee et al., 2011). In contrast, other microbes have a protective effect in EAE, for example *Bacteroides fragilis*, which stimulates IL-10-producing T_{reg} cells via its capsular polysaccharide A (Ochoa-Reparaz et al., 2010).

However, the microbiota can also influence innate immune processes in the brain, which we have seen to be important for remyelination. This was elegantly demonstrated by Erny et al. (2015), in a comparison of microglia between adult GF and control specific-pathogen-free (SPF) mice. GF mice showed more numerous microglia, which were transcriptionally and morphologically immature compared to their SPF counterparts. In response to *in vivo* stimulation by LPS or viral challenge, GF microglia showed impaired activation. These changes were partially mimicked by antibiotic treatment, and partially reversed by colonisation in adulthood – suggesting that the microbiota is important both in microglia development, and in maintenance throughout adulthood. Single-cell RNA sequencing has revealed that microglia sequentially adopt different states reflecting their changing roles from development through to adulthood, and exposure to a microbiome is important for transition into their adult stage (Matcovitch-Natan et al., 2016).

The implications of microbial control of the brain's microglia has recently been shown in a model of Parkinson's disease (Sampson et al., 2016). Mice overexpressing the α-synuclein protein were rederived into GF conditions or fed antibiotics, both of which provided resistance to α-synuclein aggregation and the associated motor dysfunction. The protective effects involved reduced microglia activation, as microglia would normally respond to α-synuclein aggregates and in turn promote further aggregation in a positive feedback loop (Gao et al., 2011). Interestingly, FMT from Parkinson's disease patients resulted in more microglial activation, protein aggregation and motor dysfunction that FMT from healthy human controls (Sampson et al., 2016).

There has been much focus on the short-chain fatty acids (SCFAs) as a mediator between the microbiota and microglia (Fig. 1.8). These are small carboxylic acids, produced by bacterial fermentation of dietary fibre and the most abundantly produced are acetate, propionate

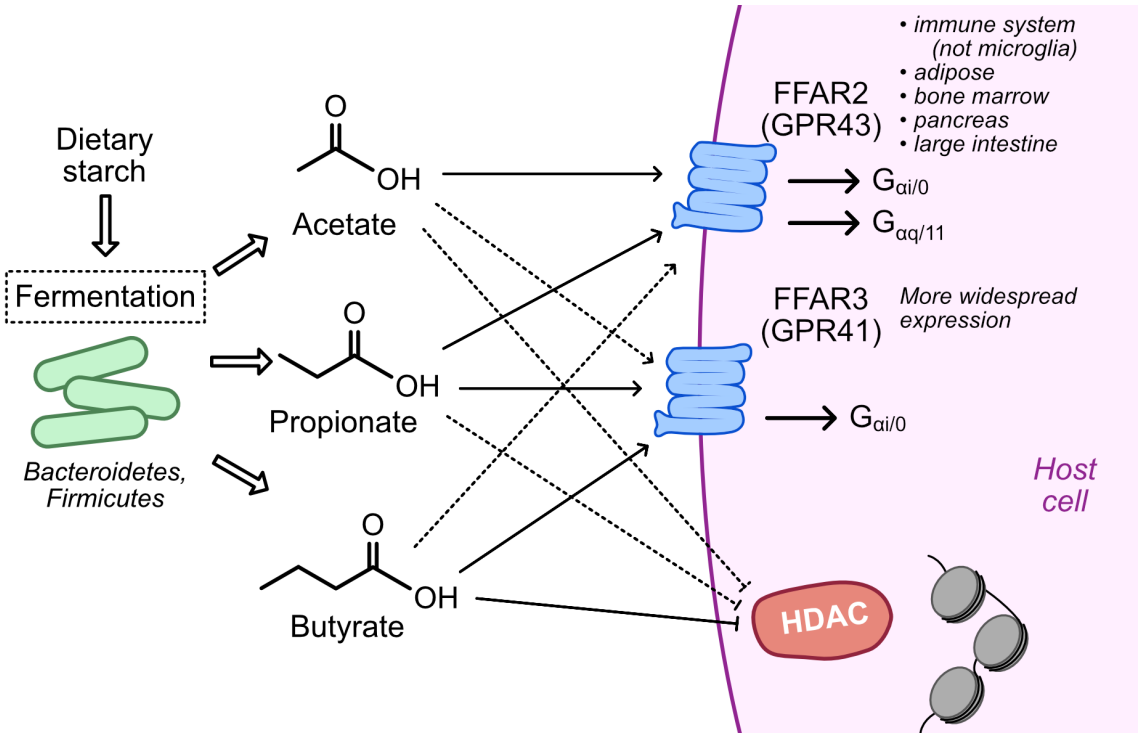

Fig. 1.8 **SCFA signalling from microbiota to host.** Various types of bacteria are able to produce the short chain fatty acids acetate, propionate and butyrate by fermentation of dietary fibre. This includes many members of the *Firmicutes* and *Bacteroidetes* phyla. SCFAs can travel around body and signal to host cells through GPCRs and inhibition of histone-deacetylase (HDAC). *Summarised from Besten et al., 2013.*

and butyrate (Vinolo et al., 2011). These small molecules can reach distant sites in the body and are known to signal to host cells through G-protein coupled receptors (GPCRs) and as inhibitors of histone deacetylation (Boffa et al., 1978; Brown et al., 2003; Maslowski et al., 2009). By feeding GF mice SCFAs, many of the microglial deficits can be restored (Erny et al., 2015) and resistance to α-synuclein pathology is lost (Sampson et al., 2016). The effect of SCFAs on microglia seemed to depend on signalling through the GPCR FFAR2, which is in fact not expressed by microglia themselves (Erny et al., 2015). Thus, it is likely that SCFAs can have indirect effects on the CNS, perhaps through signalling to peripheral immune cells.

As we saw, following demyelination microglia are supplemented by macrophages that arise from infiltrating monocytes, and this second population can be pivotal for the outcome of remyelination (Ruckh et al., 2012). Circulating microbial products such as TLR ligands also drive the emigration of monocytes from the bone marrow into the blood (Shi et al., 2011). This phenomenon was recently shown to impact on neurogenesis in the adult hippocampus, which itself is regulated by cells of the immune system (Möhle et al., 2016; Shi et al.,

2011). Following antibiotic treatment, mice had fewer Ly6C^{hi} monocytes in the CNS and fewer proliferating neural progenitor cells in the hippocampus (Möhle et al., 2016). These changes were rescued by treatment with the probiotic VSL#3 or adoptive transfer of monocytes. Intriguingly, in another study which used GF rather than antibiotics-treated mice, hippocampal neurogenesis was *increased* compared to controls (Ogbonnaya et al., 2015). This points towards the importance of reconciling results from different model systems and recognising the strengths and limitations of each. This disparity could have resulted from effects in different developmental windows, varying antibiotic sensitivity between microbial species or off-target effects of antibiotic treatment.

1.3.3 The microbiota can influence CNS myelination

Besides these effects on inflammation in the CNS, the microbiota also appear to influence myelin directly, through mechanisms that are apparently independent of the immune system. GF mice are hypermyelinated in the prefrontal cortex (PFC), with upregulation of myelin-associated genes and thicker myelin sheaths seen by electron microscopy (Hoban et al., 2016). This phenomenon was not seen outside the PFC, and might involve myelin plasticity in response to heightened electrical activity within this region in GF mice. In contrast, a PFC *hypo*myelination phenotype could be transferred by FMT from vehicle-gavaged non-obese diabetic (NOD) mouse donors to C57BL/6 recipients (Gacias et al., 2016). This was associated changes in microbial metabolites in the recipient's gut, including increased levels of cresol, which was shown to impair OPC differentiation *in vitro*.

1.3.4 The microbiota can influence CNS injury and resolution

A role of the microbiota, and subsequent changes in the immune system have been implicated in several other paradigms of CNS injury and repair. In a model of ischaemic stroke, in which the middle cerebral artery was temporarily occluded, mice treated with the antibiotic amoxicillin-clavulanic acid had a reduced infarct size and less decline in sensorimotor function (Benakis et al., 2016). Antibiotic treatment was associated with increased induction of T_{reg} cells in the gut, which might prevent $\gamma\delta$ T cells from trafficking to the meninges and releasing pro-inflammatory cytokines such as IL-17. This illustrates an example of how the microbiota may modulate CNS inflammation indirectly, mediated via local immune cells in the gut. The exact antibiotic regime appears to be important, as another study with a broader spectrum treatment observed a worse outcome in a similar ischaemia model (Winek et al., 2016). This suggests that, as we have seen elsewhere, different bacterial species could have opposing effects on processes in the CNS.

Another disabling acute neurological injury is spinal cord contusion (bruising) and Kigerl et al. (2016) showed a bidirectional interaction between the microbiota and spinal cord contusion in mice. Injured mice exhibited changes in their microbiota and a more permeable gut, with translocation of bacteria to the blood, liver and spleen. In the opposite direction, antibiotics-treated mice had more severe neurological impairment and spinal cord pathology associated with increased numbers of macrophages/microglia, B cells and CD8+ T cells. Administering mice the probiotic VSL#3 could improve pathology and functional recovery in the same model.

These examples are consistent with roles for the microbiota in injury and successful regeneration in other tissues outside the CNS. Examples include enhanced skin wound resolution in GF mice (Canesso et al., 2014), a role for bacterial LPS in promoting liver regeneration (Cornell et al., 1990) and an effect of Gram-positive bacteria on the bone marrow haematopoietic niche (Luo et al., 2015). All of these cases involve the sensing of microbe-derived molecules by components of the immune system. There is therefore a large evidence base to warrant studies into an influence of the microbiota on the immune response to demyelination and subsequent remyelination in the CNS.

1.4 Summary and aims

In summary, there are several potential routes by which the microbiota might impact upon CNS remyelination (Figure 1.9). I have investigated this hypothesis by studying remyelination in mice following a range of interventions to alter the microbiome: antibiotic treatment (Chapter 3), germ-free mice (Chapter 4) and probiotic treatment (Chapter 5).

The aims of this project were as follows:

1. Characterise how the microbiota can alter inflammatory responses to demyelination in the CNS
2. Determine whether the microbiota can influence OPC responses and remyelination
3. Explore the microbiome-brain axis as a candidate therapy to enhance remyelination.

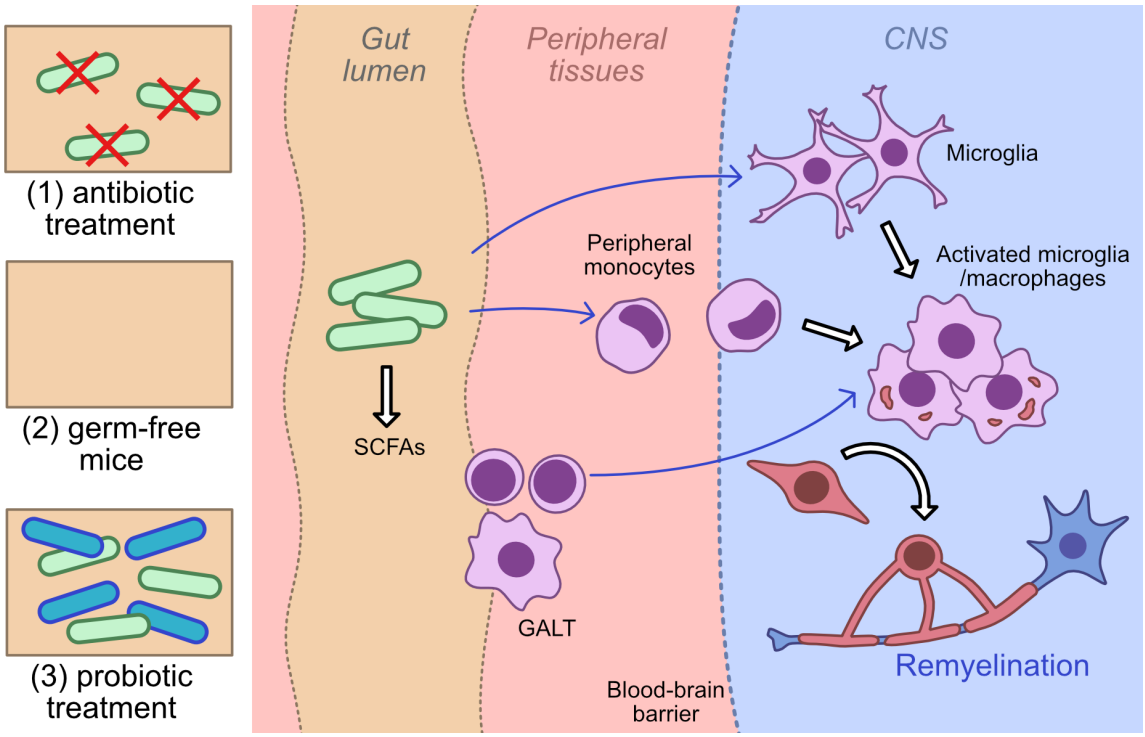

Fig. 1.9 **How the microbiota might influence remyelination.** GALT, gut-associated lymphoid tissue; SCFAs, short chain fatty acids; BBB, blood-brain barrier.

Chapter 2

Materials and methods

2.1 Animal models of demyelination

All animal work was performed using C57BL/6 mice and complied with the requirements and regulations of the United Kingdom Home Office. The antibiotics study (Chapter 3) was conducted at Queen's University, Belfast, with input from Ofra Zidon, Denise Fitzgerald, Markus Heimesaat, Yvonne Dombrowski, Rosana Penalva and John Falconer, and I carried out the histological analysis in Cambridge. The germ-free study (Chapter 4) was performed at the University of East Anglia in cooperation with Arlaine Brion and Andrew Goldson, who provided careful husbandry of the gnotobiotic mice. The probiotic study (Chapter 5) was carried out at the University of Cambridge with surgical assistance from Ginez Gonzalez and Alerie Guzmann and much help from Jon Lock and Chris Brown in administering the gavage treatment. Robin Franklin and Chao Zhao both provided expert advice on these models throughout.

2.1.1 Induction of demyelination by injection of lysolecithin into the spinal cord

C57BL/6 mice were anaesthetised by inhalation of 2-3% isoflurane in oxygen. Once unconscious, each animal received $0.05\,\mathrm{mg\,kg^{-1}}$ subcutaneous buprenorphine (Vetergesic, Animalcare Ltd.) as analgaesia, and the thoraco-lumbar area of the back was shaved and cleaned using chlorhexidine gluconate. The mouse was placed on a heat pad, and rectal temperature monitored and maintained at 37 °C throughout the procedure.

A 0.5 cm midline incision was made in the thoraco-lumbar region and the subcutaneous tissue cut away to expose the muscle layer. Under a dissection microscope, an intervertebral space was located using a pair of fine-toothed forceps. These forceps were then used to

carefully remove the muscle and ligament to reach the surface of the spinal cord. At this point, the soft tissue rostral to this area was clamped to a stand using a pair of curved mosquito forceps to minimise movement of the injection site from breathing. A bevelled 30G dental needle was used to open the dura close to the central vein on the right hand side. Through this gap in the dura, a glass-tipped Hamilton syringe, filled with sterile 1% lysolecithin (Sigma L4129) in phosphate-buffered saline (PBS) and connected to a 3-way manipulator, was advanced at a 70° angle relative to horizontal.

In total, 1 µl 1% lysolecithin was injected into the ventral white matter of the spinal cord. First, the ventral edge of the spinal cord was located by finding the point at which the needle deflected on the vertebral body. At this point, 0.5 µl were injected over the course of 20 seconds. The tip of the needle was then withdrawn by 0.25 mm, and another 0.5 µl injected. The needle was then kept in place for 1 minute before withdrawal. Finally, the wound was closed with 3-4 cutaneous sutures (6-0 Ethilon) and the mouse was transferred to a warm chamber for recovery.

2.1.2 Induction of demyelination by dietary administration of cuprizone

Cuprizone diet was produced by SDS (RM3(P) + 0.2% cuprizone) and received 50 kGy irradiation to sterilise it for use in a gnotobiotic isolator. Mice were given the cuprizone diet instead of their standard chow for 5 weeks, then returned to standard chow for a period of 2 weeks afterwards. Cuprizone diet was stored sealed at 4 °C and replaced every 2-3 days during administration. Mouse weights were also monitored every 2-3 days.

2.1.3 Choice of timepoints for lesion models

Timepoints were selected in discussion with Robin Franklin and Chao Zhao based on their previous work and other published literature on lysolecithin (Keough et al., 2015; Miron et al., 2013; Natrajan et al., 2015; Ruckh et al., 2012) and cuprizone (Gudi et al., 2014; Lampron et al., 2015; Praet et al., 2014; Steelman et al., 2012).

For lysolecithin lesions in antibiotics-treated mice (Chapter 3), 7 days postlesion (dpl) was chosen as a timepoint at which the OPC pool is expanding and differentiation has not yet occured, whereas 14dpl was selected to observe OPC differentiation into new oligodendrocytes. Given the lack of difference in OPC proliferation at 7dpl after antibiotics treatment, a 5dpl timepoint was chosen instead of 7dpl for the probiotic experiment (Chapter 5), to observe an earlier stage in the onset of inflammation. This study also had a later, 21dpl timepoint to look for differences in remyelination in semi-thin resin sections.

For cuprizone administration to germ-free mice (Chapter 4), 5 weeks 0.2% cuprizone treatment was selected as a timepoint by which near-complete demyelination normally occurs, and by 2 weeks later (on regular diet), remyelination is typically under way but not complete.

2.1.4 Perfusion fixation

To perfuse CNS tissue for histology, mice were sacrificed by perfusion fixation. Mice received a terminal intraperitoneal dose of 100 µl pentobarbitone sodium (Pentoject, Animalcare Ltd.) and absence of reflexes was confirmed. The mouse was pinned to a dissection board, the skin was opened over the thorax and the ribs cut laterally to expose the heart. At this point, any necessary fresh tissue was taken. 100-200 µl blood was collected from the left ventricle. Fresh gut tissue for flow cytometry was dissected by making a small abdominal incision then ligating and removing a loop of bowel from proximal jejunum to distal colon.

After collection of fresh tissue, a cold (4 °C) fixative solution was infused into the left ventricle and an incision made in the right atrial wall. This was applied at 13 rpm for 5 minutes. The perfusion solution was either:

- 4% paraformaldehyde (PFA) in PBS, pH 7.4: for immunohistochemistry
- 4% glutaraldehyde in PBS + 10 mM $MgCl_2$, pH 7.4: for resin embedding

Brain or spinal cord was then dissected and post-fixed in the same solution. PFA-fixed tissue was post-fixed for 4-6 hours at 4 °C, whilst glutaraldehyde-fixed tissue was post-fixed at least 24 hours at 4 °C.

2.2 CNS Tissue Processing

2.2.1 CNS tissue sectioning

To produce cryosections for immunohistochemistry, PFA-fixed tissue was cryoprotected by transferring to 20% sucrose in PBS overnight at 4 °C. The following morning, the tissue was rapidly frozen in OCT media (Ted Pella Inc.) in moulds on dry ice. 12 µm sections were collected using a cryostat (Bright Instruments Ltd.) onto Superfrost slides (VWR), with 3-4 sections per slide separated longitudinally by >100 µm. For spinal cord lesions, transverse sections were taken throughout the core of the lesion. For cuprizone-induced lesions, coronal sections of the left hemisphere were taken from bregma −1.5 to −2.0 mm. Slides were dried and stored at −80 °C.

To produce semi-thin resin sections for toluidine blue staining, glutaraldehyde-fixed tissue was dissected into pieces of maximum 1 mm thickness and stained with 2% osmium tetroxide overnight at 4 °C. Sections were then washed 3 times with water and dehydrated over the course of 1 hour with an ethanol gradient (75%-90%-100%). Ethanol was then removed by incubating in propylene oxide (BDH Merck) for 20 minutes. Following this, tissue was incubated for 6 hours with a 50:50 mix of propylene oxide and TAAB resin (TAAB Laboratories Equipment Ltd.), then 3 x 12 hours in 100% resin. After this, tissue was mounted in resin using plastic moulds, and incubated at 60 °C overnight to polymerise the resin. 0.75 µm sections were cut from these blocks using a microtome (Leica RM 2065) and collected onto a slide floating on water. The slides were heated on a hot plate until the water was removed, then alkaline toluidine blue was applied for 30 seconds before washing off with tap water. I am grateful to Michal Presz for his microtome assistance.

2.2.2 Immunohistochemistry

Cryosections on glass slides were brought to room temperature (RT) and allowed to dry for 30 minutes. These were rehydrated with PBS, prior to an antigen retrieval step, consisting of a 10 minute RT incubation with boiling 1x antigen retrieval solution (Dako). Slides were washed three times with PBS, and blocked for 1 hour with 5% Normal Donkey Serum (NDS, Sigma) and 0.3% triton X-100 in PBS. Sections were then incubated with primary antibodies (Table 2.1) diluted in blocking solution in a humidity chamber overnight at 4 °C. Following primary antibody incubation, slides were washed three times with PBS and incubated with relevant fluorophore-conjugated secondary antibodies (Table 2.2) diluted in blocking solution for 2 hours at RT and protected from light. Nucleic acids were stained by 10 minutes incubation with 1 µg ml^{-1} Hoechst. After three more PBS washes, sections were washed with water then mounted using Fluoromount-G (SouthernBiotech) with glass coverslips (VWR).

Where mouse-derived primary antibodies were to be used on mouse tissue, an additional blocking step was introduced before applying primaries to reduce noise from endogenous mouse immunoglobulins. This consisted of 1 hour in M.O.M. Mouse Ig Blocking Reagent (Vector), diluted in PBS according the manufacturer's instructions. Primaries were applied in a dilution of M.O.M. Protein Concentrate (Vector), and subsequent steps were as outlined above.

Fluorescently immunolabelled sections were imaged using a Leica-SP5 confocal microscope with *LAS* software (Leica). Z-stacks were collected with images 3 µm apart, spanning the section width, with either a 20x or 40x lens.

Antigen	Species	Manufacturer	Cat. Number	Dilution
In vivo				
Arg1	Goat	Santa Cruz	sc-18351	1:200
CC1	Mouse	Calbiochem	OP80	1:100
CD68	Rabbit	Abcam	ab125212	1:500
CD68	Rat	Serotec	MCA1957	1:200
dMBP	Rabbit	Millipore	AB5864	1:500
GFAP	Chicken	Abcam	ab4674	1:1000
Iba1	Goat	Abcam	ab5076	1:200
Iba1	Rabbit	Wako	019-19741	1:500
iNOS	Rabbit	Abcam	ab136918	1:200
Ki67	Rabbit	Abcam	ab15580	1:300
MBP	Rat	Serotec	MCA409S	1:500
MHCII	Rat	eBioscience	14-5321-82	1:500
MR	Goat	R&D Systems	AF2535	1:500
NF	Rabbit	Abcam	ab8135	1:500
Olig2	Rabbit	Millipore	AB9610	1:500
Sox10	Goat	Santa Cruz	sc-17342	1:200
In vitro				
CD11b	Mouse	Serotec	MCA275R	1:300
CNPase	Mouse	Abcam	ab6319	1:500
MBP	Rat	Serotec	MCA409S	1:500
Olig2	Rabbit	Millipore	AB9610	1:500

Table 2.1 **Primary antibodies used for immunohistochemistry and immunocytochemistry.**

Species	Manufacturer	Cat. Number	Dilution
Alexa 488 donkey anti-mouse	Invitrogen	A21202	1:500
Alexa 488 donkey anti-rabbit	Invitrogen	A21206	1:500
Alexa 488 donkey anti-rat	Invitrogen	A21208	1:500
Alexa 568 donkey anti-goat	Invitrogen	A11057	1:500
Alexa 568 donkey anti-mouse	Invitrogen	A10037	1:500
Alexa 568 donkey anti-rabbit	Invitrogen	A10042	1:500
Alexa 594 goat anti-chicken	Stratech	703-585-155-JIR	1:500
Alexa 647 donkey anti-mouse	Invitrogen	A31571	1:500
Alexa 647 donkey anti-rabbit	Invitrogen	A31573	1:500

Table 2.2 **Secondary antibodies used for immunohistochemistry and immunocytochemistry.**

2.2.3 Osmium tetroxide staining

Cryosections on glass slides were brought to RT and allowed to dry for 30 minutes, rehydrated with PBS, then post-fixed with 2% glutaraldehyde in PBS for 1 hour. After two PBS washes, sections were then stained with (0.1%) osmium tetroxide (OsO_4) for 45 minutes RT. Following this, sections were washed with PBS, then water, then dehydrated with an ethanol gradient (50%-70%-90%-95%-100%) followed by xylene. These were then mounted using DPX (Sigma) with glass coverslips (VWR). Images of these OsO_4-stained sections were acquired at 10x with a Nikon Eclipse E400 microscope.

2.3 Processing of peripheral tissues

2.3.1 Faecal PCR

Fresh faecal pellets were collected from mice and stored in sterile Eppendorf tubes at −80 °C. To confirm the presence or absence of a bacterial microbiota, DNA was isolated from the pellets using a QIAamp DNA Stool Mini Kit (Qiagen) following the manufacturer's instructions. 1 µl eluted DNA was added to 24 µl PCR SuperMix (Thermo Fisher) with 200 nM UniF/R primer pairs (Packey et al., 2013), which recognise a 147bp conserved region of bacterial 16S rRNA. The conditions for the polymerase chain reaction (PCR) were 95 °C for 5 minutes, then 25 cycles of 95 °C for 30 s, 52 °C for 30 s and 72 °C for 45 s, and finally 72 °C for 7 minutes. The PCR products were then separated on a 1% agarose gel, and visualised under UV light.

2.3.2 Detection of faecal / serum metabolites using GC-MS

Fresh faecal pellets were collected from mice and stored in sterile Eppendorf tubes at −80 °C, as for PCR. Serum samples were obtained from 100-200 µl left ventricular blood collected prior to perfusion. The blood samples were incubated in sterile Eppendorf tubes for 1 hour at RT to allow coagulation, then separated by centrifugation for 15 minutes at 1500 g. Serum was collected and stored at −80 °C.

Concentrations of short chain fatty acids (SCFAs) were investigated by gas chromatography-mass spectrometry (GC-MS) with the assistance of Fynn Krause in the Department of Biochemistry, using a protocol he derived. All reagents were of HPLC-grade. For faecal samples, 15 to 25 mg of faeces was placed in a pre-chilled 2 ml plastic tube, and 150 µl of an ice-cold 2:1 v/v methanol:chloroform mixture was added, followed by 30 ul of 130 µM norvaline as an internal standard. Samples were then homogenised by vortex and sonication, after

which phase separation was initiated by adding 100 µl ice-cold chloroform and 100 µl water, vortexing and 20 minutes centrifugation at 15 871 g. 150 µl of the aqueous fraction was transferred to a pre-chilled glass tube, the extraction was repeated and both aqueous phases combined.

For serum samples, 20 µl of sample were placed in pre-chilled 1.5 ml plastic tube, and 150 µl of an ice-cold 2:1 v/v methanol:chloroform mixture was added, followed by 30 ul of 130 µM norvaline as an internal standard. Samples were vortexed, after which phase separation was initiated by adding 100 µl ice-cold chloroform and 50 µl water, vortexing and 20 minutes centrifugation at 50 g. 100 µl of the aqueous fraction was transferred to a pre-chilled glass tube.

For both sets of samples, after drying the extracts under nitrogen stream at $-4\,^{\circ}\mathrm{C}$, the samples were reconstituted in 30 µl of 20 $\mathrm{mg\,ml^{-1}}$ methoxyamine hydrochloride in pyridine and incubated at for 16 hours at RT. Samples were derivatised by addition of 30 µl MSTFA (*N*-Methyl-*N*-(trimethylsilyl) trifluoroacetamide), and after one hour at RT 50 µl of the derivatised sample was transferred to a new glass vial and diluted with 50 µl hexane.

Purified samples were analysed on a Thermo Trace GC Ultra coupled to an Thermo DSQ II. 2 ml sample was injected. The oven temperature was increased from 70 to 130 °C at 10 °C/min, then to 230 °C at 5 °C/min, and finally to 320 °C at 20 °C/min and held for 5 minutes. The MS was operated in positive ion mode from 4 to 35 minutes at a scan rate of 3.0030 scans/s and 1927.3 amu/s, over a mass range of 50 to 650. Data processing was carried out using the *Xcalibur* software (Thermo) and the *National Institute of Standards and Technology (NIST)* library. Concentrations were calculated based on the peak areas from the known concentration of norvaline, and adjusted to the original quantity of sample.

2.3.3 Flow cytometry of gut lymphoid tissue

In the probiotics study, a loop of gut from proximal jejunum to distal colon was ligated and removed prior to perfusion fixation. 4-6 Peyer's patches (PPs) and the mesenteric lymph nodes (MLNs) were harvested and transferred into HALF (Appendix A.3) with 1:100 penicillin-streptomycin (Sigma) at 4 °C, and all subsequent steps were carried out at this temperature unless otherwise specified. Populations of immune cells were interrogated using a flow cytometry protocol developed by Dan Ma. The tissue was homogenised by grinding between the frosted parts of two sterilised microscope slides and then passed through a 70 µm filter (Millipore). Samples were centrifuged for 5 minutes at 350 g and pellets of single cells were then resuspended at 1×10^7 cells/ml in Cell Staining Buffer (BioLegend).

Next, 100 µl suspension, containing 1×10^6 cells was incubated for 10 minutes with 2 µl TruStain FcX (BioLegend) to block Fc receptors. Fluorescently-conjugated antibodies

were then added to the tubes at the dilutions indicated in Table 2.3, and incubated in the dark for 30 minutes. After primary incubation cells were washed twice by resuspension in 1.8 ml Cell Staining Buffer and 5 minutes 350 g centrifugations. To fix the cells, pellets were then resuspended in 500 µl Fixation Buffer (BioLegend) and incubated in the dark at RT for 20 minutes. As Foxp3 is an intracellular antigen, this was stained after fixation and a permeabilisation step in which cells were washed twice with 2 ml Intracellular Staining Permeabilization Wash Buffer (BioLegend). The Foxp3 antibody was then incubated with cells in 100 µl for 30 minutes at RT (Table 2.3), followed by two washes with 2 ml of the Intracellular Staining Permeabilization Wash Buffer. Finally, cells were resuspended in 500 µl Cell Staining Buffer for flow cytometry. Unstained and single-stained controls were subject to an identical protocol with the relevant antibodies omitted. Samples were run on an Attune NxT (Thermo Fisher), with subsequent analysis using *FlowJo 10* software.

Antigen	Fluorophore	Manufacturer	Cat. Number	Dilution
B220	Pacific blue	BioLegend	103230	1:50
CD11c	PE/Cy7	BioLegend	117317	1:100
CD3	AF-594	BioLegend	100240	1:200
CD4	PE/Cy7	BioLegend	100527	1:100
CD45	PerCP/Cy5.5	BioLegend	103131	1:80
Foxp3	AF-488	BioLegend	126409	1:50

Table 2.3 **Antibodies used for flow cytometry.**

2.4 Cell culture

2.4.1 Myelin debris isolation

Myelin debris was purified from the brains of young adult C57BL/6 mice (age 2-3 months), using discontinuous sucrose gradient centrifugation. Mice were sacrificed by cervical dislocation and brains were homogenised on ice in 0.32 M sucrose, layered over 0.85 M sucrose in an Ultra-Clear centrifuge tube (Beckman) and spun for 30 minutes at 75 000 g at 4 °C. Crude myelin was then collected from the interface and homogenised in ddH_2O for osmotic disintegration, before centrifuging for 10 minutes at 12 000 g at 4 °C. The sucrose gradient centrifugation was then repeated to increase the purity of the myelin, followed by another osmotic disintegration step with a spin for 15 minutes at 75 000 g, 4 °C. Finally, the pellet was resuspend in PBS and the concentration of the protein component quantified using a Pierce BCA Protein Assay Kit (Thermo Fisher). Aliquots were stored at −80 °C.

2.4.2 Microglia isolation and culture

Microglia were isolated from P6-8 C57/B6 mouse pups using a Magnetic-Activated Cell Sorting (MACS) protocol. Pups were euthenised by overdose of Pentoject (Animalcare Ltd.) and their brains transferred to ice-cold HALF (Appendix A.3). Brains from 2-3 pups were pooled per replicate. Tissue was diced into small pieces ($<1\,\mathrm{mm}^3$) using a scalpel and washed once with HBSS-- (without Ca^{++} or Mg^{++}), followed by 1 minute centrifugation at 100 g. Tissue was then incubated at 37 °C on a 50 rpm shaker for 30 minutes in a dissociation solution, consisting of 34 U/ml papain (Worthington) and $20\,\mu\mathrm{g\,ml}^{-1}$ DNAse (Gibco) in HALF.

Following this incubation, tissue was washed with HBSS--, centrifuged (5 minutes, 200 g) then resuspended in HALF supplemented with 2% B27 (Thermo Fisher), 500 µM *N*-acetylcysteine (NAC, Sigma) and 1 mM sodium pyruvate (Gibco). Tissue was then triturated using a 5 ml serological pipette and twice more with fire-polished glass pipettes. After each round or trituration, the tissue was allowed to settle and supernatant containing single cells was collected. Supernatant was passed through a 70 µm cell strainer (Millipore) and suspended in DMEM/F12 (Gibco) with isotonic Percoll (90% Percoll (GE Healthcare) in 10x PBS pH7.2 (Lifetech)) to give a final Percoll concentration of 22.5%. This tube was then centrifuged for 20 mins at 800 g, RT to separate single cells from acellular debris based on density. Following this, single cells were washed with HBSS-- and centrifuged for 5 minutes at 300 g.

Next, cells were labelled with magnetic bead-conjugated antibodies for CD11b (Miltenyi Biotec). 1×10^6 cells were incubated at 4 °C for 15 minutes with 5 µl CD11b-beads in 95 µl modified Miltenyi Wash Buffer (MWB, Appendix A.4). After this, cells were washed once with MWB, centrifuged for 5 minutes at 300 g and resuspended in 500 µl MWB. MACS was performed according to the manufacturer's recommendations. Briefly, an MS column (Miltenyi Biotec) was held in a magnets and washed with 500 µl MWB. The labelled cells were then run through the column and washed the 1.5 ml MWB. Finally, the column was removed from the magnetic field and CD11b+ microglia were eluted in pre-warmed microglia medium containing 10% fetal bovine serum (FBS, Biosera) (Appendix A.1).

96-well clear bottom black microplates (Corning) were coated in advance by incubating with $5\,\mu\mathrm{g\,ml}^{-1}$ poly-D-lysine (Sigma) for 1 hour at 37 °C then washed 3 times with water. Eluted microglia were plated at a density of 10 000 cells per well in 100 µl microglia medium. By 48 hours, microglia had adhered and adopted a ramified morphology, indicating recovery from the stress of isolation. At this point, treatments were applied and the medium was changed to a serum-free formulation, Macrophage-SFM (Thermo Fisher), to reduce the effects of serum-derived factors, to which microglia are not normally exposed *in vivo*.

Microglia were incubated with the treatments for 48 hours, which is sufficient time for minocycline - a known immunomodulatory antibiotic - and for other HDAC-inhibitors to have effects on cultured microglia (Kannan et al., 2013; Kobayashi et al., 2013). Following treatments, the myelin debris assay was carried out, in which 10 µg ml^{-1} myelin debris was added to the wells and incubated with the cells for 4 hours. A pilot study showed that this combination of concentration and timepoint, phagocytosis would have just been completed in untreated microglia, thus any deficit in phagocytosis should be detected (Fig. 2.1). Following the phagocytosis assay, uninternalised myelin debris was removed by washing with cold PBS, and cells were fixed by 10 minutes incubation in 4% PFA at RT.

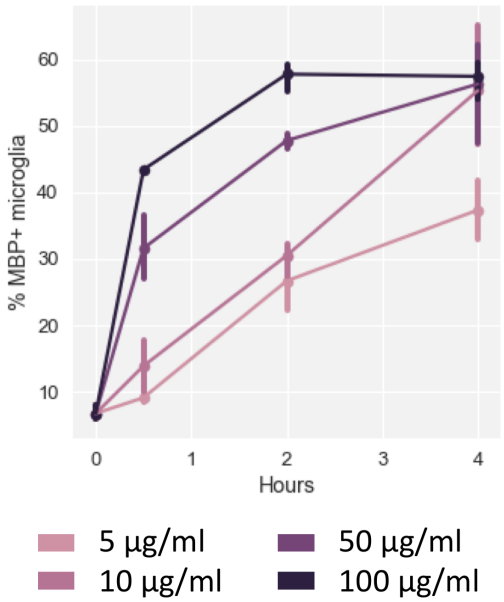

Fig. 2.1 **Myelin debris phagocytosis pilot study.** Microglial phagocytosis of myelin over time was measured for different concentrations of myelin debris, identifying 10 µg ml^{-1} for 4 hours as a regime at which any deficit in myelin phagocytosis would be apparent. Error bars show ± SEM. MBP, myelin basic protein.

2.4.3 OPC isolation and culture

OPCs were isolated from P6-8 C57/B6 mouse pups using a MACS protocol. This was identical to the microglia protocol until the labelling stage. Instead of CD11b-beads, OPCs were detected using an antibody for A2B5, mouse-anti-rat-A2B5-IgM (RD systems).

Following the 22.5% Percoll centrifugation step, single cells were resuspended in 500 µl MWB per 1×10^7 cells and incubated at 4 °C for 25 minutes with 1:250 anti-A2B5. Cells were then washed with MWB, centrifuged for 5 minutes at 300 g and resuspended in 80 µl MWB per 1×10^7 cells. To this, 20 µl of a magnetic bead-coupled goat-anti-mouse-IgM antibody (Miltenyi Biotec) was added, and incubated at 4 °C for 15 minutes. MACS was then performed as described for microglia, but with the final elution of A2B5+ OPCs into OPC medium (Appendix A.2).

96-well clear bottom black microplates (Corning) were precoated overnight with poly-L-ornithine (Sigma) at 37 °C, washed three times with water, then incubated for 3 hours with laminin 1:250 in HBSS++ (with Ca^{++} and Mg^{++}) and washed twice with HBSS++ before use. Eluted OPCs were plated at a density of 7500 cells per well in 100 µl OPC medium, with 10 ng ml^{-1} each of PDGF-AA and FGF-basic (both recombinant human, Preprotech). The timecourse for OPC treatments *in vitro* was based on assays established in the Franklin lab that can successfully show either enhancement or impairment of OPC proliferation or differentiation. After 24 hours, treatments were added and medium was changed to differentiation conditions, without growth factors and with 40 ng ml^{-1} triiodothyronine (T3, Sigma). This was maintained for 8 days, with media changed and treatments replaced on days 4 and 7. Cells were then incubated with 10 µM 5-ethynyl-2'-deoxyuridine (EdU) for 4 hours to label proliferating cells, washed with PBS and finally fixed by 10 minutes incubation in 4% PFA at RT.

2.4.4 Cell treatments

For short chain fatty acid (SCFA) treatments *in vitro*, sodium acetate, sodium propionate and sodium butyrate (all Sigma) were dissolved in PBS as 1 M stocks and aliquots stored at −80 °C.

To apply antibiotics treatments at doses equivalent to *in vivo* exposure, steady state plasma concentrations ($C_{ss(P)}$) were estimated for each antibiotic administered to mice in their drinking water (Chapter 3). These estimations were based on literature values of oral bioavailability (F), clearance (CL), and area-under-the-curve ratio of cerebrospinal fluid (CSF) to plasma (AUC_{CSF}/AUC_P), for ampicillin and sulbactam (English et al., 1984; Foulds et al., 1987; Liu et al., 1990), ciprofloxacin (Drusano et al., 1986; Nau et al., 2010; Vallee et al., 1992) and metronidazole (Al-Dabagh and Mohammad, 2008; Lau et al., 1992; Nau et al., 2010) (Table 2.4). Daily water consumption was assumed to be 4 ml/day/mouse, and estimated $C_{ss(P)}$ was calculated using the equation:

$$C_{ss} = \frac{F \times dose\ rate}{CL}$$

All antibiotics for *in vitro* studies were purchased from Sigma.

Drug	Orally absorbed?	Conc. in drinking water ($mg l^{-1}$)	Dose rate (mg/day)	F	CL (ml/min)	AUC_{CSF} $/AUC_P$	$C_{ss(P)}$ ($ng ml^{-1}$)	$C_{ss(CNS)}$ ($ng ml^{-1}$)
Ampicillin	✓	1000	4.0	0.23	1.8	0.39*	360	140
Sulbactam	✓	500	2.0	0.19	3.9	0.34*	68	23
Ciprofloxacin	✓	200	0.8	0.7*	0.81	0.6*	480	290
Metronidazole	✓	1000	4.0	0.95*	0.068	0.87*	40000	34000
Imipenem	✗							0
Vancomycin	✗							0

Table 2.4 **Pharmacokinetics of antibiotics used to deplete the murine microbiota.** Asterisks denotes values extrapolated from human studies.

2.4.5 Immunocytochemistry

Fixed cells in 96-well plates were blocked for 1 hour with 5% NDS and 0.1% triton X-100 in PBS. For the cell proliferation assay, EdU was labelled at this point by 30 minutes incubation at RT with the Click-iT reaction cocktail from the Click-iT EdU Alexa Fluor 647 Imaging Kit (Thermo Fisher) before two PBS washes. Cells were then incubated with primary antibodies (Table 2.1) diluted in blocking solution overnight at 4 °C. Following primary antibody incubation, cells were washed three times with PBS and incubated with relevant fluorophore-conjugated secondary antibodies (Table 2.2) diluted in blocking solution for 1 hour at RT and protected from light. Nucleic acids were stained by 10 minutes incubation with $1\,\mu g\,ml^{-1}$ Hoechst (check source and stock conc), followed by three more PBS washes. Images were acquired automatically using an InCell2200 (GE-Healthcare).

2.5 Image analysis

2.5.1 Cell counting

All cell counts were automated using a combination of *Fiji*, *CellProfiler* and *CellProfiler Analyst* software, based on the pipeline outlined in Fig. 2.2. This employed a machine-learning approach, which reduced the time taken and removed any effects of human bias in the image analysis. The accuracy of each classifier was verified by comparison to manual counts in a random subset of images.

2.5.2 Cell morphology analysis

Cell morphology analysis was also carried out using *Fiji*, *CellProfiler* and *CellProfiler Analyst* software. First, microglia (Iba1+) or astrocytes (GFAP+) were identified using the supervised learning approach described (Fig. 2.2). The set of rules used by the classified

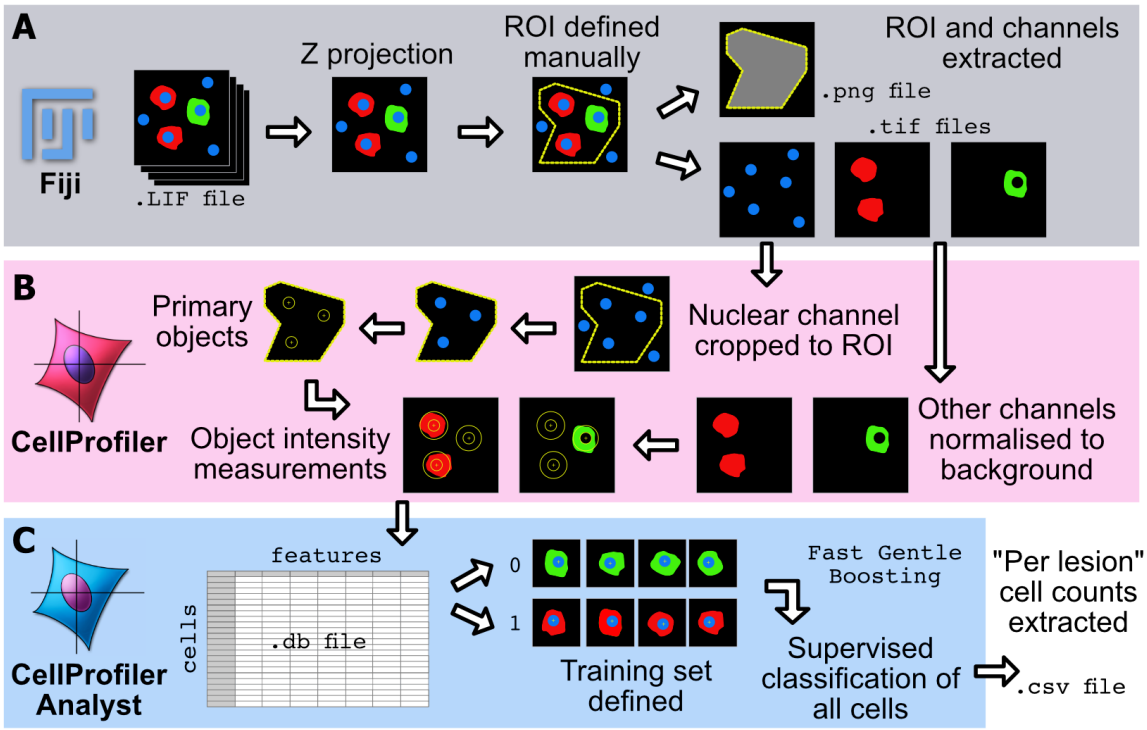

Fig. 2.2 **Pipeline for performing automated cell counting.** (A) *Fiji* software was used to create maximum projections of Z-stacks acquired by confocal microscopy. The region of interest (ROI e.g. the lesion area) was manually defined and individual channels extracted. (B) These images were imported into *CellProfiler*, where the nuclear channel (Hoechst) was cropped to the pre-defined region-of-interest (ROI), and nuclei were identified as primary objects. Other channels were normalised to the median backgroud intensity to correct for variability in staining. A number of intensity features were measured for the nuclear and peri-nuclear regions of each cell in every channel, and this data was exported as a master database file. (C) In *CellProfiler Analyst*, a training set of >50 cells was specified per group and used to train a classifier with a Fast Gentle Boosting algorithm, based on the featureset. The training data was increased until the classifier gave consistently comparable results to manual counting in sample images. Finally, "per lesion" cell counts were extracted for each image using this classifier.

were then exported, to allow identification of microglia and astrocytes within the *CellProfiler* pipeline. Two categories of morphological measurement were then derived from each cell:

- **cell mask measurements**, by propagation of a secondary object from the nucleus to the border of the cell using the relevant channel; including area, compactness, solidity, minor/major axis, perimeter etc.

- **cell skeleton measurements**, by skeletonisation of the relevant channel image and identifying neurites seeding from the nuclei; including number of trunks, number of branches, total process length etc.

2.5.3 Other image quantification

To quantify the area of a lesion occupied by myelin debris, images of tissue stained for MBP or dMBP were imported into a *CellProfiler* pipeline, which applied a threshold to each image determined by the background (median) staining. The area of the image above this threshold was considered positive for myelin debris, and was expressed as a fraction of the total lesion area.

To quantify the area of corpus callosum occupied by myelin (MBP+ or OsO_4+) or axons (NF+), blinded, randomised images were manually assigned a threshold for the respective stain using *Fiji*. The area of image above this threshold was expressed as a fraction of the total lesion area.

To quantify remyelination from toluidine blue-stained resin sections, slides were independently ranked by two experienced, blinded investigators (GG and CZ) according to the extent of remyelination. The assigned numerical ranks were used for subsequent statistical tests.

2.6 Statistical analysis

All statistical analysis was carried out using a *Jupyter* Notebook with *Python 2*. *In vivo* experiments were carried out once each, with the following numbers of biological replicates per group:

- **antibiotics lysolecithin study** (Chapter 3): n = 4-6
- **germ-free cuprizone study** (Chapter 4): n = 5
- **probiotic lysolecithin study** (Chapter 5): n = 3-5

These group sizes were chosen in discussion with Robin Franklin and Chao Zhao based on previous work, and were thought to be sufficiently powered to detect meaningful differences in the OPC response to demyelination. For *in vivo* cell counts, generally 3-4 technical replicate sections were counted and averaged per biological replicate. For *in vitro* cell assays, 3 technical replicate wells were averaged for each of 4 biological replicate studies.

Data was tested for normality of residuals (Kolmogorov-Smirnov test) and homogeneity of variance (Levene's test). Data sets passing both of these criteria were compared by

either Student's *t*-test (unpaired) (if two groups), or one-way ANOVA with Tukey HSD *post hoc* tests (if three or more groups). For *in vitro* assays, to reduce the effect of variability between replicates, results were quantified relative to an internal control. Treated conditions were then compared to this control using a one-sample *t*-test with H_0: $\mu = 100\%$, and p adjusted for multiple comparisons using the Holm-Bonferroni method. For ranking analysis of remyelination, groups were compared using the Mann-Whitney *U* test, and for comparing survival curves following high-dose probiotic treatment, the log-rank test was used. For all statistical tests, differences were considered significant if $p<0.05$.

In all bar plots, the heigh of the bar represents the group mean, with an error bar representing the standard error of the mean (SEM). As there was often considerable within-group variability in the *in vivo* data, these are overlaid with strip plots, in which a grey point represents the value for each individual animal. The colour schemes and abbreviations used to represent experimental groups for *in vivo* studies are summarised in Fig 2.3.

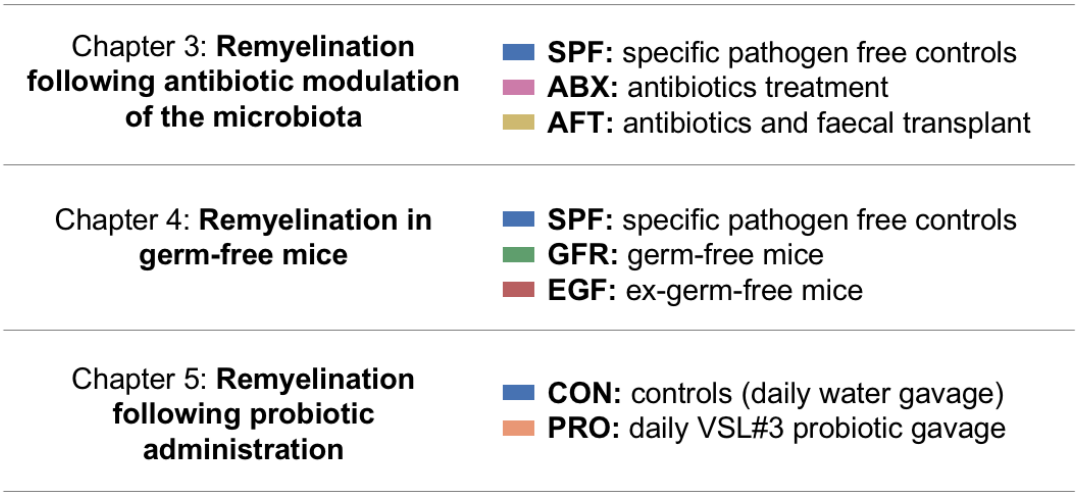

Fig. 2.3 **Colour scheme and abbreviations for representation of *in vivo* studies.**

Chapter 3

Remyelination following antibiotic modulation of the microbiota

3.1 Introduction

3.1.1 Antibiotics and the microbiota

Antibiotics are drugs that kill or inhibit the growth of bacteria. The antibiotic revolution of the last century is undoubtedly one of the greatest advancements in the history of medicine, credited with dramatically reducing death due to bacterial infection (Aminov, 2010). Antibiotic use is now widespread, ranging from the treatment of severe infections to prophylactic use in agricultural animals.

Whilst generally used for their inhibitory effects on pathogens, antibiotics are also one of the strongest determinents of the composition of our microbiota. Human volunteers receiving a 7 day course of clindamycin had disturbances in their microbiota that persisted for over two years (Jernberg et al., 2007). The functional implications of this can be very undesirable, as is exemplified by cases of *Clostridium difficile* (*C. diff*) infection following antibiotic therapy. The pathogenic *C. diff* bacteria are ordinarily constrained by commensal species in the colon, with which they compete for space and nutrients. Following antibiotic treatment for another infection, commensal microbes are depleted, allowing *C. diff* to thrive and cause debilitating illness (Kumar and Clark, 2012, p.122). Faecal microbial transplant (FMT) treatment has been used successfully in *C. diff* infection to restore the integrity of the microbiota and limit the consequences of infection (Aas et al., 2003).

The implications of antibiotics disturbing the microbiota indeed extend beyond the gut (Becattini et al., 2016). Recent preclinical studies have shown that disturbing the microbiota with broad-spectrum antibiotics can impair microglial function (Erny et al.,

2015), reduce monocyte trafficking into the CNS (Möhle et al., 2016) and alter outcome in mouse models of MS (Ochoa-Reparaz et al., 2009), spinal cord contusion (Kigerl et al., 2016) and stroke (Benakis et al., 2016; Winek et al., 2016). On this basis, our first set of experiments investigated whether oral antibiotic treatment would influence the immune and OPC responses underlying remyelination.

3.1.2 Experimental design

A cocktail of five antibiotics was administered to female C57BL/6 mice in their drinking water, over a period of 8 weeks: ampicillin/sulbactam, ciprofloxacin, vancomycin, metronidazole and imipenem. This regimen of antibiotic treatment has been employed previously to cause substantial depletion of microbes in the gut (Heimesaat et al., 2006, 2013; Möhle et al., 2016). The antibiotics-treated group (**ABX**) were administered this antibiotic cocktail from age 4 months until completion of the experiment at 7.5 months. Another group were treated with antibiotics from 4-6 months, after which the treatment was stopped, and mice were orally gavaged with faecal material from control mice, once per day for 5 days (antibiotics with faecal microbial transplantation group, **AFT**). These two treatment groups were compared with age-matched specific-pathogen-free controls (**SPF**). All groups received an injection of 1 µl lysolecithin into the spinal cord ventral white matter to cause focal demyelination at 7 months of age. Mice were then sacrificed by perfusion-fixation at either 7 or 14 days post lesion (**7dpl** and **14dpl**) (Fig. 3.1).

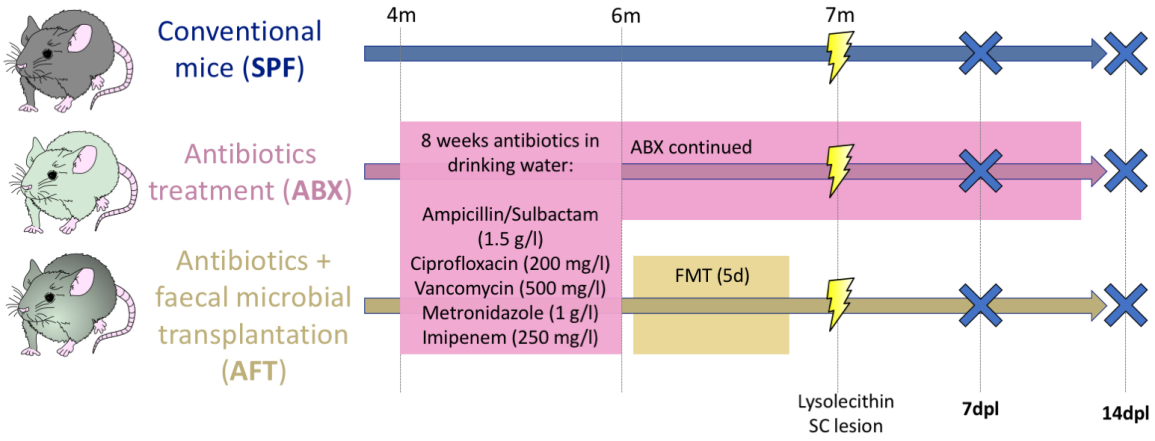

Fig. 3.1 **Schematic diagram of the antibiotics study**, showing the timings of antibiotic administration, FMT treatment, lesioning and perfusion.

The efficacy of the antibiotic treatment was verified by collection of faecal samples from each mouse prior to perfusion. From these, DNA was extracted and quantitive RT-PCR used to determine the copy numbers of a 16S rRNA amplicon common to all bacteria (Fig. 3.2). Faecal samples from a fourth experimental group, which received FMT from human donors, were also included, with the intention of verifying successful colonisation by human microbiota for future studies. The ABX group had ≈100-fold fewer copies of this common bacterial amplicon than the other groups, demonstrating substantial depletion of the microbiota following antibiotics, with restoration one month after AFT ($p<0.01$). The bacterial load within each group also tended to be less at 14dpl compared to 7dpl and this was particularly significant in the SPF group ($p<0.05$).

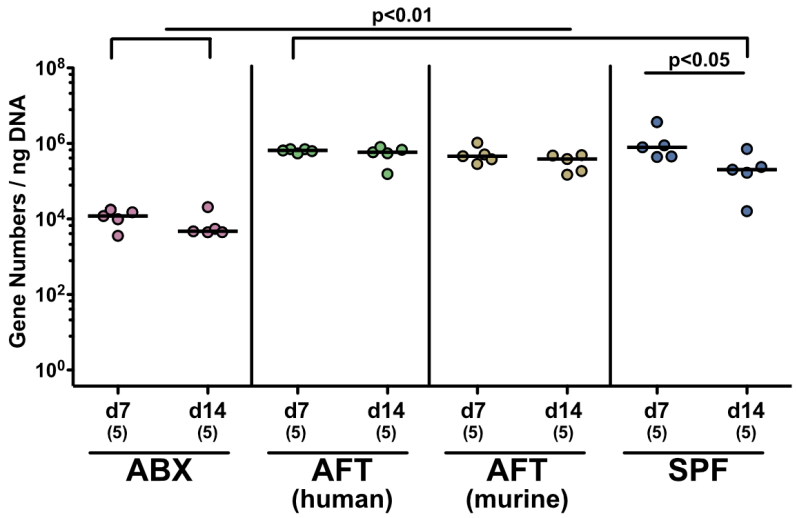

Fig. 3.2 **Quantification of faecal bacteria load following antibiotic and FMT treatments.** Bacterial content of faecal pellets was quantified by quantitative PCR for a common bacterial amplicon. A group receiving FMT from human donors was also included. The antibiotic-treated group (ABX) had approximately a 100-fold depletion of bacterial gene numbers compared to SPF controls and the two groups that had received AFT treatment following antibiotics. Points represent individual mice, with horizontal lines showing the median value for each group. SPF, specific-pathogen-free controls; ABX, antibiotics-treated; AFT, antibiotics and faecal transplant. Mann–Whitney *U* test. *Figure adapted from Markus Heimesaat.*

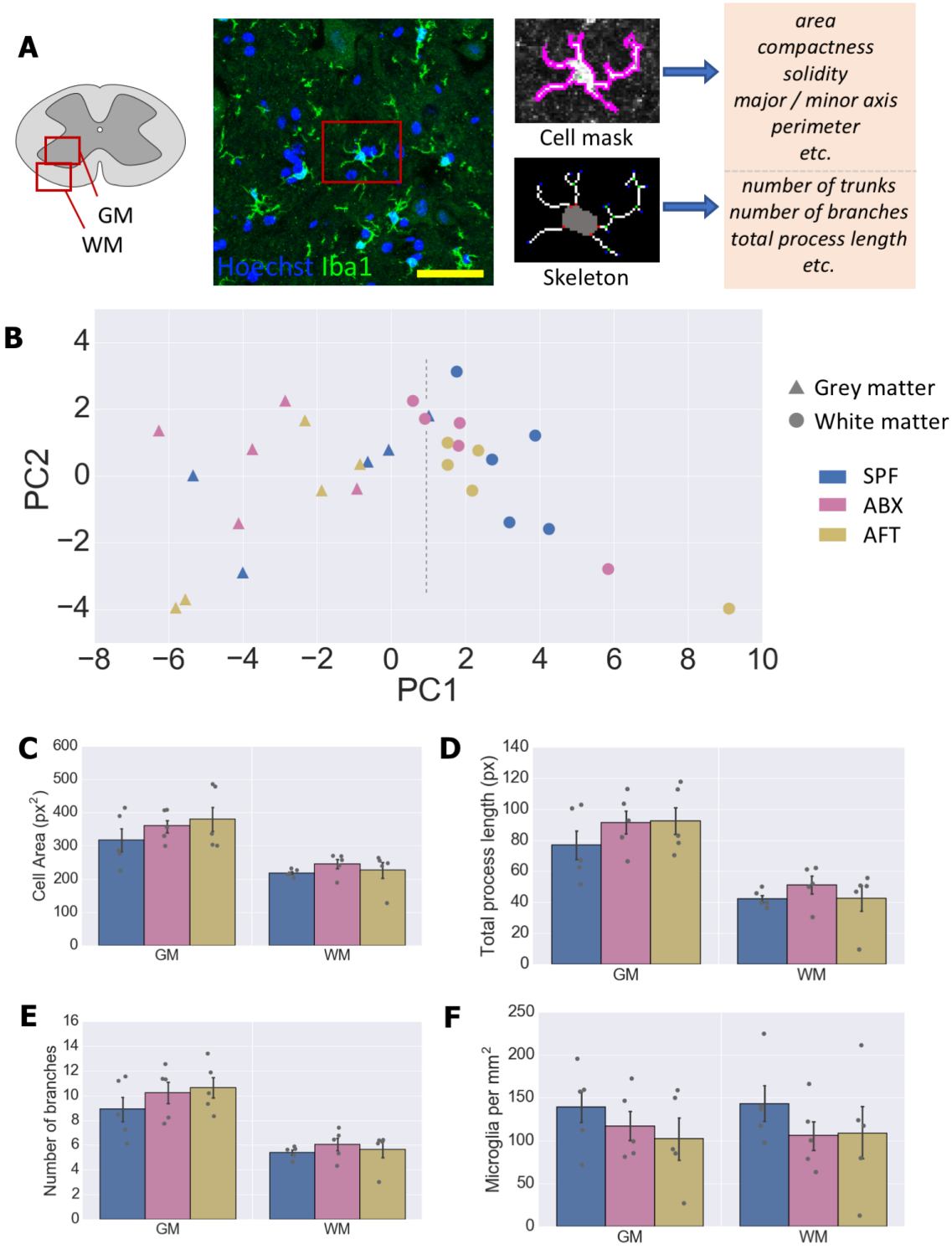
A
GM
WM
Hoechst Iba1
Cell mask
Skeleton
area
compactness
solidity
major / minor axis
perimeter
etc.
number of trunks
number of branches
total process length
etc.
B
PC2
PC1
Grey matter
White matter
SPF
ABX
AFT
C
Cell Area (px²)
GM
WM
D
Total process length (px)
E
Number of branches
F
Microglia per mm²

Fig. 3.3 **Morphological analysis of microglia in unlesioned spinal cord of antibiotics-treated mice.** (A) Spinal cord sections were stained for Iba1, and images taken in the ventral horn grey matter and ventrolateral white matter, contralateral to the lesion. Microglia (Iba1+) were identified and reconstructed using *CellProfiler* software and a number of morphological features were extracted. (B) A plot of principal components 1 and 2 from this dataset shows clustering of grey versus white matter microglia (dotted line), but no clear differences between experimental groups. (C-E) examples of parameters within this dataset including mean cell area (C), total length of cellular processes per cell (D) and mean number of branches (E). (F) Density of microglia in white and grey matter across experimental groups. Bars show mean ± SEM; scale bar: A = 50 µm. GM, grey matter; WM, white matter; SPF, specific-pathogen-free controls; ABX, antibiotics-treated; AFT, antibiotics and faecal transplant; PC, principal component; px, pixels.

This experimental plan was devised in consultation with Ofra Zidon (Franklin Lab, Cambridge) with input from Robin Franklin (Cambridge), Denise Fitzgerald (Queen's University, Belfast (QUB)) and Markus Heimesaat (Charité – Universitätsmedizin Berlin). The mice were prepared in the laboratory of Markus Heimesaat, who also verified the microbial load of the faecal samples. From there they were shipped to QUB, where the lesions were performed with input from Rosana Penalva, Yvonne Dombrowski and John Falconer. I carried out histological analysis of the tissue and the accompanying *in vitro* studies, with assistance from Alerie Guzman de la Fuente.

3.2 Results

3.2.1 Microbial depletion does not influence glia in uninjured spinal cord

Before determining if remyelination was affected in antibiotics-treated mice, I quantified the baseline states of relevant cell types in unlesioned spinal cord. I used immunohistochemistry to count microglia, astrocytes, OPCs and oligodendrocytes on the contralateral side of the spinal cord, several millimetres away from the lesion. To gain insight into the microglial and astrocyte activity, I also assessed the morphology of these cells in grey and white matter.

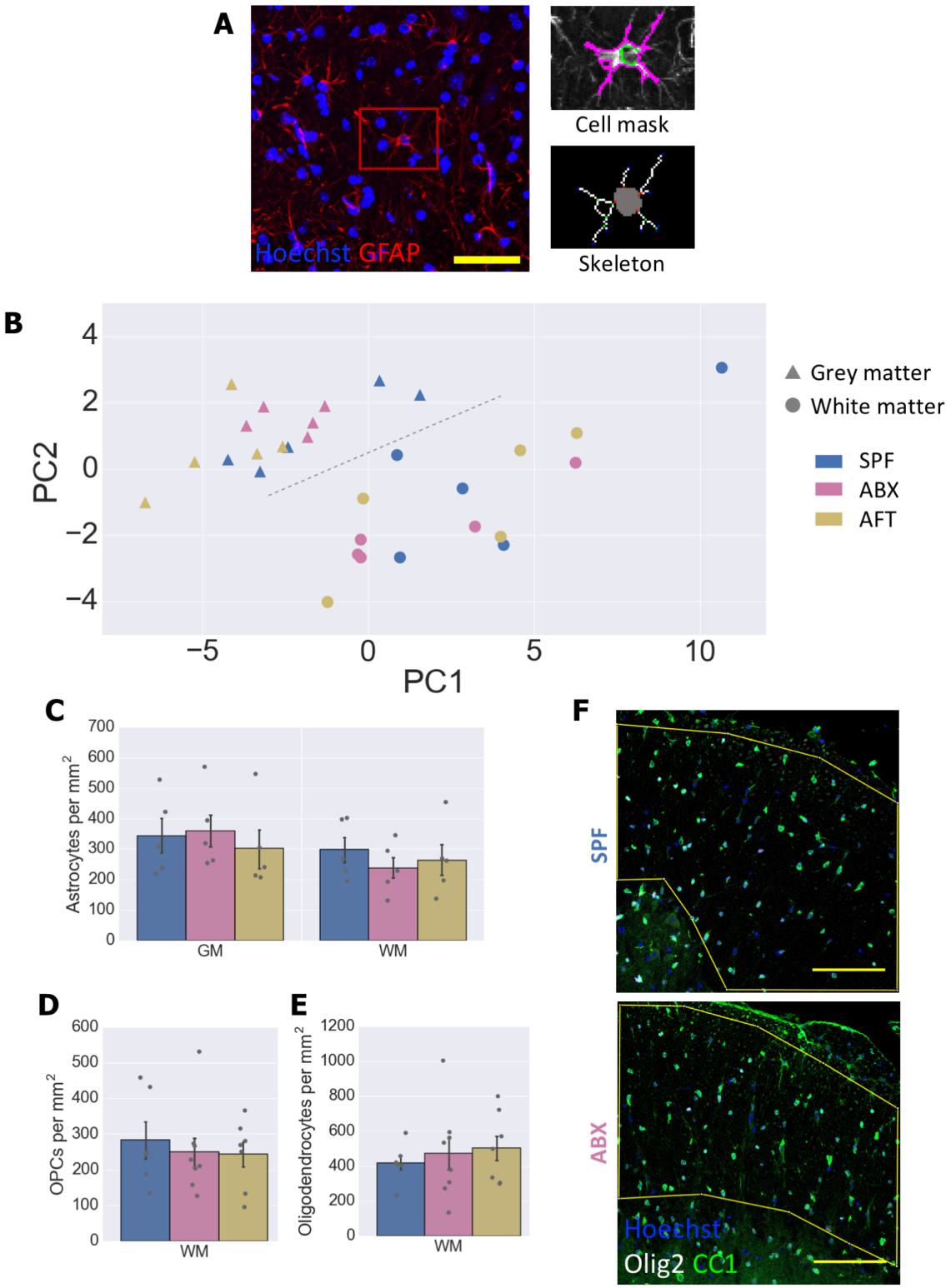
A
Hoechst GFAP
Cell mask
Skeleton
B
PC2
PC1
Grey matter
White matter
SPF
ABX
AFT
C
Astrocytes per mm2
GM
WM
D
OPCs per mm2
WM
E
Oligodendrocytes per mm2
WM
F
SPF
ABX
Hoechst
Olig2 CC1

Fig. 3.4 **Astrocytes, OPCs and oligodendrocytes in unlesioned spinal cord of antibiotics-treated mice.** (A) Astrocyte morphological features were extracted from GFAP-stained spinal cord sections, using the same methodology as for microglia in 3.3. (B) A plot of principal components 1 and 2 from the astrocyte dataset again shows clustering of grey versus white matter microglia (dotted line), but no clear differences between experimental groups. There was no difference in the density of astrocytes (C), OPCs (D) or oligodendrocytes (E) between groups. (F) representative images of unlesioned white matter stained for Olig2 and CC1 to assess OPC and oligodendrocyte densities. Bars show mean ± SEM; scale bars: A = 50 µm, F = 100 µm. GM, grey matter; WM, white matter; SPF, specific-pathogen-free controls; ABX, antibiotics-treated; AFT, antibiotics and faecal transplant; PC, principal component; px, pixels.

Morphometric analysis has previously been used to indicate functional differences in microglia, in the context of changes in the microbiome (Erny et al., 2015; Sampson et al., 2016). Microglia from the uninjured cortex of GF or antibiotics-treated mice have an immature phenotype characterised by longer, heavily branched dendritic trees, consistent with functional deficits (Erny et al., 2015). I performed a semi-automated morphometric analysis using *CellProfiler* software to determine if similar changes were visible in the spinal cord following our antibiotic regime. Ionized calcium-binding adapter molecule 1 (Iba1)+ microglia were detected in projections of Z-stacks spanning 12 µm thickness. A mask and a skeletonised version of each cell were derived, which allowed a number of morphological features to be extracted (Fig. 3.3A). This dataset showed clear clustering between microglia from grey versus white matter in the first principal component (PC1), but no clear segregation between antibiotics-treated mice and SPF controls (Fig. 3.3B).

The microglia used for this "baseline" analysis were from contralateral spinal cord in lesioned mice rather than strictly control animals. The features of this contralateral side observed by immunohistochemistry were consistent with unlesioned CNS tissue: namely low density of Hoechst+ nuclei, a ramified microglial morphology and little CD68+ to indicate activated microglia or infiltrating macrophages (Fig. 3.3A & Fig. 3.5A). However, this analysis comes with the caveat that cells here could be more subtly influenced by longer range signals originating from the lesion.

Astrocytes are another important cell population to consider, as they are responsive to signals from the microbiota (Rothhammer et al., 2016) and secrete factors that influence remyelination (Domingues et al., 2016; Franklin et al., 1991). As with microglia, the morphology of astrocytes is highly plastic in response to their state of activity (Phatnani and Maniatis, 2015). I carried out a similar mophometric analysis, but this time looking at glial

fibrillary acidic protein (GFAP)+ astrocytes (Fig. 3.4A). Again, the astrocytes from grey and white matter clustered apart but without clear differences between antibiotics-treated mice and controls (Fig. 3.4B). Neither were there differences in the density of astrocytes (Fig. 3.4C). Finally, I quantified baseline densities of oligodendrocyte lineage cells expressing oligodendrocyte transcription factor (Olig2), using the antibody CC1 to distinguish between OPCs and oligodendrocytes. I observed no effect of antibiotic treatment on the density of OPCs (Olig2+CC1-, Fig. 3.4D) or oligodendrocytes (Olig2+CC1+, Fig. 3.4E) in unlesioned spinal cord white matter.

3.2.2 Antibiotic treatment results in a prolonged inflammatory response to demyelination

Having established that there were no significant baseline effects of microbial depletion on glia in the unlesioned white matter of the contralateral spinal cord, I turned my attention to the pattern of inflammation in demyelinated white matter lesions caused by focal lysolecithin injection. Whilst Iba1 is a useful marker for ramified microglia in uninjured CNS, CD68 can be used more specifically to stain the activated microglia and infiltrating macrophages in a lesion (Korzhevskii and Kirik, 2016). As expected, the lesion sites had a high density of CD68+ cells in comparison to the surrounding normal tissue (Fig. 3.5A).

This inflammatory response was consistent between all groups at 7dpl ($p=0.74$). However, at 14dpl, the CD68+ density of antibiotics-treated group increased significantly above the SPF controls ($p=0.043$, Fig. 3.5B). This effect was not reversed by FMT, as the AFT group also had $\approx$50% higher CD68+ cell density than controls ($p=0.012$). There was no significant difference in lesion size between groups at either 7dpl ($p=0.44$) or 14dpl ($p=0.47$, Fig. 3.5C).

3.2.3 Antibiotic treatment and FMT disrupt expression of inflammatory markers following demyelination

CD68+ macrophages/microglia can express a wide range of phenotypes during CNS inflammation (Kigerl et al., 2009). To look in more detail at how the inflammatory response to demyelination is perturbed in antibiotics-treated mice, I used more specific markers for these different phenotypes. Efficient remyelination has previously been associated with a high density of M1 macrophages/microglia at early timepoints, giving way to M2 macrophages/microglia coinciding with the onset of OPC differentiation (Miron et al., 2013). As my timepoints (7, 14dpl) were intermediate to those previously studied (3, 10, 21dpl; Miron et al. (2013)), my results likely reflect snapshots of inflammation during this shift.

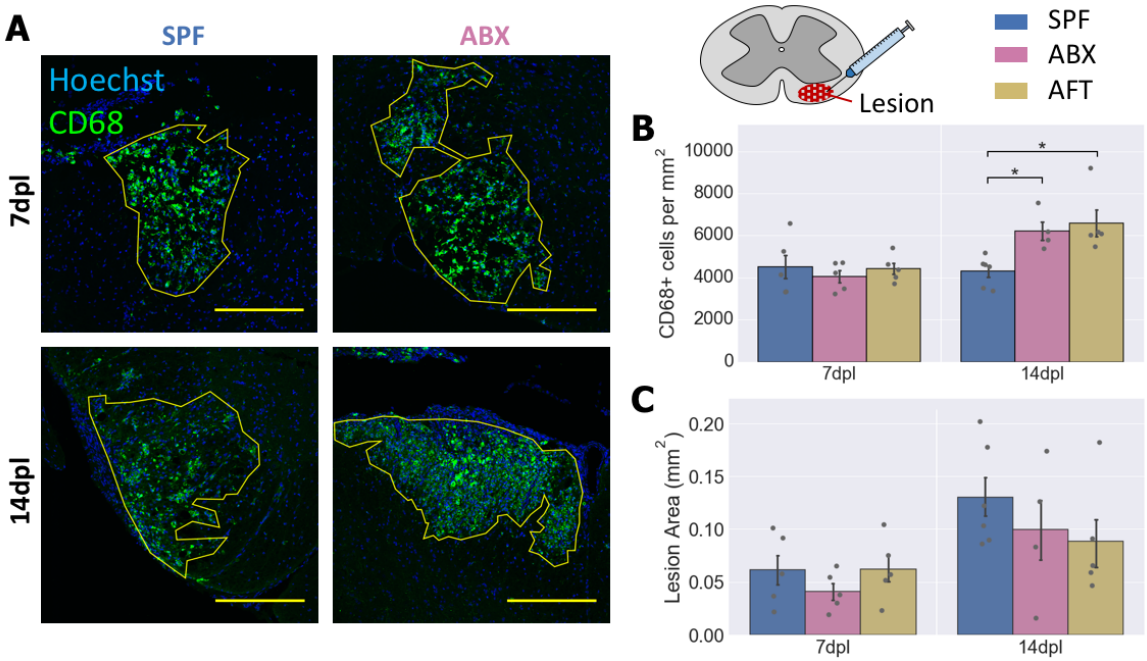

Fig. 3.5 **Activated microglia and macrophages in the lesions of antibiotics-treated mice.** (A) Tissue from 7 and 14 days post lesion (dpl) was stained for CD68 to mark activated microglia and infiltrating macrophages. (B) The density of these CD68+ cells was consistent across groups at 7dpl, but at 14dpl the antibiotics-treated groups had ≈40% more CD68+ cells. This effect was not reversed by our FMT regime. (C) There was no significant difference in lesion size at either timepoint. Bars show mean ± SEM; scale bar: A = 250 µm. SPF, specific-pathogen-free controls; ABX, antibiotics-treated; AFT, antibiotics and faecal transplant. *p<0.05, one-way ANOVA with Tukey HSD *post hoc* test.

To determine microglia/macrophages phenotypes, I stained for two classical M1 markers: inducible nitric oxide synthase (iNOS) and the major histocompatibility complex class II (MHCII). iNOS is used by microglia and macrophages to produce high quantities of nitric oxide (NO) during inflammation, whilst MHCII presents sampled antigens to activate other immune cells (Lan et al., 2017). I also stained for the M2 markers arginase-1 (Arg1) and mannose receptor (MR, also known as CD206). Arg1 competes with iNOS for its substrate arginine and suppresses inflammation, whilst MR is a surface receptor with roles in endocytosis and phagocytosis (Lan et al., 2017). As some of these markers are expressed in other cell types, only cells co-expressing CD68 were counted.

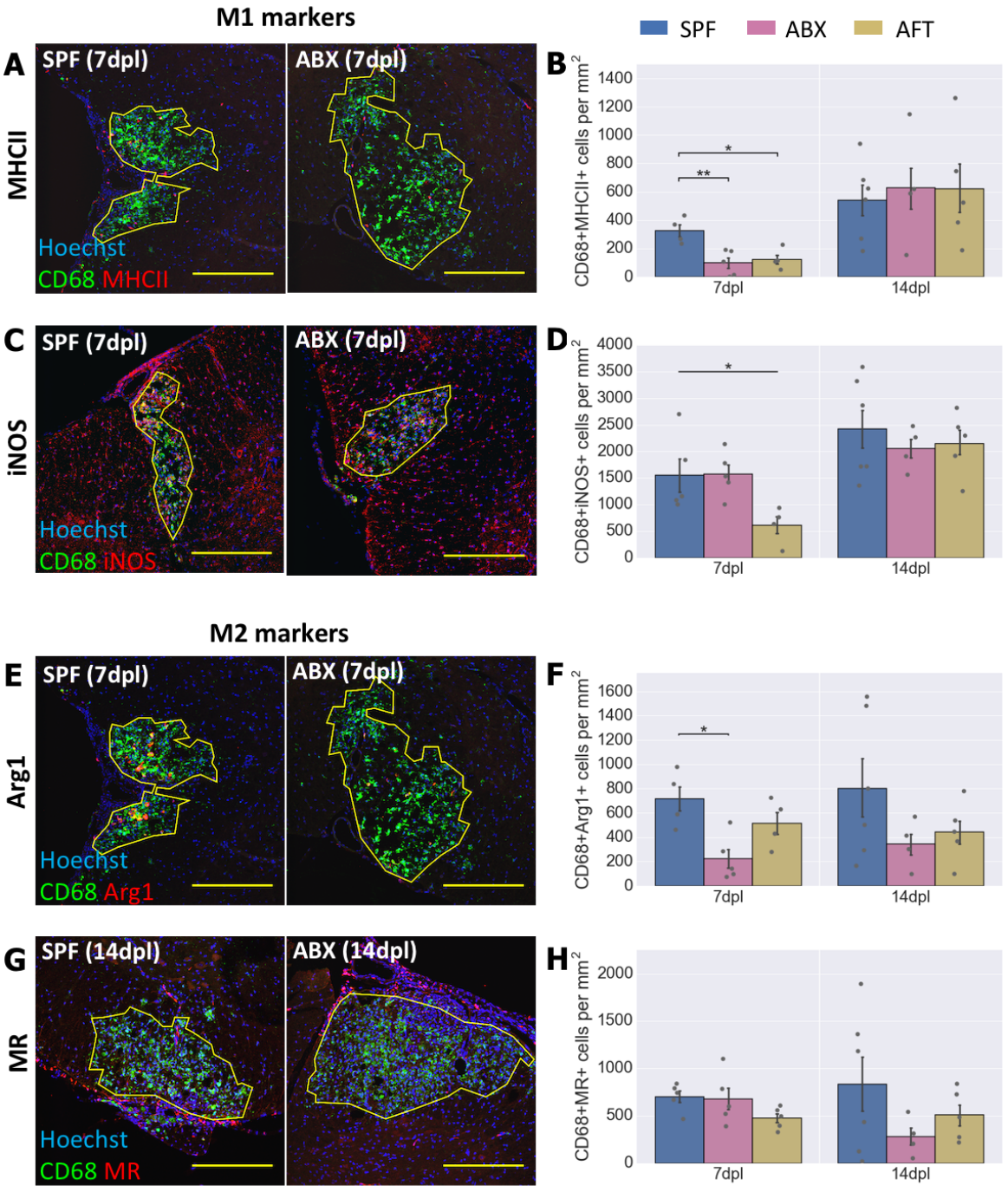
M1 markers
A
MHCII
SPF (7dpl)
ABX (7dpl)
Hoechst
CD68 MHCII
B
SPF
ABX
AFT
CD68+MHCII+ cells per mm2
1400
1200
1000
800
600
400
200
0
*
**
7dpl
14dpl
C
iNOS
SPF (7dpl)
ABX (7dpl)
Hoechst
CD68 iNOS
D
CD68+iNOS+ cells per mm2
4000
3500
3000
2500
2000
1500
1000
500
0
*
7dpl
14dpl
M2 markers
E
Arg1
SPF (7dpl)
ABX (7dpl)
Hoechst
CD68 Arg1
F
CD68+Arg1+ cells per mm2
1600
1400
1200
1000
800
600
400
200
0
*
7dpl
14dpl
G
MR
SPF (14dpl)
ABX (14dpl)
Hoechst
CD68 MR
H
CD68+MR+ cells per mm2
2000
1500
1000
500
0
7dpl
14dpl

Fig. 3.6 **Antibiotic treatment and FMT affect expression of different inflammatory markers following demyelination.** Lesion tissue from 7 and 14dpl was co-stained with CD68 and different M1 (A-D) and M2 (E-H) markers. MHCII+CD68+ cells were reduced at 7dpl following antibiotic treatment (A,B), whilst iNOS+CD68+ cells were observed in similar numbers between groups at both timepoints (C,D). Arg1 was also reduced at 7dpl, but partially reversed by the FMT treatment (E,F), and there were no significant differences in MR expression (G,H). Bars show mean ± SEM; scale bar (A,C,E,G) = 250 µm. SPF, specific-pathogen-free controls; ABX, antibiotics-treated; AFT, antibiotics and faecal transplant. *p<0.05, **p<0.01, one-way ANOVA with Tukey HSD *post hoc* test.

The general pattern observed was a suppressive effect of antibiotics on macrophage /microglia inflammatory marker expression. This affected both M1 and M2 markers, and the effect of the FMT depended on the marker. MHCII showed a clear reduction in the ABX group compared to SPF controls at 7dpl (p=0.007, Fig. 3.6A,B). The AFT group also had a lower density of MHCII+CD68+ cells than controls (p=0.020), indicating that this deficit was not rescued by the FMT. These differences between groups were absent by 14dpl, suggesting that the picture at 7dpl reflects a delay rather than a complete lack of CD68+MHCII+ cells in the lesion. There were also differences in CD68+iNOS+ cell density at 7dpl (p=0.037, ANOVA, Fig. 3.6C,D). This could reflect a consequence of the faecal transplant itself, as the AFT group had lower numbers than either of the other groups, though there was no significant difference in *post hoc* tests (Tukey HSD: AFT vs. SPF p=0.057, AFT vs. ABX p=0.053).

As for the M2 markers, CD68+Arg1+ cells were also diminished by antibiotic treatment compared to in SPF controls (p=0.013, Fig. 3.6E,F). The densities in the AFT group were intermediate levels, pointing towards a degree of rescue by the faecal transplant. There were no significant differences between M2 markers at the 14dpl timepoint, with a large spread within the SPF controls (Arg1 p=0.23, ANOVA; MR p=0.28, ANOVA).

In summary, as well as causing increased numbers of macrophages/microglia at the later timepoint, antibiotic treatment also influences the expression of some of the functional molecules used by different macrophage/microglia phenotypes. These differences were more apparent at the earlier timepoint (7dpl) and involved suppression of Arg1, which is involved in the pro-regenerative effects of macrophages (Rath et al., 2014) and MHCII, which is necessary for antigen presentation by microglia to other immune cells (Perry, 1998), and also important in remyelination (Arnett et al., 2003). The faecal microbial transplant partially reversed the reduction in CD68+Arg1+ cell numbers, but not CD68+MHCII+ cells.

3.2.4 Antibiotic treatment impairs OPC differentiation following demyelination

After determining that there were indeed differences in the inflammatory response to demyelination following our antibiotic regime, we investigated whether this might impact the OPC responses necessary for remyelination. The lesion tissue was stained for Olig2 to label cells of the oligodendrocyte lineage, along with either Ki67 (for proliferating cells) or CC1 (mature oligodendrocytes). The total number of OPCs (Olig2+CC1-) was consistent between the ABX and SPF groups at both timepoints (Fig. 3.7B,E). Neither were there differences in the number of Olig2+Ki67+ proliferating OPCs at 7dpl, a timepoint at which the OPC population is expected to be expanding (Fig. 3.7C,D).

However, there was a difference in the number of Olig2+CC1+ differentiated oligodendrocytes at the later timepoint (14dpl, Fig. 3.7E,F). The SPF control lesions had approximately double the number of oligodendrocytes compared to both the ABX ($p=0.020$) and AFT groups ($p=0.016$). Thus, antibiotic treatment prevented the expected increase in oligodendrocyte number as a result of OPC differentiation, and this was not restored by FMT. In summary, our antibiotic regime did not significantly alter OPC number or proliferation, but did cause an impairment in OPC differentiation.

3.2.5 Antibiotic treatment impairs myelin debris clearance following demyelination

Having observed both a disruption of the immune response and an impairment of OPC differentiation following antibiotic-treatment, I explored how these two processes might be linked. An important means by which microglia/macrophage responses contribute to remyelination is the phagocytosis of myelin debris, which is inhibitory to OPC differentiation (Kotter et al., 2006; Robinson and Miller, 1999). I quantified myelin debris in the lesion by staining for MBP (myelin basic protein), an abundant protein component of the sheath. MBP staining was uniform throughout normal white matter, and absent throughout most of the lesion, with small patches of hyperintense staining representing myelin debris (Fig. 3.8A,B). I also used an antibody for a degenerate form of MBP (dMBP), which specifically labels an epitope unmasked in myelin debris (Matsuo et al. (1997), Fig. 3.8A,B).

In lesions of SPF control mice, there were substantial areas of myelin debris at 7dpl as visualised by MBP+ and dMBP+ staining. These areas were much smaller at 14dpl (Fig. 3.8C,D), by which point the clearance of myelin debris is expected to be largely complete to make way for OPC differentiation. At 7dpl, the regions of hyperintense MBP+ and dMBP staining were similar between all groups (Fig. 3.8C). At 14dpl, both the ABX and

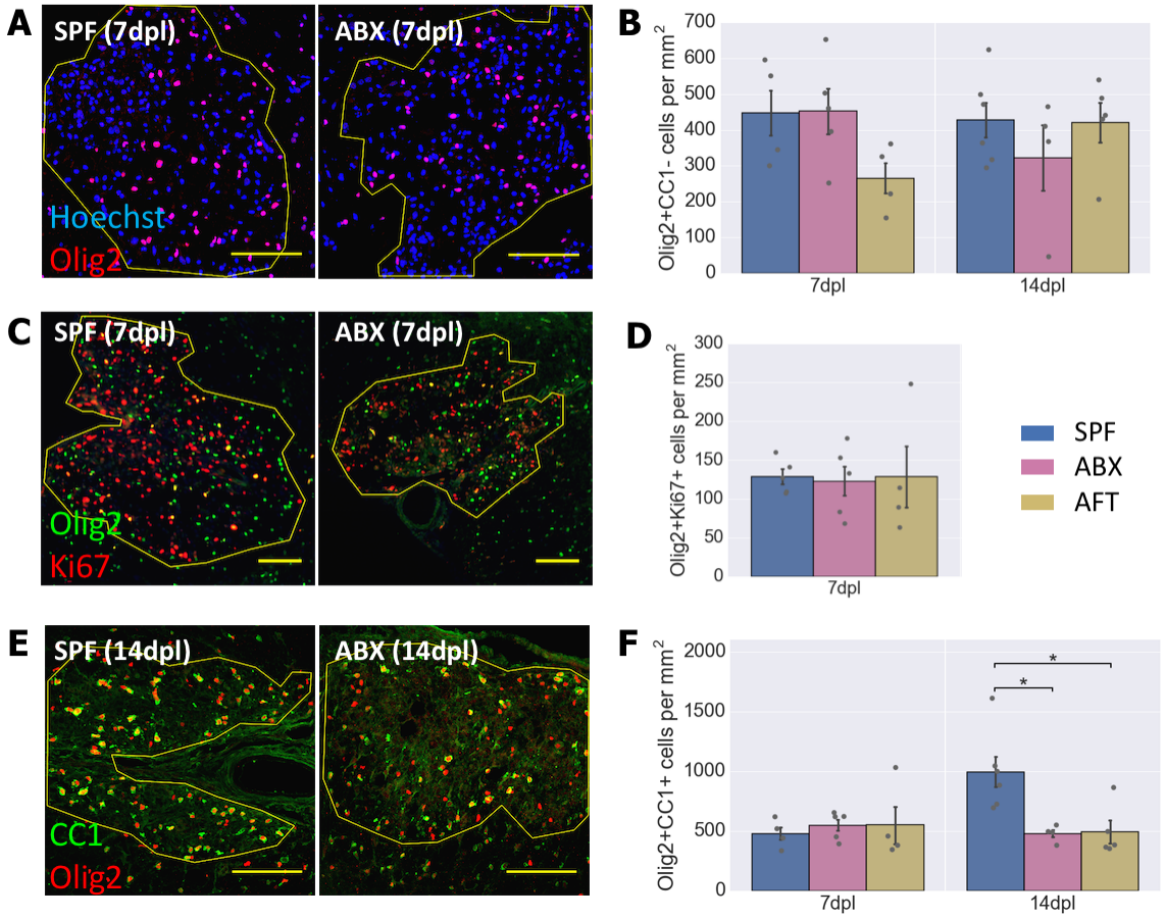

Fig. 3.7 **OPC responses to demyelination in antibiotics-treated mice.** Tissue from 7 and 14 days post lesion (dpl) was stained for Olig2 to mark cells of the oligodendrocyte lineage (A). This was co-stained with CC1 to visualise OPCs (Olig2+CC1-, E,B) and mature oligodendrocytes (Olig2+CC1+, E,F) or with Ki67 to show proliferating OPCs (C,D). Antibiotics-treated mice had fewer differentiated oligodendrocytes at the 14 dpl timepoint, and this was not reversed by FMT. Bars show mean ± SEM; scale bar (A,C,E) = 100 µm. SPF, specific-pathogen-free controls; ABX, antibiotics-treated; AFT, antibiotics and faecal transplant. *p<0.05, one-way ANOVA with Tukey HSD *post hoc* test.

AFT groups showed differences from the SPF controls indicative of impaired myelin debris clearance. The area of MBP+ hyperintensity was significantly greater than SPF controls in both the ABX (p=0.034) and the AFT group (p=0.013, Fig. 3.8C). Additionally the ABX group had significantly larger regions of dMBP+ staining than controls (p=0.012), though the abundance of this degraded epitope in the AFT group was in line with control levels (Fig. 3.8D). The different patterns in hyperintense MBP and dMBP staining, particularly

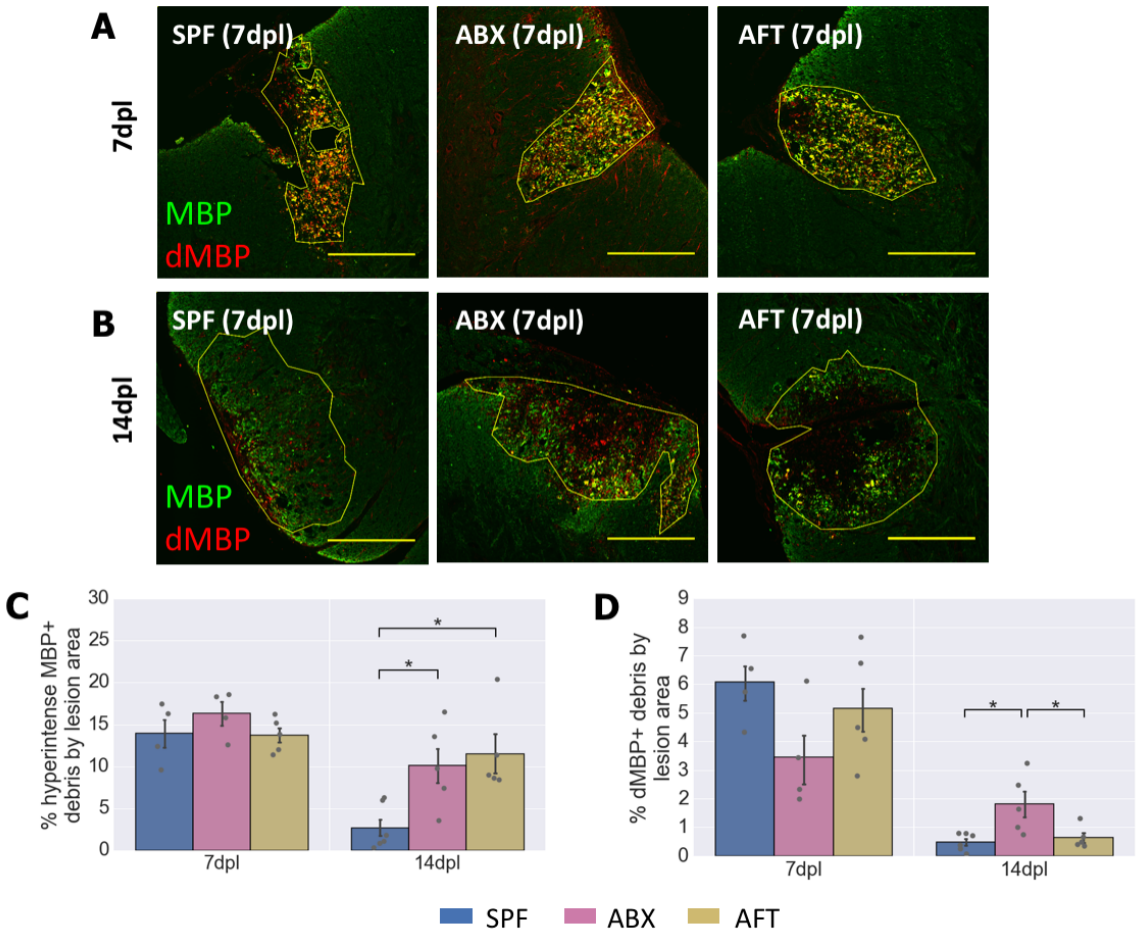

Fig. 3.8 **Myelin debris clearance following demyelination in antibiotics-treated mice.** Tissue from 7 (A) and 14 days (B) post lesion (dpl) was stained for MBP and dMBP to visualise myelin debris. The area of positive staining for each marker is expressed as a percentage of the total lesion area for each group at each timepoint (C,D). The SPF controls displayed a reduction in both markers as debris was cleared from 7 to 14 dpl. However at 14dpl, there was still substantial MBP+ staining in both the ABX and AFT groups, and dMBP+ staining in the ABX group. Bars show mean ± SEM; scale bar (A) = 250 µm. SPF, specific-pathogen-free controls; ABX, antibiotics-treated; AFT, antibiotics and faecal transplant. *p<0.05, one-way ANOVA with Tukey HSD *post hoc* test.

in the AFT group, might reflect contrasting dynamics of these two epitopes during myelin degradation and phagocytosis.

In summary, the lesions of the antibiotics-treated group and, to some extent, the faecal-transplant recipients, showed markers indicative of persistent myelin debris at the later

timepoint - a possible mechanistic link between the reduced inflammatory response and OPC differentiation.

3.2.6 Antibiotics do not impair myelin debris phagocytosis *in vitro*

Whilst we have used oral antibiotic treatment as an intervention to target the microbiota, it is also possible that the antibiotics have other "off-target" effects. For example, if any of the antibiotics can penetrate the CNS in substantial concentrations, it is possible that they might:

- directly impair clearance of myelin debris by microglia
- directly impair OPC differentiation

I investigated these two possibilities by isolating microglia or OPCs by magnetic-activated cell sorting (MACS) and exposing them to antibiotics *in vitro*. Five antibiotics were used in the study as well as sulbactam, an adjuvant β-lactamase inhibitor (referred to here as an "antibiotic" for ease). Of these, four were considered as candidates for direct CNS effects: ampicillin, sulbactam, ciprofloxacin and metronidazole (Table 3.1). Their CNS concentrations were estimated based on literature values for their bioavailability, clearance and BBB penetration. The remaining two antibiotics (imipenem, vancomycin) were not considered to have sufficient bioavailability for any activity outside the gastrointestinal tract (see Materials and Methods for calculations and literature sources).

Antibiotic	Drinking water concentration ($\mu g\,ml^{-1}$)	Estimated CNS concentration ($ng\,ml^{-1}$)
Ampicillin	1000	15
Sulbactam	500	2.5
Ciprofloxacin	200	30
Metronidazole	1000	3.5×10^4
Imipenem	250	(0)
Vancomycin	500	(0)

Table 3.1 **Estimated CNS concentrations of orally-administered antibiotics.**

Primary microglia were isolated from P6-8 mice using MACS for CD11b and cultured for 48 hours in the presence of antibiotics. Each antibiotic was administered at its estimated CNS concentration (++), as well as a 10% dose (+) to look for a graded dose response. The four antibiotics were also tested in combination. Microglia were then exposed to myelin debris for 4 hours and stained for MBP to visualise their phagocytic uptake (Fig. 3.9A), which was confirmed to be internalised by confocal Z-stack imaging (Fig. 3.9C). None of

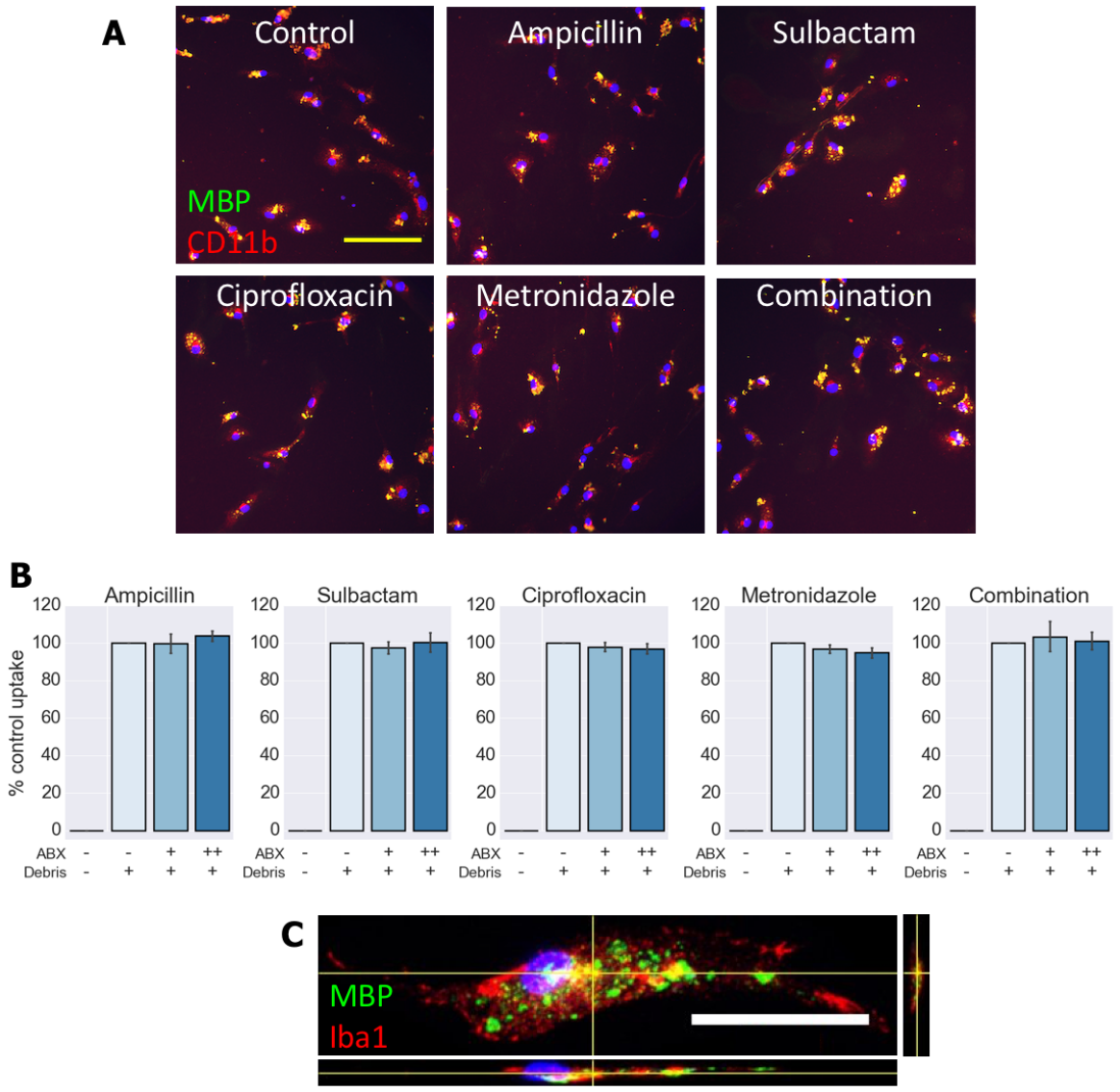

Fig. 3.9 **Phagocytosis of myelin debris by microglia *in vitro* following antibiotic treatment.** (A) Primary microglia were isolated by MACS for CD11b, treated with antibiotics then exposed to myelin debris for 4 hours. These were stained for CD11b to mark microglia, and MBP to identify cells that had taken up myelin debris. (B) The fraction of cells that had phagocytosed myelin debris after 4 hours is expressed relative to microglia in control conditions with no antibiotic treatment. (C) Higher resolution Z-stack imaging using confocal microscopy confirmed that MBP+ debris was internalised within Iba1+ microglia. ABX++ = estimated CNS concentration, ABX+ = 10% of this concentration. None of these treatments significantly modulated phagocytosis relative to control conditions. Bars show mean ± SEM; scale bars: A = 100 µm, C = 50 µm; ABX, antibiotics. One-sample *t*-test with H_0: µ = 100%, and p adjusted for multiple comparisons using the Holm-Bonferroni method.

the antibiotic treatments used caused a deviation of myelin phagocytosis from control levels 3.9B). This suggests that the impaired myelin debris clearance seen following antibiotic administration *in vivo* is not due to direct effects of antibiotics on microglia in the CNS.

3.2.7 Antibiotics can modulate OPC activity *in vitro*

Another possibility to explore was that the doses of antibiotics used could directly inhibit OPC differentiation, which might account for the reduced numbers of oligodendrocytes at 14dpl (Fig. 3.7E, F). To investigate this, primary OPCs were isolated from P6-8 mice using MACS for A2B5, and cultured for eight days to allow differentiation in the presence of antibiotics. As for microglia, each antibiotic was administered at its estimated CNS concentration (++), as well as a 10% dose (+).

Differentiation was assessed as the fraction of Olig2+ cells expressing the oligodendrocyte marker CNPase. Control rates of differentiation varied from 3-9% between replicates and no antibiotic caused a significant decrease in differentiation from control levels.

Prior to fixation, OPC cultures were also labelled with a 3 hour pulse of (EdU) 5-ethynyl-2'-deoxyuridine, which allows the detection of any cell proliferating during this time window. Between 1-7% of Olig2+CNPase- OPCs were EdU+ in control conditions. Again, no antibiotic alone caused a significant difference in the proliferative fraction of OPCs. However, the combination treatment did significantly inhibit proliferation ($p=0.0027$, Fig. 3.10C, D), suggesting a synergistic effect of the antibiotics. As no difference in Ki67+Olig2+ proliferative OPCs was observed in remyelinating lesions of antibiotics-treated mice *in vivo* (Fig. 3.7C, D), this could be an artefact of the *in vitro* assay, which is a reductive model of the lesion environment.

3.3 Discussion

The aim of this first set of experiments was to determine if an intervention that alters the microbiota could influence the process of remyelination. In particular, this antibiotics model has some clinical relevance as all of these antibiotics are used routinely in humans at equivalent scaled doses (see Materials and Methods), albeit generally not in combination and for such great lengths of time.

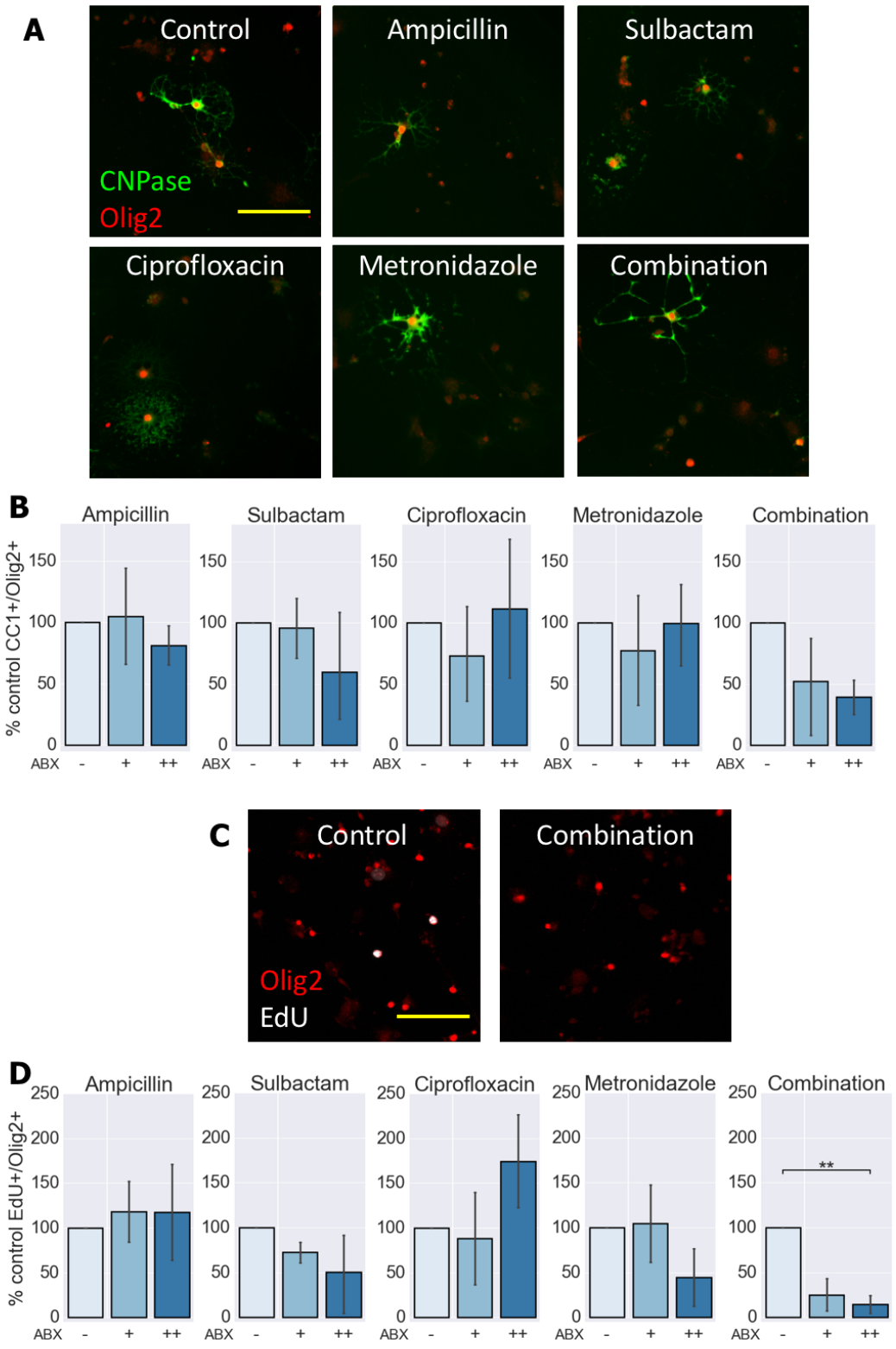
A
Control
Ampicillin
Sulbactam
CNPase
Olig2
Ciprofloxacin
Metronidazole
Combination
B
Ampicillin
Sulbactam
Ciprofloxacin
Metronidazole
Combination
% control CC1+/Olig2+
150
100
50
0
ABX - + ++
C
Control
Combination
Olig2
EdU
D
Ampicillin
Sulbactam
Ciprofloxacin
Metronidazole
Combination
% control EdU+/Olig2+
250
200
150
100
50
0
**
ABX - + ++

Fig. 3.10 **OPC differentiation and proliferation *in vitro* following antibiotic treatment.** (A) Primary OPCs were isolated by MACS for A2B5, and cultured with antibiotic treatments for 8 days. These were stained for Olig2 to label cells of the oligodendrocyte lineage and CNPase as a marker for differentiation. (B) The fraction of CNPase+ Olig2+ cells is expressed relative to control OPCs. (C) Cells were pulse-labelled with EdU to mark proliferating cells prior to fixation. (D) The fraction of EdU+ Olig2+CNPase- cells was reduced relative to control levels in the combination treatment. ABX++ = estimated CNS concentration, ABX+ = 10% of this concentration. Bars show mean ± SEM; scale bar (A,C) = 100 µm; ABX, antibiotics. One-sample *t*-test with H_0: µ = 100%, and p adjusted for multiple comparisons using the Holm-Bonferroni method.

We observed several deficits in the response to toxin-mediated demyelination following antibiotic depletion of 99% of the murine gut microbiota. Firstly, there was a late peak in inflammation in antibiotics-treated mice, with an increase in CD68+ cell numbers from 7 to 14dpl, which was not observed in SPF mice (Fig. 3.5B). Whilst inflammation is an important prerequisite for remyelination (Kotter et al., 2001), a prolonged inflammatory response with poor resolution is associated with poor remyelination, as occurs in older animals (Hinks and Franklin, 2000). As our focus was on OPC responses, this study lacked a very early timepoint, which would have been informative for observing differences in the onset of inflammation.

However, staining for markers of more specific microglia/macrophage phenotypes did reveal some deficiencies in the immune response mounted by antibiotics-treated mice. In particular, there were fewer CD68+ cells expressing MHCII or arginase-1 (Fig. 3.6). Arginase-1 is a marker for pro-regenerative macrophages/microglia, which are associated with timely resolution of inflammation and efficient remyelination (Miron et al., 2013). Meanwhile, MHCII is an important complex for antigen presentation to T cells, but is also known to have T cell-independent roles in promoting remyelination (Arnett et al., 2003). Thus, the antibiotics-treated group have reduced expression of multiple macrophage/microglia markers known to be important for remyelination.

The phagocytosis of myelin debris is one important function of microglia/macrophages, and is necessary to allow OPC differentiation to take place (Kotter et al., 2006; Robinson and Miller, 1999). Consistent with the observed inflammatory deficits in the antibiotics-treated mice, this group also exhibited reduced debris clearance compared to SPF mice at 14 dpl (Fig. 3.8). Direct antibiotic treatment of microglia *in vitro* did not affect their phagocytosis of myelin debris (Fig. 3.9), supporting the hypothesis that an intact microbiome bolsters this

pro-regenerative function of microglia. Other evidence can be drawn from recent studies showing that microbiota-derived signals support the capacity of microglia to respond to viral infection (Erny et al., 2015), as well as their role in neurodegenerative disease (Sampson et al., 2016).

It would be interesting to know whether direct antibiotic treatment can influence peripherally-derived macrophages, which also contribute to efficient myelin debris clearance (Ruckh et al., 2012). Other work has shown that depletion of the intestinal microbiota reduces monocyte entry into the CNS (Möhle et al., 2016) and impairs phagocytosis in peripheral macrophage populations (Schuijt et al., 2016), but an off-target effect of antibiotic treatment is a possible confounding factor in both studies.

Importantly, the OPC response to demyelination was also impaired in antibiotics-treated mice (Fig. 3.7). Whilst OPC proliferation and number were unaffected, there were fewer Olig2+CC1+ oligodendrocytes at the 14 dpl timepoint, suggesting that OPC differentiation was reduced. Part of this is likely due to the increased myelin debris load of these lesions, which is known to inhibit OPC differentiation during remyelination (Kotter et al., 2006; Lampron et al., 2015). Other possible contributing factors to this include non-phagocytic roles of microglia/macrophages (namely secretion of differentiation-promoting factors), or other direct or indirect routes of communication with the microbiota. For example, components of the adaptive immune system, which is similarly dependent on the microbiota (Belkaid and Hand, 2014), have also been shown to contribute to remyelination (Bieber et al., 2003; Dombrowski et al., 2017). Independent of the immune system, microbiota-derived metabolites can penetrate the CNS, signalling to neurons (Arentsen et al., 2017) and astrocytes (Rothhammer et al., 2016), and may offer a more direct route of communication to OPCs.

We must also consider that high doses of antibiotics could themselves inhibit OPC function. My experiments on primary OPC cultures suggested that, at the estimated CNS antibiotic concentrations, proliferation was markedly reduced, and there was also a tendency towards reduced differentiation (Fig. 3.10). This is a possible contributing factor, though these results must be interpreted with the caveat that OPCs *in vivo* would be exposed to antibiotics in the context of many other cues from the lesion environment, which may affect their response. Additionally, *in vivo* metabolism of these exogenous compounds might create byproducts with different potencies. For example, the reduced proliferation rate *in vitro* did not translate to changes in OPC proliferation within the lysolecithin lesions (Fig. 3.7C,D).

As OPC differentiation is commonly the rate-limiting step in remyelination of MS lesions (Chang et al., 2000; Wolswijk, 2002), the changes observed in this study have implications as to the success of remyelination following microbial depletion. However, without a later

timepoint with higher resolution imaging of the myelin sheaths, we cannot make conclusive claims about the ultimate result of remyelination in these mice.

The role of the faecal transplant group was to determine the reversibility of any changes we observed following antibiotic treatment. Any effect that was not reversed might point towards either longer-term effects of temporary microbial depletion, or a direct effect of the antibiotics themselves. Interestingly, some antibiotics-induced changes were more susceptible to reversal than others. The delayed peak of CD68+ inflammation was similar following antibiotics, regardless of faecal transplant (Fig. 3.5), as was the reduced differentiation of OPCs (Fig. 3.7). In contrast, the presence of arginase-1+ macrophages/microglia (Fig. 3.6E,F) and the clearance of dMBP+ myelin debris (Fig. 3.8D) did show some evidence of reversal. This disparity suggests several underlying mechanisms are likely contributing to the effect of antibiotic treatment on the processes of remyelination.

The density of iNOS+ macrophages/microglia, which was similar between the SPF and antibiotics groups, was reduced following the faecal transplant treatment (Fig. 3.6C,D). iNOS is considered a marker for the M1 phenotype, which has an important role in early inflammation, but must give way to M2 macrophages/microglia at later timepoints for efficient remyelination (Miron et al., 2013). The pattern observed here is worth considering as it suggests that, whilst faecal transplant is generally considered a "rescue treatment" in microbial depletion studies, the process of transferring donor microbes may have its own effects on the immune system.

In conclusion, this experiment shows that mice have defects in their remyelination response following microbial depletion by an oral antibiotic regimen. This encompasses a reduction in important populations of macrophages/microglia, diminished clearance of myelin debris and impaired differentiation of OPCs into new oligodendrocytes. Some, but not all, of these changes were rescued by transplanting donor microbiota into antibiotics-treated mice by oral gavage. Accompanying studies *in vitro* showed that these doses of antibiotics had little direct effect on microglial phagocytosis of myelin debris, though they may be sufficient to alter OPC responses. Thus, the effects seen could be a combination of microbial signalling to immune cells in the CNS and some direct effect of the antibiotics.

Chapter 4

Remyelination in germ-free mice

4.1 Introduction

4.1.1 The germ-free environment

As all experimental systems available to study the microbiome have their advantages and shortcomings, it is clear that consolidating findings in different models is essential to investigate causative links from gut to brain. In particular, a limitation of our antibiotics study was that the antibiotics may have unintended effects, besides depleting the microbiota. With this in mind, we investigated whether the findings made following demyelination in antibiotics-treated mice - notably altered microglia/macrophage and OPC responses - would be recapitulated in a germ-free system.

Germ-free (GF) mice have two major differences to the mice of our antibiotics-study. Firstly, they have a negligible microbial load. Whilst the antibiotics regime caused a 100-fold decrease in total bacterial load (Fig. 3.2), some bacterial DNA was still detectable in the faeces - particularly of the *Lactobacilli* and *Bifidobacteria* groups (approximately 10^3 and 10^1 gene copies per ng of DNA respectively, see Appendix B). In contrast, GF mice are generally considered to be completely devoid of a microbiome, being derived by sterile caesarean section and housed in a germ-free isolator (Luczynski et al., 2016). In practice, some contamination has been detected in isolators previously considered to be "germ-free" (Fontaine et al., 2015; Packey et al., 2013), necessitating careful screening throughout our experiment[1].

[1]It should also be mentioned that mammalian genomes (including those of GF mice) contain various endogenous retroviruses, which are sometimes described as a component of our microbiome (Nicklas et al., 2015).

As well as exhibiting a more extreme microbial depletion, GF animals are sterile throughout their development, in contrast to our antibiotics regime which was initiated in adult mice (at 4 months old). This feature of the model has been useful for identifying roles of the microbiota during development, but permanent developmental deficits can also be a confounding factor for effects later in life (Luczynski et al., 2016). To control for this, we included a group of "ex-GF mice", which were conventionalised by introduction of a control microbiome after weaning.

Several decades of research have shown that the lifespan of mice is not reduced in the absence of a microbiome - in fact, GF mice tend to outlive conventionally colonised mice, which can suffer morbidity from subclinical pathological infections (Luczynski et al., 2016). However, GF mice do display some important characteristics reflecting roles of gut microbes in normal physiology. Of relevance to this study, they are known to have reduced microglia and monocyte function (Erny et al., 2015; Khosravi et al., 2014), and different patterns of myelination in the medial prefrontal cortex (Hoban et al., 2016). The aim of this study was to determine whether the total absence of a microbiome impairs remyelination.

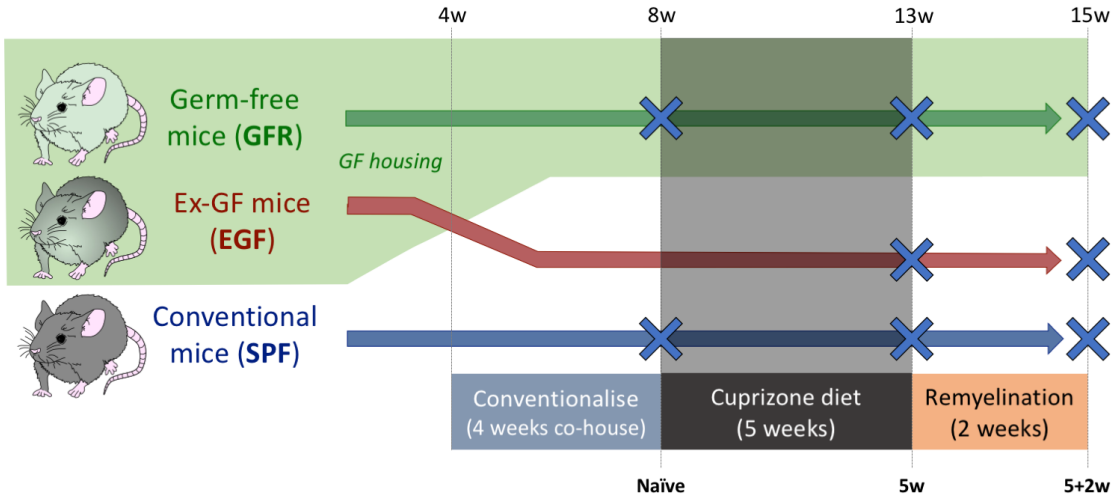

Fig. 4.1 **Schematic diagram of the germ-free study**, showing the timings of conventionalisation, cuprizone administration and the timepoints used for perfusion.

4.1.2 Experimental design

C57BL/6 male mice were bred from a GF nucleus colony at the University of East Anglia (UEA), Norwich, and maintained in a flexible-film isolator, supplied with sterilised air, food, water and bedding. The GF group (**GFR**) were maintained in these conditions throughout the experiment and compared to aged-matched specific-pathogen-free controls (**SPF** group). An

"ex-GF" group (**EGF**) were also included to disentangle the effects of GF development from the need for microbiota-derived signals throughout adult life. The EGF mice were littermates of the GFR group, and remained GF until after weaning (4 weeks old), at which point they acquired a microbiome by co-housing with the SPF mice.

The constraints of the germ-free housing made the use of sterotactic lysolecithin injection impossible, as had been employed to cause demyelination in the antibiotics system (see Chapter 3). Instead, we opted for the cuprizone model: another toxin-mediated model in which demyelination occurs following administration of 0.2% cuprizone in the diet. The cuprizone was incorporated into RM3(P) diet (SDS), processed into pellets and then received 50 kGy γ-irradiation for sterilisation. Mice received the cuprizone diet for 5 weeks in place of their regular diet, and were then returned to regular diet for 2 weeks afterwards. There were three timepoints at which animals were sacrificed by perfusion-fixation: prior to cuprizone administration (**Naïve**), at the end of cuprizone administration (**5w**) or after two more weeks of normal diet (**5+2w**) (Fig. 4.1).

The microbial status of the mice was confirmed by several approaches. Firstly, faecal pellets were collected prior to perfusion, and the DNA isolated and amplified by polymerase chain reaction, using a universal primer pair (UniF/R). UniF/R flank a 147 base pair region of the 16S rRNA gene that is common to all bacterial groups (Fuller et al., 2007; Packey et al., 2013). Agarose gel electrophoresis revealed this amplicon to be present in the SPF and EGF groups, absent in the GFR group (Fig. 4.2A). Another feature of GF mice is their grossly enlarged caeca (Smith et al., 2007). The caecal appearances and weights in our study were consistent with this, and changes were completely reversed in the EGF group by 4 weeks cohousing with SPF controls (Fig. 4.2B,C). In addition, the animals and isolators were monitored by routine in-house screening using aerobic and anaerobic culture methods, as well as microscopy of faecal smears. This array of quality control measures confirmed that the mice in our GFR group were indeed germ-free, whilst the co-housing regime returned the bacterial load to normal levels in the EGF group.

This experiment using GF mice was made possible thanks to the expertise of Andrew Goldson and Arlaine Brion (Institute for Food Research, UEA), who were responsible for the husbandry of the animals. I designed the study, with input from Robin Franklin, Chao Zhao and Alerie Guzman de la Fuente (Cambridge), and carried out the perfusions and subsequent analysis of the tissue, as well as the accompanying *in vitro* studies. Fynn Krause (Department of Biochemistry, Cambridge) advised and assisted with the gas chromatography-mass spectrometry.

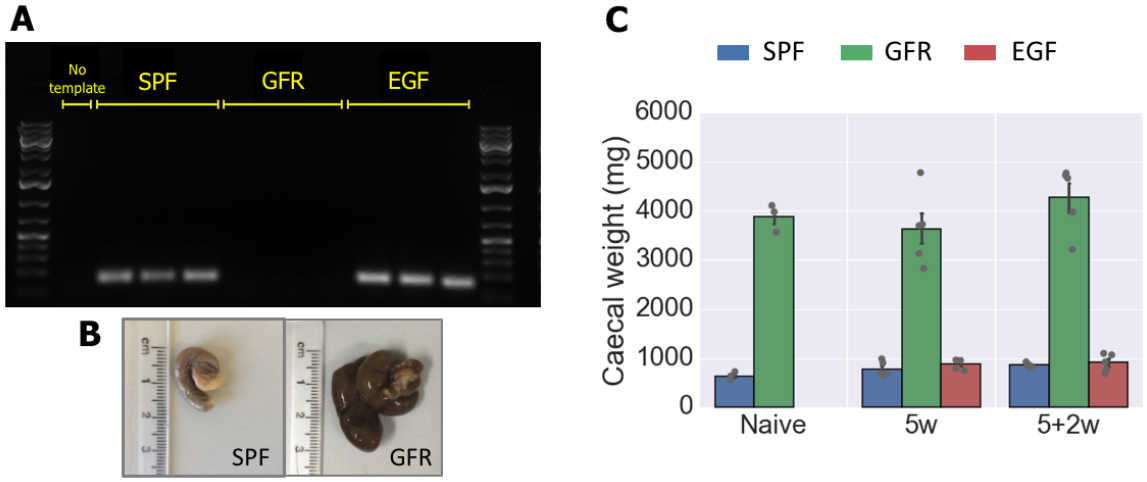

Fig. 4.2 **Confirmation of the microbial status of mice used in the study.** (A) DNA extracted from faecal pellets was used to amplify a universal prokaryotic 16S sequence, and this was absent in the faeces of the GFR group. (B) The GFR mice also displayed grossly enlarged caeca, a hallmark of axenic mice. (C) This was reversed in the EGF group following cohabitation with the SPF controls. SPF, specific-pathogen-free controls; GFR, germ-free; EGF, ex-germ-free.

4.2 Results

4.2.1 Characterising glia in the corpus callosum of unlesioned germ-free mice

As with the antibiotics model, I first investigated whether the chronic absence of a microbiome would affect baseline glial populations in the corpus callosum (CC). SPF (n=3) and GF (n=3) cuprizone-naive mice were perfused and sections from the caudal CC were stained with markers to distinguish microglia (Iba1+), astrocytes (GFAP+), oligodendrocytes (Sox10+CC1+) and OPCs (Sox10+CC1-) (Fig. 4.3). A semi-automated morphometric analysis was performed using *CellProfiler* software, in the same manner as described for the antibiotics model.

An increased microglial density has previously been described in GF mice in the CC, in parallel with other brain regions (Erny et al., 2015). I observed the same result here with approximately 50% more Iba1+ microglia per mm^2 in the CC of the GFR group compared to the SPF group (p=0.0095, Fig. 4.3B,D). However, I did not detect any morphological

differences in the GFR microglia, which did not separate clearly from the SPF group on a PCA plot (Fig. 4.3C).

GF mice have similar CNS densities of astrocytes compared to SPF mice (Erny et al., 2015), though astrocytes are known to respond to microbiota-derived metabolites through activation of the aryl hydrocarbon receptor (Rothhammer et al., 2016). Using a similar strategy as for microglia, I stained sections with the astrocyte marker GFAP (Fig. 4.3E). There were no significant differences in either astrocyte morphology or density in the corpus callosum, though with considerable variability observed between mice within the same group (Fig. 4.3F,G).

Finally, I quantified the numbers of oligodendrocytes and OPCs in the germ-free CC. A higher abundance of oligodendrocyte-associated mRNAs has previously been reported in the medial prefrontal cortex of GF mice, but not other grey-matter regions of the brain, though the CC was not investigated in this study (Hoban et al., 2016). I detected no baseline difference between GF and SPF mice in their density of oligodendrocytes (Olig2+CC1+, Fig. 4.3I) or OPCs (Olig2+CC1-, Fig. 4.3J) in the CC.

In summary, prior to cuprizone administration, the CC of GF mice had enhanced numbers of microglia, but no difference in astrocyte, oligodendrocyte or OPC numbers compared to SPF mice.

4.2.2 Germ-free mice have a blunted peak in inflammation following toxin-induced demyelination

I next turned my attention to how these glia populations behave during demyelination and remyelination. As in the lysolecithin lesions, there was a substantial increase in the density of CD68+ activated microglia/macrophages following demyelination (Fig. 4.4). In the SPF controls, this peaked at the end of cuprizone administration, and by two weeks later was returning back towards control levels. In the GFR group the density of CD68+ cells at the end of cuprizone was less than in SPF controls ($p=0.048$). Furthermore, the density of activated macrophages/microglia did not resolve following two weeks without cuprizone, and in fact was higher than in the SPF ($p=0.043$) or EGF ($p=0.022$) groups by this timepoint. The CD68+ cell density in the EGF group tracked similarly to the SPF controls, showing that the differences seen in GF mice could be reversed by colonisation in adulthood.

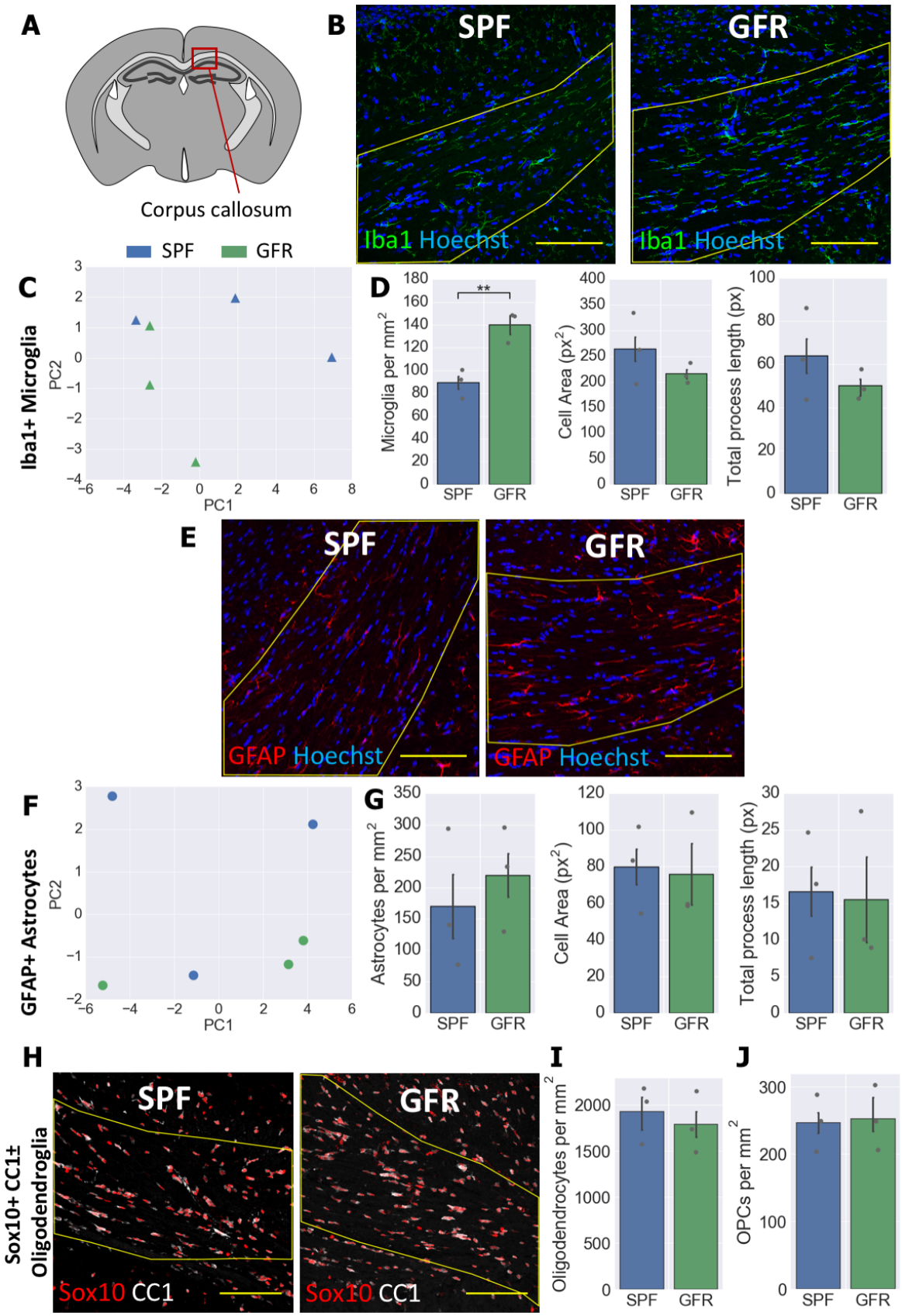
A
Corpus callosum
B
SPF
GFR
Iba1 Hoechst
Iba1 Hoechst
C
SPF
GFR
Iba1+ Microglia
PC2
PC1
D
Microglia per mm2
Cell Area (px2)
Total process length (px)
SPF
GFR
E
SPF
GFR
GFAP Hoechst
GFAP Hoechst
F
GFAP+ Astrocytes
PC2
PC1
G
Astrocytes per mm2
Cell Area (px2)
Total process length (px)
SPF
GFR
H
Sox10+ CC1± Oligodendroglia
SPF
GFR
Sox10 CC1
Sox10 CC1
I
Oligodendrocytes per mm2
J
OPCs per mm2
SPF
GFR

Fig. 4.3 **Morphological analysis of glia in the corpus callosum of germ-free mice.** (A) Coronal brain sections were stained for glial markers, and images taken in the CC 500 µm lateral to the midline. Morphology of microglia and astrocytes were analysed as in Fig. 3.3. (B) Iba1+ microglia in the CC of cuprizone-naive SPF and GFR mice. (C) PCA of morphological features of microglia. (D) Plots of the density, mean cell area and mean process length of microglia. GFR mice had ≈50% more microglia per unit area than SPF controls. (E) GFAP+ astrocytes in the CC of cuprizone-naive SPF and GFR mice. (F) PCA of morphological features of astrocytes. (G) Plots of the density, mean cell area and mean process length of astrocytes. (H) Sox10+CC1+ oligodendrocytes and Sox10+CC1- OPCs in the CC of cuprizone-naive SPF and GFR mice. The density of oligodendrocytes (I) and OPCs (J) were also quantified. Bars show mean ± SEM; scale bar in B, E and H = 100 µm; CC, corpus callosum; px, pixels. **p<0.01, student's *t*-test.

To better characterise this difference in the inflammatory response, I looked at the expression of MHCII, an M1 marker which was reduced in the microglia/macrophages of antibiotics-treated mice (Fig. 3.6C,D). Mirroring the result in the antibiotics-treated mice, the GF mice had fewer MHCII+ macrophages/microglia at the end of cuprizone administration (p=0.043, Fig. 4.5A,B). As there tended to be fewer total Iba1+ microglia/macrophages in the GFR mice (Fig. 4.5C), I also quantified the MHCII+ percentage of this total pool. The MHCII+ proportion of total Iba1+ cells was also reduced in GF mice (p=0.011, Fig. 4.5D), suggesting that as well as a reduced number of microglia and macrophages, these cells are less responsive to cuprizone-induced demyelination.

Arginase-1 expression was also reduced in antibiotics-treated mice lesioned with lysolecithin (Fig. 3.6E,F). However, in the GF cuprizone study there was minimal arginase-1 expression across all groups and timepoints. This is consistent with other studies reporting negligible expression of arginase-1 during cuprizone-induced demyelination and remyelination (Le Blon et al., 2016; Olah et al., 2012) and reflects differences in the regenerative pathways at play in the two models.

Similarly myelin debris, which was cleared more slowly in antibiotics-treated mice, was absent at the timepoints studied in this cuprizone study. Validation of the dMBP staining at earlier timepoints in SPF mice showed that a peak of myelin debris at 3 weeks of cuprizone administration was cleared by 5 weeks. Thus if there was a similar delay in myelin debris clearance in GF mice, this did not extend to 5 weeks of cuprizone treatment.

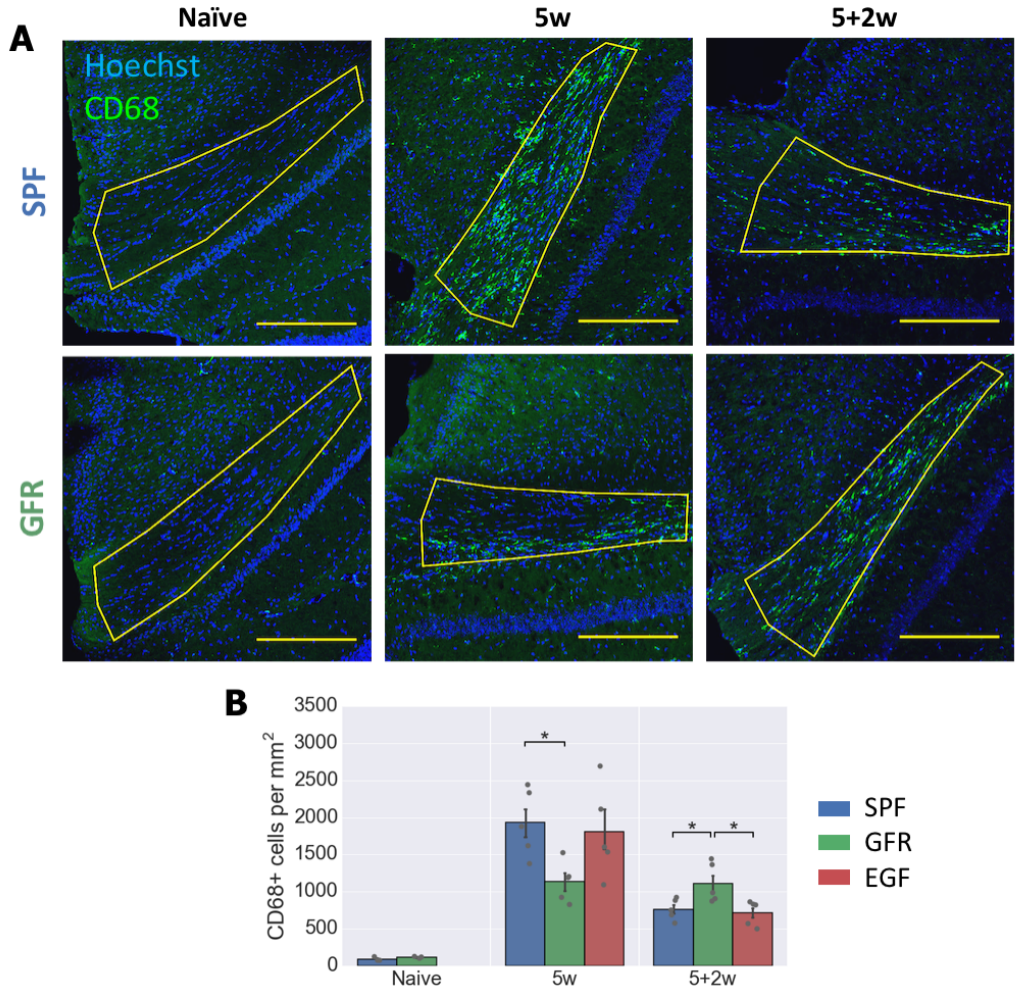

Fig. 4.4 **Activated microglia and macrophages in the demyelinated corpus callosum of GF mice.** (A) Tissue from mice before cuprizone, at the end of cuprizone and two weeks after cuprizone treatment was stained for CD68 to mark activated microglia and infiltrating macrophages. (B) 5 weeks of cuprizone treatment caused an increase in CD68+ density, but this was ≈40% less in the GFR group than the SPF controls. In contrast, the GFR group had significantly more CD68+ cells than either SPF or EGF groups two weeks later. Bars show mean ± SEM; scale bar: A = 250 µm. SPF, specific-pathogen-free controls; GFR, germ-free; EGF, ex-germ-free. *p<0.05, one-way ANOVA with Tukey HSD *post hoc* test.

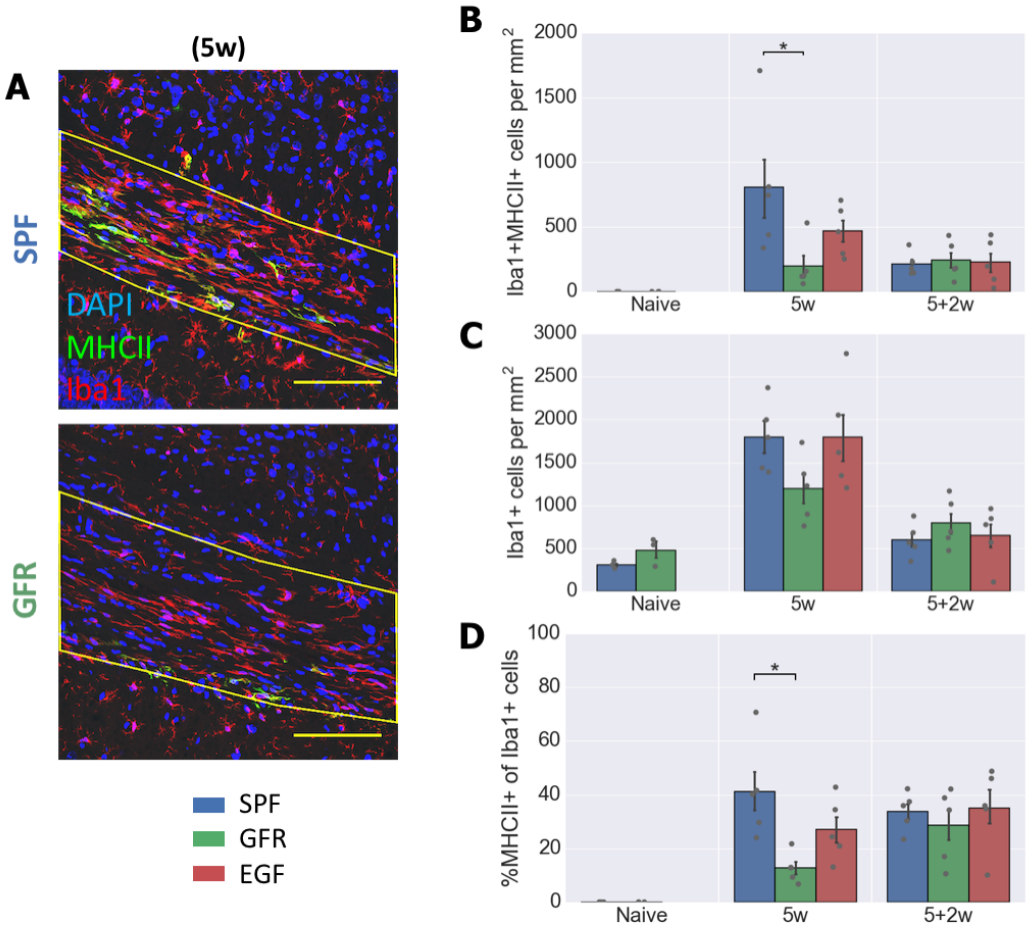

Fig. 4.5 **MHCII+ microglia and macrophages in the demyelinated corpus callosum of GF mice.** (A) Tissue from the three timepoints was stained for the M1 marker MHCII, as well as Iba1 to mark all microglia and infiltrating macrophages. (B) The density of MHCII+ microglia/macrophages was less in the GFR group than in SPF controls at the end of cuprizone treatment, an effect partially rescued in the EGF group. (C) The GFR group tended to have fewer total microglia/macrophages than the other groups at the end of cuprizone. (D) The MHCII+ proportion of total microglia/macrophages was less in the GFR compared to SPF group following cuprizone. Bars show mean ± SEM; scale bar: A = 100 µm. SPF, specific-pathogen-free controls; GFR, germ-free; EGF, ex-germ-free. *p<0.05, one-way ANOVA with Tukey HSD *post hoc* test.

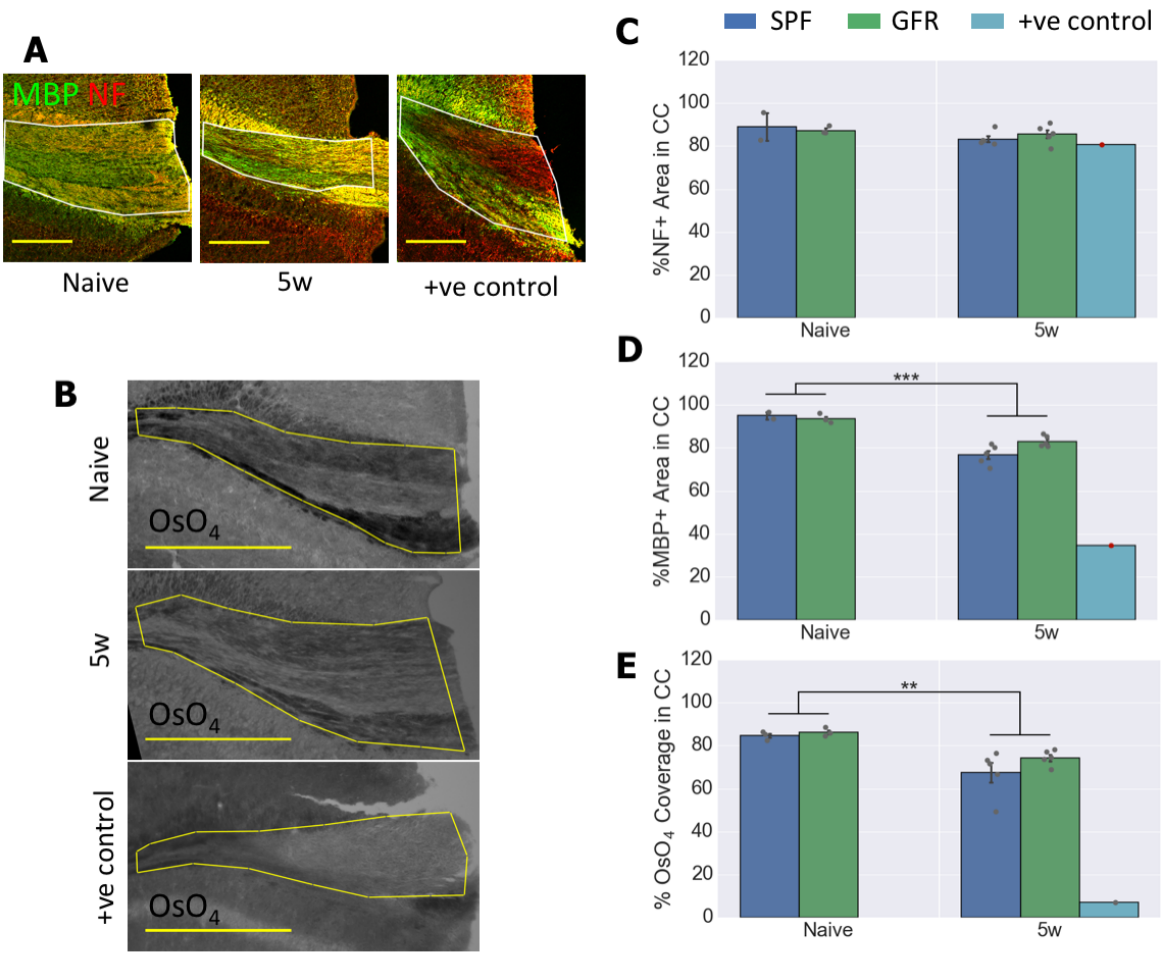

Fig. 4.6 **Quantification of myelin in the CC following cuprizone treatment.** (A) Tissue from the experiment and from a positive control animal was stained for NF to label axons along with MBP to show myelin. (B) Tissue was also stained with OsO_4 to label lipids (dark). The proportion of the CC area above a threshold for NF (C), MBP (D) and OsO_4 (E) was then quantified. Bars show mean ± SEM; scale bar: A = 250 µm, A = 500 µm. SPF, specific-pathogen-free controls; GFR, germ-free. **p<0.01, ***p<0.001, two-way ANOVA.

4.2.3 Demyelination was limited in our cuprizone model

Further analysis revealed that, unfortunately, our cuprizone regimen had not caused robust demyelination in the CC of this cohort of mice. This was determined by comparing the degree of demyelination with positive control tissue from a pilot study using an irradiated cuprizone diet (Fig. 4.6). In the CC of this positive control mouse, after 5 weeks cuprizone treatment there was maintained intensity of the neuronal marker neurofilament (NF, Fig. 4.6C), but a 60% reduction in MBP staining (Fig. 4.6D). However, in the GF study, there was only a 15% reduction in MBP positivity. To confirm this, sections were stained with

osmium tetroxide (OsO_4), which stains lipids and has been used previously to quantify the extent of demyelination (Mei et al., 2016). Similarly, the loss of OsO_4 staining in the CC was much subtler than in the positive control (Fig. 4.6B,E). This meant that, whilst the study gave us valuable insights into the inflammatory response following cuprizone administration in GF mice, its scope for studying remyelination was limited.

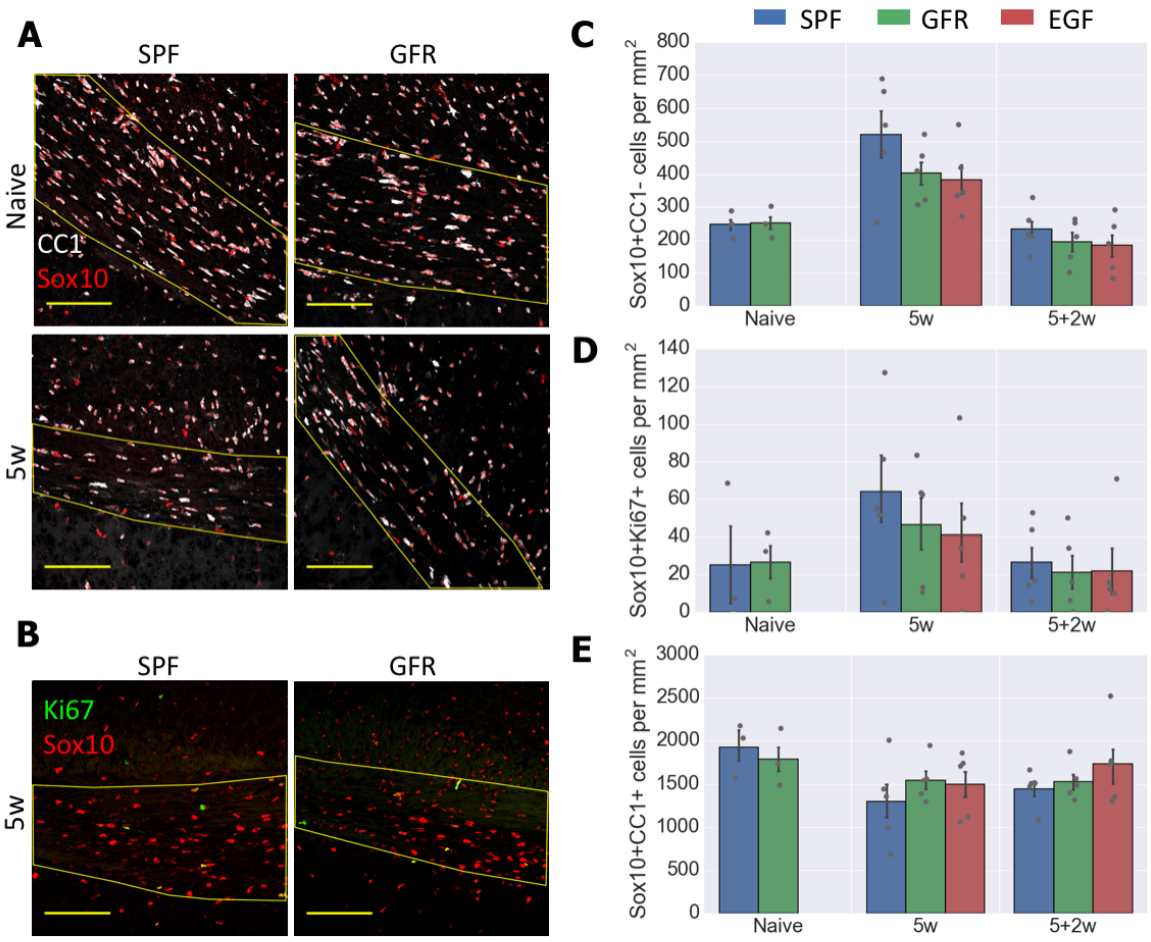

Fig. 4.7 **Oligodendrocyte lineage populations following cuprizone administration in GF mice.** Tissue from the three timepoints was stained for Sox10 to mark cells of the oligodendrocyte lineage, along with CC1 to distinguish OPCs and oligodendrocytes (A) and Ki67 to mark proliferative cells (B). The densities of Sox10+CC1- OPCs (C), Sox10+CC1-Ki67+ proliferative OPCs (D) and Sox10+CC1+ oligodendrocytes (E) were then quantified. Bars show mean ± SEM; scale bar: A,B = 100 µm. SPF, specific-pathogen-free controls; GFR, germ-free; EGF, ex-germ-free.

Nevertheless, I stained for oligodendrocyte lineage markers to investigate how these populations changed even in the context of limited demyelination and remyelination. Sox10 was used to mark all cells of the oligodendrocyte lineage, with CC1 staining for mature oligodendrocytes and Ki67 for proliferative cells (Fig. 4.7).

Following the 5 week cuprizone treatment, there was an increase in the number of OPCs in the CC, which returned to baseline levels by 2 weeks after cuprizone cessation (Fig. 4.7A,C). There were no significant differences between the experimental groups, which all displayed considerable variability. For example, there was one mouse in the SPF group that did not show an increase in OPC number, likely reflecting the fact that the demyelination was patchy throughout the CC. Consistent with an increase in OPC number, the Ki67+ proliferative population increased following cuprizone treatment, though again with substantial variability between individual mice (Fig. 4.7B,D).

The changes in Sox10+CC1+ oligodendrocyte numbers were consistent with the quantification of myelin throughout the experiment (Fig. 4.6). The cuprizone treatment did reduce the density of oligodendrocytes, though there was not a complete depletion and some animals were affected considerably more than others (Fig. 4.7A,E). In summary, whilst the efficacy of our cuprizone had been sufficient to cause inflammation, with differences between GF and SPF mice, the effects on myelin, oligodendrocytes and OPCs were less substantial and this could have obscured any inter-group differences.

4.2.4 GF mice have systemically reduced concentrations of short chain fatty acids

Some of the key mediators thought to mediate communication between the microbiota and the brain are short chain fatty acids (SCFAs), in particular acetate, propionate and butyrate (Fung et al., 2017). These are produced by the fermentation of dietary carbohydrates by certain bacteria and travel to distant sites in the host, where they can act as ligands at specific G-protein coupled receptors as well as inhibiting histone deacetylase (HDAC) activity (Fig. 1.8, den Besten et al. (2013)). Oral administration of SCFAs to GF mice can rescue much of the microglial function (Erny et al., 2015; Sampson et al., 2016); however, high millimolar doses are generally used in these studies, which likely exceeds the physiological load produced by the microbiota. As I had the opportunity to analyse peripheral tissue from GF mice, I measured the concentrations of these SCFAs in the faeces and serum by gas chromatography–mass spectrometry (GC-MS) to determine whether this could be contributing to the deficits seen in GF and antibiotics-treated mice following demyelination.

As expected, the faeces of GF mice had lower levels of all three SCFAs compared to control mice, and this was completely reversed by colonisation (Fig. 4.8A-C). In the serum, both propionate and butyrate were reduced in GF mice, whilst acetate was not significantly different (Fig. 4.8D-F). All three SCFAs were measured in the low micromolar range in serum.

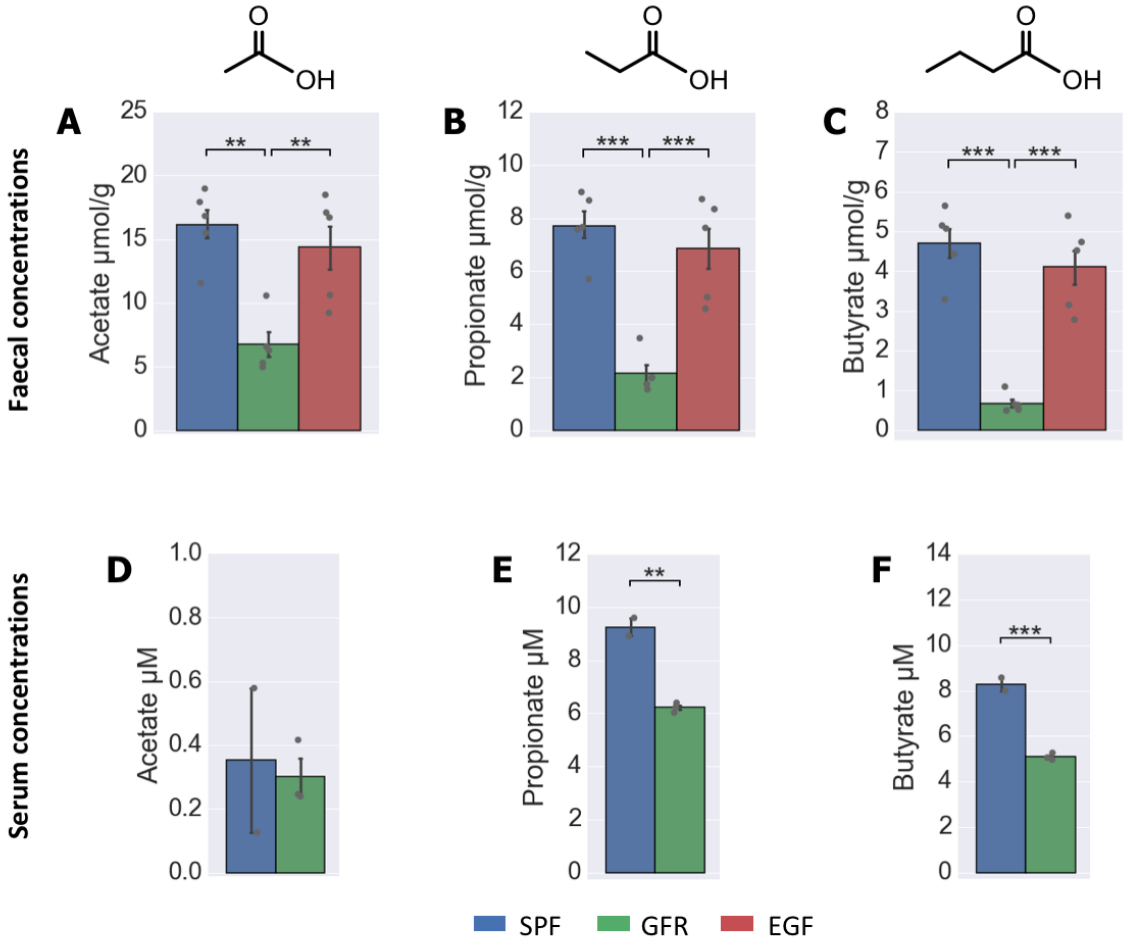

Fig. 4.8 **SCFA concentrations in the faeces and serum of GF mice.** Concentrations of of acetate, propionate and butyrate were determined by GC-MS for faecal samples (A-C) and serum samples (D-F) of mice that had not been exposed to cuprizone.Bars show mean ± SEM. SPF, specific-pathogen-free controls; GFR, germ-free; EGF, ex-germ-free. *p<0.05, **p<0.01, ***p<0.001, A-C: one-way ANOVA with Tukey HSD *post hoc* test, D-F: student's *t*-test.

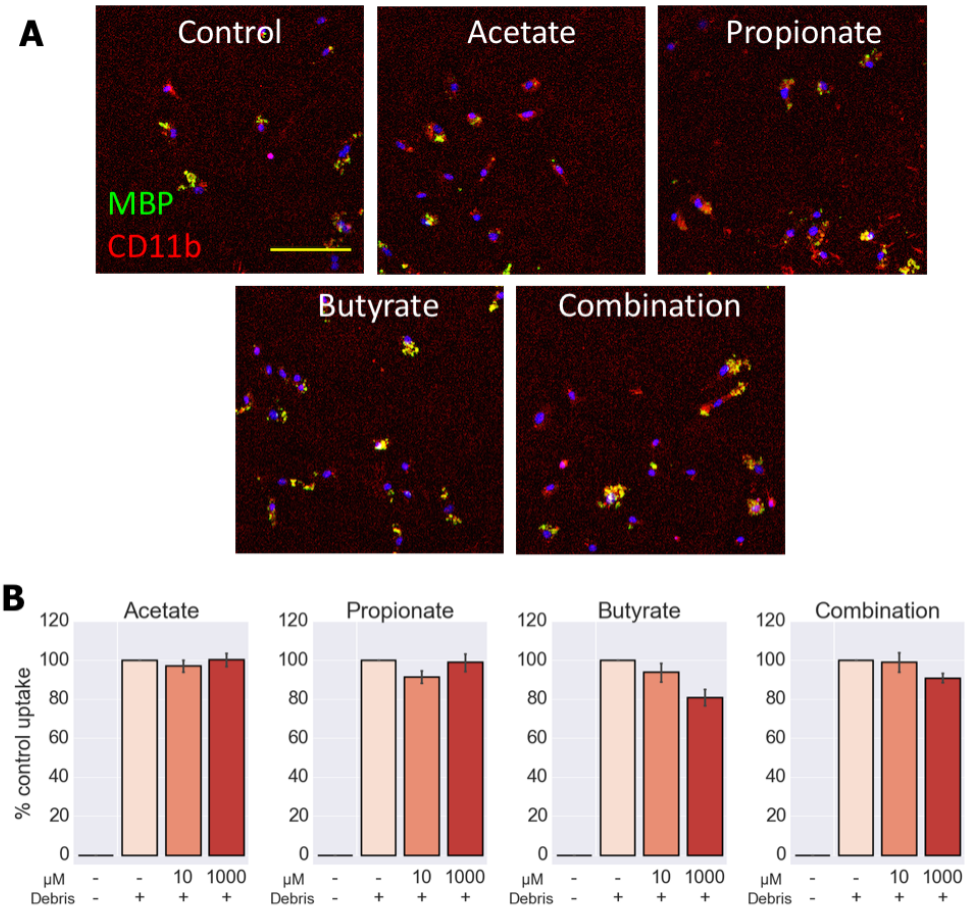

Fig. 4.9 **Phagocytosis of myelin debris by microglia *in vitro* following SCFA treatment.** (A) Primary microglia were isolated by MACS for CD11b, treated with SCFAs then exposed to myelin debris for 4 hours. These were stained for CD11b to mark microglia, and MBP to identify cells that had taken up myelin debris. (B) The fraction of cells that had phagocytosed myelin debris after 4 hours is expressed relative to microglia in control conditions with no antibiotic treatment. None of these treatments significantly modulated phagocytosis relative to control conditions. Bars show mean ± SEM; scale bar (A) = 100 μm; One-sample *t*-test with H_0: μ = 100%, and p adjusted for multiple comparisons using the Holm-Bonferroni method.

4.2.5 SCFAs influence OPC responses in vitro, but not at physiological doses

To explore whether these observed differences in SCFA concentrations could contribute to the results seen in antibiotics-treated and GF mice, I investigated the effect of acetate, propionate or butyrate when applied to microglia or OPC cultures *in vitro*. For example, it could be

that circulating SCFAs help to support a robust inflammatory response to demyelination and efficient myelin debris clearance. Mice that lack the SCFA receptor FFAR2 were indeed seen to have phenotypically similar microglia to GF mice (Erny et al., 2015). Alternatively, SCFAs may directly modulate OPC proliferation or differentiation. For these experiments, I used the same system as for assessing antibiotic efficacy *in vitro*.

Primary CD11b+ microglia from P6-8 mice were isolated by MACS and cultured with SCFA treatments consisting of acetate, propionate and butyrate at 10 µM or 1 mM concentration, either alone or in combination. After 48 hours treatment, myelin debris was added for 4 hours and stained for MBP to visualised phagocytic uptake (Fig. 4.9A). There were no differences in the phagocytic activity of microglia following any of the SCFA treatments.

Primary A2B5+ OPCs were isolated from P6-8 mice by MACS and allowed to differentiate for 8 days in the presence of SCFA treatments (Fig. 4.10). Differentiation at this timepoint was quantified as the fraction of Olig2+ cells expressing the oligodendrocyte marker CNPase. OPC differentiation was inhibited by butyrate at 1 mM concentration, either alone ($p=0.004$) or in combination with acetate and propionate ($p=0.006$). To assess proliferation, OPCs received a 3 hour pulse of EdU prior to fixation. Butyrate alone ($p<0.001$) or in combination with other SCFAs ($p<0.001$) also inhibited OPC proliferation. Again, these effects were only seen with the 1 mM treatment and not with the more physiological 10 µM concentration, which better reflects my quantification of butyrate *in vivo* (8 µM, Fig. 4.8F). In summary, the results here suggest that at physiological concentrations produced by the microbiota of SPF mice, SCFAs do not directly modulate microglia phagocytosis or OPC proliferation or differentiation.

4.3 Discussion

The aim of this study was to determine whether the deficits observed during remyelination after antibiotic treatment would be recapitulated in a germ-free system. This would provide further evidence for a role of the microbiome in supporting remyelination, rather than confounding effects of high doses of antibiotics. The technical requirements of working with GF mice made it impossible to carry out surgical lysolecithin lesions, and instead we opted for the dietary cuprizone model as a means to induce demyelination non-invasively.

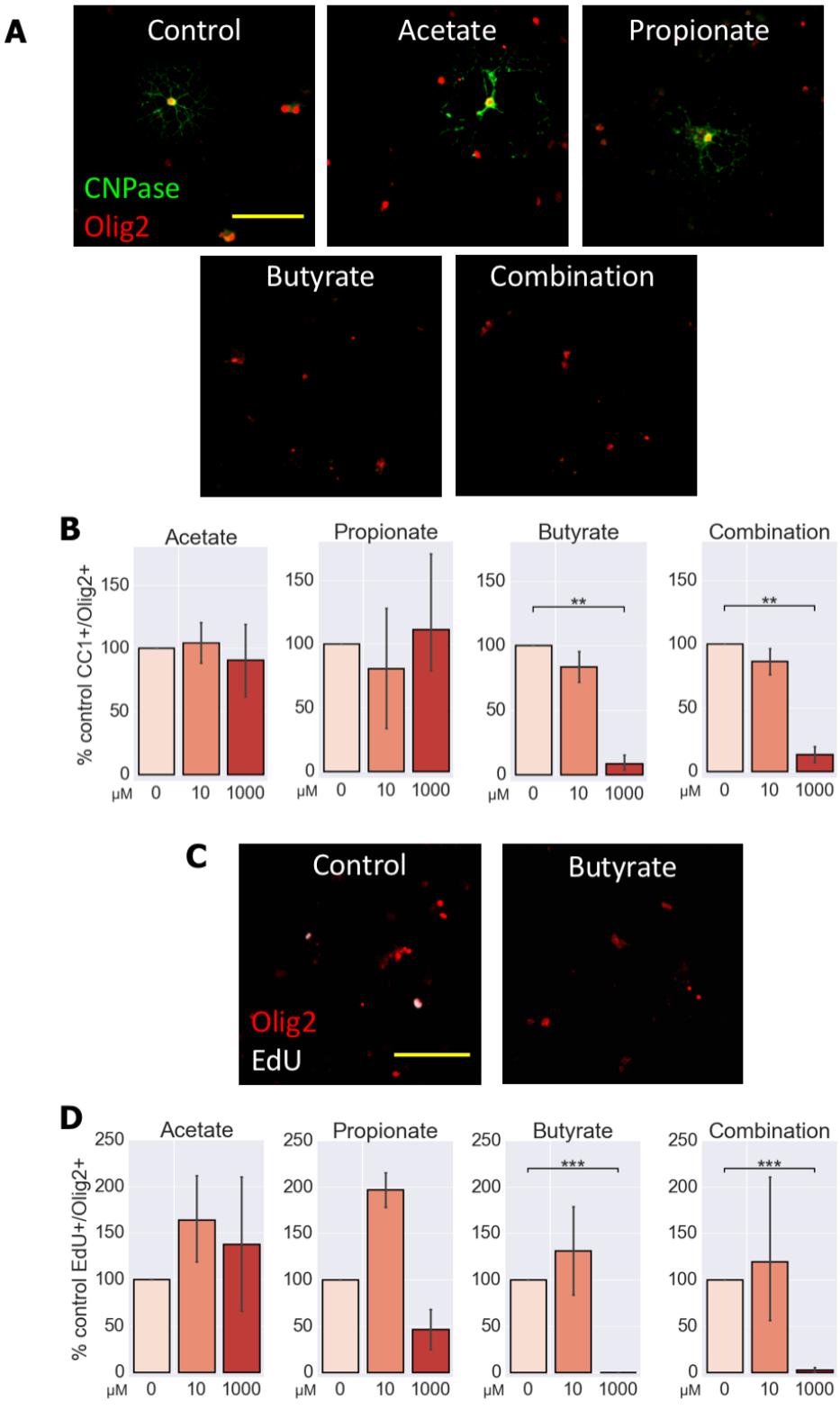
A
Control
Acetate
Propionate
CNPase
Olig2
Butyrate
Combination
B
Acetate
Propionate
Butyrate
Combination
% control CC1+/Olig2+
150
100
50
0
μM 0 10 1000
**
C
Control
Butyrate
Olig2
EdU
D
Acetate
Propionate
Butyrate
Combination
% control EdU+/Olig2+
250
200
150
100
50
0
μM 0 10 1000
***

Fig. 4.10 **OPC differentiation and proliferation *in vitro* following SCFA treatment.** (A) Primary OPCs were isolated by MACS for A2B5, and cultured with SCFA treatments for 8 days. These were stained for Olig2 to label cells of the oligodendrocyte lineage and CNPase as a marker for differentiation. (B) The fraction of CNPase+ Olig2+ cells is expressed relative to control OPCs. Both butyrate and the combination treatment inhibited proliferation at the 1 mM dose. (C) Cells were pulse-labelled with EdU to mark proliferating cells prior to fixation. (D) The EdU+ fraction of Olig2+CNPase- cells was effectively abolished by 1 mM butyrate or combination SCFA treatment. Bars show mean ± SEM; scale bar (A,C) = 100 µm. One-sample *t*-test with H_0: $\mu = 100\%$, and p adjusted for multiple comparisons using the Holm-Bonferroni method.

Despite the different mechanism, anatomical location and timecourse of cuprizone compared to lysolecithin, a similar pattern was observed in the GF mice. In particular, a blunted peak in CD68+ activated microglia/macrophages was seen, suggesting an impaired response of the innate immune system to myelin damage in the absence of a microbiome (Fig. 4.4). At the end of 5 weeks cuprizone treatment the density of CD68+ cells in the CC of GF mice was roughly half that of SPF mice, and this was rescued in the ex-GF group. The pattern was reversed by 2 weeks after cuprizone cessation: whilst inflammation had begun to resolve in the SPF and ex-GF mice, the density of CD68+ cells was maintained in the GF group.

Similarly, the expression of MHCII by Iba1+ microglia/macrophages was less in GF mice (Fig. 4.5), reproducing another finding of the antibiotics study. As well as lower counts of MHCII+Iba1+ cells, the fraction of Iba1+ microglia/macrophages expressing MHCII was reduced, suggesting that these cells are deficient not just in number, but also in function in the absence of a microbiome. Arginase-1 is an M2 macrophage/microglial marker, which also had reduced expression in antibiotics-treated mice following a lysolecithin lesion (Fig. 3.6E,F). However, arginase-1 expression has not been observed as a feature of the cuprizone model (Le Blon et al., 2016; Olah et al., 2012), so this finding could not be validated in the GF experiment.

Quantification of myelin, and oligodendrocyte/OPC numbers showed that our cuprizone regime caused only a limited degree of CC demyelination compared to positive control tissue from a pilot study (Fig. 4.6 & Fig. 4.7). This constrains the interpretation that can be made beyond differences in the innate immune response following cuprizone treatment in GF mice. Specifically, it is impossible to draw direct conclusions with regard to demyelination and remyelination. If there were indeed differences in the OPC responses consistent with the antibiotics study, the GF study was underpowered to detect these given the small effect sizes in the absence of more substantial demyelination.

Another technical consideration relates to the mechanisms at play in the cuprizone model. Whilst we are equating a robust innate immune response with conditions that are beneficial for remyelination, the innate immune system can also contribute to demyelination. This is thought to be largely driven by the adaptive immune system in diseases such as MS (Dendrou et al., 2015), but is also a well described feature of the cuprizone model, in which a direct toxicity to oligodendrocytes is compounded by a "second hit" by the immune system (Praet et al., 2014). In mice on a cuprizone diet, full demyelination is thought to depend upon microglia and neutrophils (Clarner et al., 2015; Liu et al., 2010), but not T lymphocytes or monocyte-dervied macrophages (Arnett et al., 2001; Lampron et al., 2015). Thus the reduced inflammation in the GF group could in fact have a protective effect during demyelination, had the cuprizone diet been more potent. This has been previously observed in models of demyelination that hinge more on the adaptive immune system, such as spontaneous or induced EAE in GF mice (Berer et al., 2011; Lee et al., 2011).

The deficiencies observed in the innate immune resonse of GF mice during myelin damage were generally reversed by colonisation after weaning four weeks old (Fig. 4.4 & Fig. 4.5). This effect is encouraging for the overall hypothesis, as it demonstrates a modulatory role for the microbiome throughout adulthood, rather than a peculiarity of early development in GF conditions. Consistent with this, the emerging view of the microbiota-brain axis is that a continuous input from the microbiota is required for innate immune activity in the CNS (Fung et al., 2017).

Strong candidates for this continuous signal are the short chain fatty acids - particularly acetate, propionate and butyrate - which, when administered orally to GF mice, can restore much of the morphology and function of their microglia (Erny et al., 2015; Sampson et al., 2016). Here, I confirmed by GC-MS that all three of these bacterial metabolites are found at substantially lower concentrations in the faeces of GF mice, and restored to control levels in ex-GF mice (Fig. 4.8A-C). I also saw that these differences were translated into differing concentrations in the serum, at least for propionate and butyrate (Fig. 4.8D-F). Propionate was measured at approximately 9 µM in SPF controls and 6 µM in GF mice, whereas butyrate was measured at 8 µM in SPF controls and 5 µM in GF mice. These are consistent with previous measurements of propionate and butyrate in serum (Perry et al., 2016) and the SCFAs observed in the GF mice reflects the fact that these molecules can also be produced at lower levels by endogenous host metabolism (Bourassa et al., 2016; Pouteau et al., 2003). Acetate was technically more difficult to measure, due to its smaller size and higher volatility, leading to more variable concentrations that were lower than expected (Perry et al., 2016). SCFAs are able to easily cross lipid bilayers, so the values measured in serum will reflect similar concentrations in the CNS (Mitchell et al., 2011).

I next explored whether these SCFAs *in vitro* could modulate functions of microglia and OPCs relevant to remyelination. Microglial phagocytosis was not affected by any of the SCFA treatments, even at concentrations substantially higher than measured *in vivo* (Fig. 4.9). This strongly suggests that the reduced myelin phagocytosis in antibiotics-treated mice is not due to the lack of a direct positive SCFA signal from the microbiota (Fig. 3.8). Other studies have similarly shown that, whilst high oral doses of SCFAs have a downstream stimulatory effect on microglia, this is unlikely to be a direct interaction. Erny et al. (2015) observed that the FFAR2 SCFA receptor necessary for microglial maturation is found in peripheral immune tissues but not within the CNS. Additionally, whilst the orally-administered doses of SCFAs in this study normalises colonic concentrations (Sampson et al., 2016), it likely underestimates the substantial absorption of these small, soluble molecules occurring more proximally in the digestive tract, which may give serum concentrations well above normal microbial production.

Whilst I did not investigate this here, it would also be informative to know whether SCFAs can directly modulate the polarisation of microglia or macrophages to M1 or M2 phenotypes, given the other changes in inflammation I observed *in vivo*. In a mouse colitis model, butyrate was shown to promote expression of various M2 markers in the gut, and could enhance IL-4-mediated M2 polarisation *in vitro* (Ji et al., 2016). However, this required millimolar concentrations of butyrate, which is realistic within the gut but unlikely to occur in the CNS given my serum concentration measurements.

At 1 mM concentration, I observed a strong inhibitory effect of butyrate on both OPC differentiation and proliferation *in vitro*. Whilst millimolar concentrations of butyrate have been recorded after oral administration of a precursor molecule to rats (Miyoshi et al., 2011), this is approximately 100x the concentration I measured in the serum of my SPF mice. Additionally, after antibiotic depletion of the microbiota, I observed a reduction rather than an increase in OPC differentiation, and no change in proliferation (Fig. 3.7), suggesting these results are unlikely to be relevant *in vivo*. In the high micromolar - low millimolar range, butyrate is known to exert an inhibitory effect on histone deacetylase (HDAC) enzymes (Bourassa et al., 2016; Sealy, 1978) and this is the mechanism thought to account for an inhibitory effect on human OPC differentiation at 5 mM *in vitro* (Conway et al., 2012). It may be that the most important effects of SCFAs occur locally in the colon, where they exist in high millimolar concentrations, and these could be propagated indirectly to the CNS by other means of host communication (Fung et al., 2017). However, the results of my experiments, and the wider literature, are currently inconclusive in this regard.

In summary, I have shown that in germ-free mice the inflammatory response mounted in the corpus callosum during cuprizone administration is reduced and less effective than in

control mice. Colonisation of GF mice after weaning can reverse these changes. The results here are consistent with the microglia/macrophage responses observed in lysolecithin lesions of antibiotics-treated mice, which were associated with deficits in myelin debris clearance and OPC differentiation. However, neither of these phenomena could be reliably assessed in the GF model. Mice without a microbiome had lower systemic levels of SCFAs, which have been previously linked to effects in the CNS, though my results suggest these concentrations are unlikely to influence microglia phagocytosis or OPC responses directly. These results are further evidence that the deficits seen in antibiotics-treated mice are due to depletion of the microbiota.

Chapter 5

Remyelination following probiotic administration

5.1 Introduction

5.1.1 Therapeutic uses of probiotics

Having established that a complete microbiome is essential for the normal inflammatory response to myelin injury, and that antibiotic depletion of the microbiota impairs OPC differentiation, I explored this phenomenon in a gain-of-function paradigm. Specifically, I investigated whether supplementing the microbiota with a probiotic would be a viable means to enhance remyelination.

Probiotics are formulations of live microorganisms that, when administered in adequate amounts, confer a health benefit to the host (Hill et al., 2014). The most commonly used microorganisms for this purpose are bacteria of the genera *Lactobacillus*, *Streptococcus* and *Bifidobacterium* (Scott et al., 2015). Principal advantages of probiotics as therapies are that they are non-invasive and considered relatively safe, though concerns have been raised about the lack of literature on associated risks (Sanders et al., 2010). The best established indications for probiotic therapy are diseases focussed in the gastrointestinal tract, including antibiotic-associated diarrhoea, irritable bowel syndrome and lactose intolerance (Hill et al., 2014), though a growing body of preclinical evidence suggests that probiotic efficacy can extend to sites outside the gut, including the CNS (Kigerl et al., 2016; Möhle et al., 2016; Wang et al., 2016).

For this study I used the probiotic VSL#3, a freeze-dried formulation of 8 strains of Gram-positive bacteria (Table 5.1), which has shown some clinical efficacy in treating inflammatory bowel disease and pouchitis (Ciorba, 2012). I selected this probiotic for several reasons.

Firstly, the formulation is verified to have good survival following the acidic conditions of the stomach, which is a limiting factor for many similar products (Fredua-Agyeman and Gaisford, 2015). Secondly, administration of VSL#3 has been previously associated with increased production of SCFAs, which are known to be positive regulatory signals for microglia function and were reduced in our GF mice (Yadav et al., 2013). Importantly, VSL#3 has also been recently shown to have therapeutic effects in the CNS, reversing age-related electrophysiological changes in the rat hippocampus (Distrutti et al., 2014) and improving outcome in a spinal cord contusion model in mice (Kigerl et al., 2016).

Genus	Strain
Streptococcus	*Streptococcus thermophilus*
Bifidobacterium	*Bifidobacterium breve* *Bifidobacterium longum* *Bifidobacterium infantis*
Lactobacillus	*Lactobacillus paracasei* *Lactobacillus acidophilus* *Lactobacillus delbrueckii subsp. Bulgaricus* *Lactobacillus plantarum*

Table 5.1 **Bacterial strains comprising the probiotic VSL#3.**

As I was intending to see a gain-of-function effect, I chose to use aged mice for this study, in which remyelination would be suboptimal with scope for improvement. This approach has been used in previous studies intending to enhance remyelination (Huang et al., 2011; Ruckh et al., 2012). Additionally, ageing is characterised by predictable changes in the microbiota (Claesson et al., 2012), whilst calorie restriction, an intervention known to reverse many of the hallmarks of ageing, is associated with an increase in *Lactobacillus* and *Bifidobacterium* genera (Zhang et al., 2013), both of which are represented in the probiotic VSL#3.

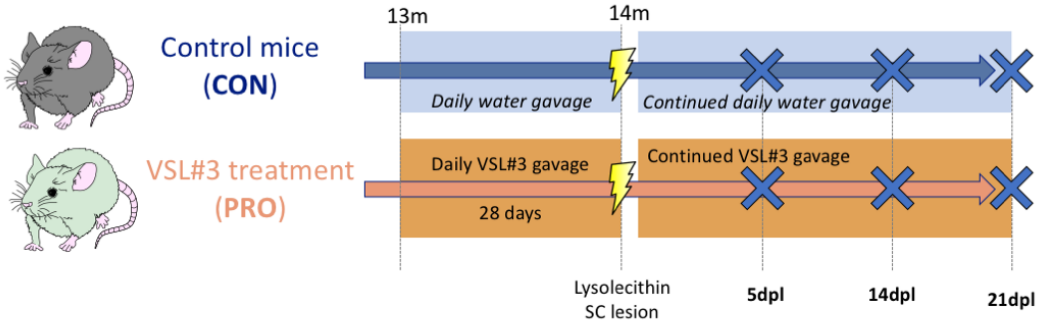

Fig. 5.1 **Schematic diagram of the probiotic study**, showing the timings of probiotic administration, lesioning and perfusion.

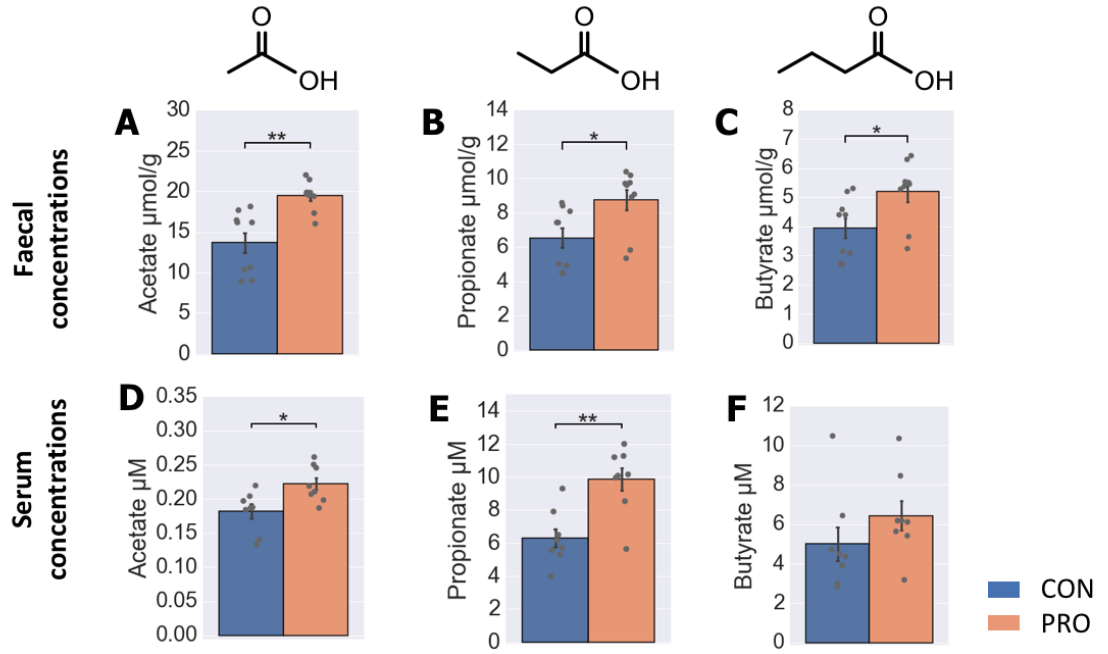

Fig. 5.2 **SCFA concentrations in the faeces and serum of probiotic-treated mice.** Concentrations of of acetate, propionate and butyrate were determined by GC-MS for faecal samples (A-C) and serum samples (D-F) of mice prior to perfusion. Bars show mean ± SEM. CON, control; PRO, probiotic. *p<0.05, **p<0.01, Student's *t*-test.

5.1.2 Experimental design

13 month old female C57BL/6 mice were administered a daily dose of 1.35×10^9 colony forming units (CFU) of VSL#3 suspended in 100 µl autoclaved water by oral gavage for 28 days (**PRO**). These were compared to age-matched control mice, which were instead gavaged daily with 100 µl water (**CON**). Control and probiotic-treated mice were housed in separate racks necessitating a change of gloves between handling, to avoid cross-contamination. Following this treatment, all groups received an injection of 1 µl lysolecithin into the spinal cord ventral white matter to cause focal demyelination. Gavage treatments were recommenced from two days after this surgery. Mice were then sacrificed by perfusion-fixation with 4% PFA at either 5 or 14 days post lesion (**5dpl** and **14dpl**) or with 4% glutaraldehyde at 21 days post lesion for resin sections (**21dpl**) (Fig. 5.1).

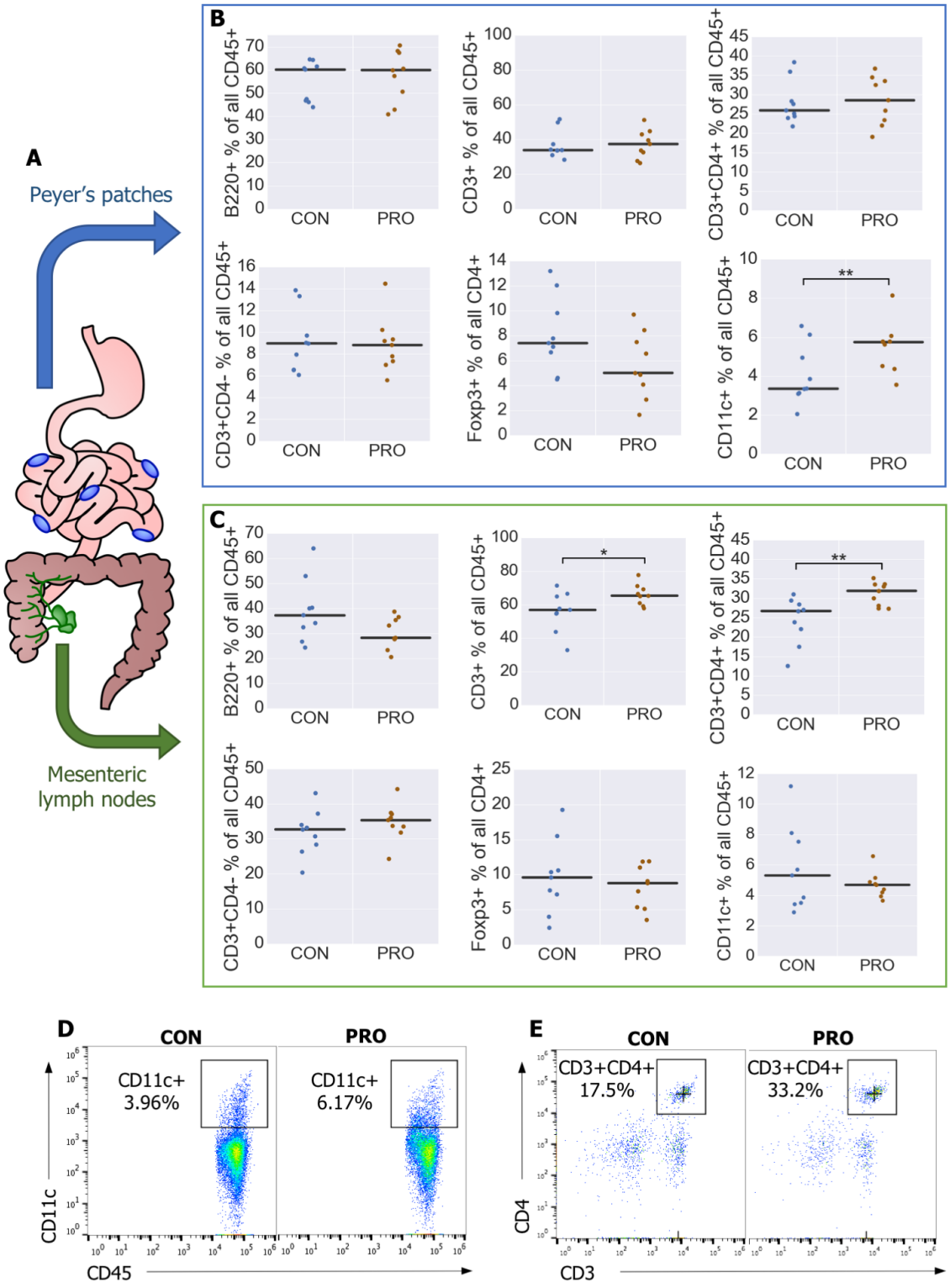
A
Peyer's patches
Mesenteric lymph nodes
B
C
B220+ % of all CD45+
CD3+ % of all CD45+
CD3+CD4+ % of all CD45+
CD3+CD4- % of all CD45+
Foxp3+ % of all CD4+
CD11c+ % of all CD45+
CON
PRO
*
**
D
CON
PRO
CD11c+ 3.96%
CD11c+ 6.17%
CD11c
CD45
E
CD3+CD4+ 17.5%
CD3+CD4+ 33.2%
CD4
CD3

Fig. 5.3 **Flow cytometry analysis of gut-associated lymphoid tissue from probiotic-treated mice.** (A) Tissue was harvested from Peyer's patches (PPs) and mesenteric lymph nodes (MLNs) prior to perfusion. (B) PP and (C) MLN quantifications for B cells (B220+), T cells (CD3+), CD4+/- T cells, T_{reg} cells (CD4+Foxp3+) and dendritic cells (CD11c+). (D) Sample plots for CD45+CD11c+ dendritic cells from PPs. (E) Sample plots for CD4+ T cells from MLNs. Horizontal lines show median value; CON, control; PRO, probiotic. *p<0.05, **p<0.01, Student's *t*-test.

I designed this experiment with input from Robin Franklin, Chao Zhao and Alerie Guzman de la Fuente (Cambridge). Ginez Gonzalez and Alerie Guzman de la Fuente (Franklin Lab, Cambridge) assisted me with the surgeries, and I carried out the perfusions and subsequent analysis of the tissue. Dan Ma (Franklin Lab, Cambridge) advised regarding the flow cytometry and Fynn Krause (Department of Biochemistry, Cambridge) advised and assisted with the gas chromatography-mass spectrometry. The VSL#3 was kindly provided by Janine de Beer (Ferring Pharmaceuticals Ltd.) and I am very grateful to Jon Lock and Chris Brown (Cambridge) for their help with the daily gavage treatments.

5.2 Results

5.2.1 VSL#3 enhances circulating SCFAs and influences the immune system in the gut

To assess whether VSL#3 administration would successfully increase concentrations of SCFAs locally and peripherally, I collected faecal and serum samples from the mice prior to perfusion. As described previously, concentrations of acetate, propionate and butyrate were quantified by GC-MS (Fig. 5.2). In the faecal samples there was an enrichment of all three SCFAs amongst the probiotic-treated group. This pattern was also seen in the serum for acetate (p=0.013) and propionate (p=0.002), whereas there was no difference detected in serum butyrate concentrations. Again, serum concentrations were detected in the lower micromolar range.

My studies *in vitro* suggested a direct effect of circulating SCFAs on microglia or OPCs was unlikely. It may be that the microbiota influence other aspects of host physiology with indirect communication to the CNS. One possibility is the modulation of immune cells in gut-associated lymphoid tissue (GALT) through high local doses of SCFAs or other molecular

signals, and it was recently demonstrated that the microbiota can influence outcome in an ischaemic stroke model by promoting the trafficking of γδ T cells between the gut and the brain (Benakis et al., 2016). I explored how my probiotic treatment would affect immune cell populations in two types of GALT: Peyer's patches (PPs), which are nodules of lymphoid tissue in the small intestinal wall, and the mesenteric lymph nodes (MLNs) draining the small and large intestine (Fig. 5.3A).

There was no effect on the total proportion of cells expressing the pan-leucocyte marker CD45 in either PPs (p=0.24) or MLNs (p=0.39), suggesting total numbers of leucocytes were not altered following probiotic treatment. Subpopulations of leucocytes were analysed as a fraction of this CD45+ population. I used a panel of antibodies that included B220 (B cells), CD3 (T cells) and CD11c (dendritic cells) (Yu et al., 2016). Within the CD3+ T cell population, I also assessed CD4+ T helper cells and CD4+Foxp3+ T_{reg} cells.

In the PPs, following probiotic treatment there was a significant increase in the proportion of CD45+ cells positive for CD11c (p=0.044), a marker expressed primarily by dendritic cells (Fig. 5.3B). There were no differences detected amongst populations of B or T cells. In the MLNs, the CD11c+ cell numbers were consistent between groups, but the probiotic treatment caused an increase in the CD3+ T cell population (p=0.046, Fig. 5.3C). This was largely attributable to an increase in CD4+ T helper cells (p=0.008); however, there was no difference in CD4+Foxp3+ T_{reg} cell numbers (p=0.51). In summary, probiotic treatment increased intenstinal and systemic levels of SCFAs, and enhanced populations of dendritic cells and CD4+ T cells in the gut-associated lymphoid tissue.

5.2.2 VSL#3 enhances the onset of inflammation following demyelination

Having established some effects on host physiology peripherally, I next investigated how the probiotic treatment might influence the innate immune response within the CNS, following toxin-mediated demyelination. As with the previous studies, I stained for CD68 to label activated microglia and infiltrating macrophages (Fig. 5.4). I observed a small increase in the density of macrophages at 5dpl amongst the probiotic group (p=0.027).

I followed this up by staining for additional macrophage/microglial markers (Fig. 5.5). Probiotic treatment caused an increase at 5dpl in the numbers of iNOS+CD68+ cells (p=0.024, Fig. 5.5C,D). However, unlike in the antibiotics and GF studies, there was no significant difference in the density of macrophages/microglia expressing MHCII, another M1 marker (p=0.14, Fig. 5.5A,B). As for M2 markers, probiotic treatment increased the number of MR+CD68+ cells at 5dpl (p=0.041, Fig. 5.5G,H), but no difference in Arg1+CD68+ mi-

croglia was observed (p=0.24, Fig. 5.5E,F). No differences were detected at 14dpl, though this may have been limited by fewer replicates at this timepoint (n=3-4, compared to n=5 at 5dpl).

Following antibiotic-mediated depletion of the microbiome, a reduced inflammatory response was associated with impaired clearance of myelin debris (Fig. 3.8). I quantified myelin debris in the lesions of probiotic-treated mice to determine if this would be cleared more rapidly following an enhanced inflammatory response (Fig. 5.6). The fraction of the lesion positive for the dMBP epitope was not altered by the probiotic treatment at either 5dpl (p=0.80) or 14dpl (p=0.65), suggesting that the increase in activated microglia/macrophages observed at 5dpl does not translate to more rapid myelin debris clearance.

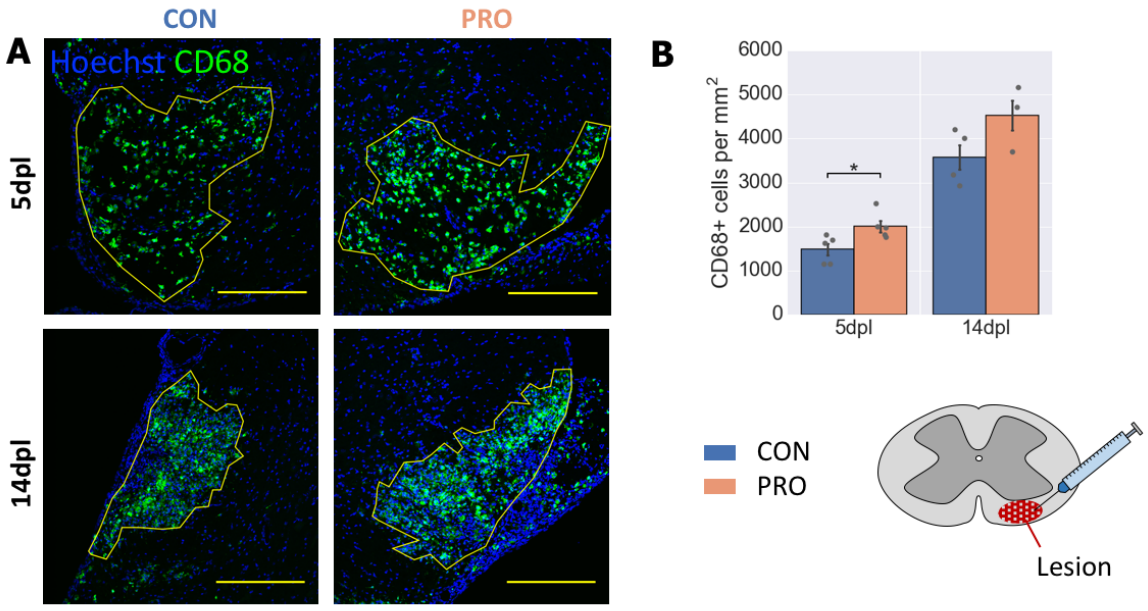

Fig. 5.4 **Activated microglia and macrophages in the lesions of probiotic-treated mice.** (A) Tissue from 5 and 14 days post lesion (dpl) was stained for CD68 to mark activated microglia and infiltrating macrophages. (B) At 5dpl, the group receiving probiotic treatment had a higher density of CD68+ cells in the lesion area. Bars show mean ± SEM; scale bar: A = 250 µm. CON, control; PRO, probiotic. *p<0.05, Student's *t*-test.

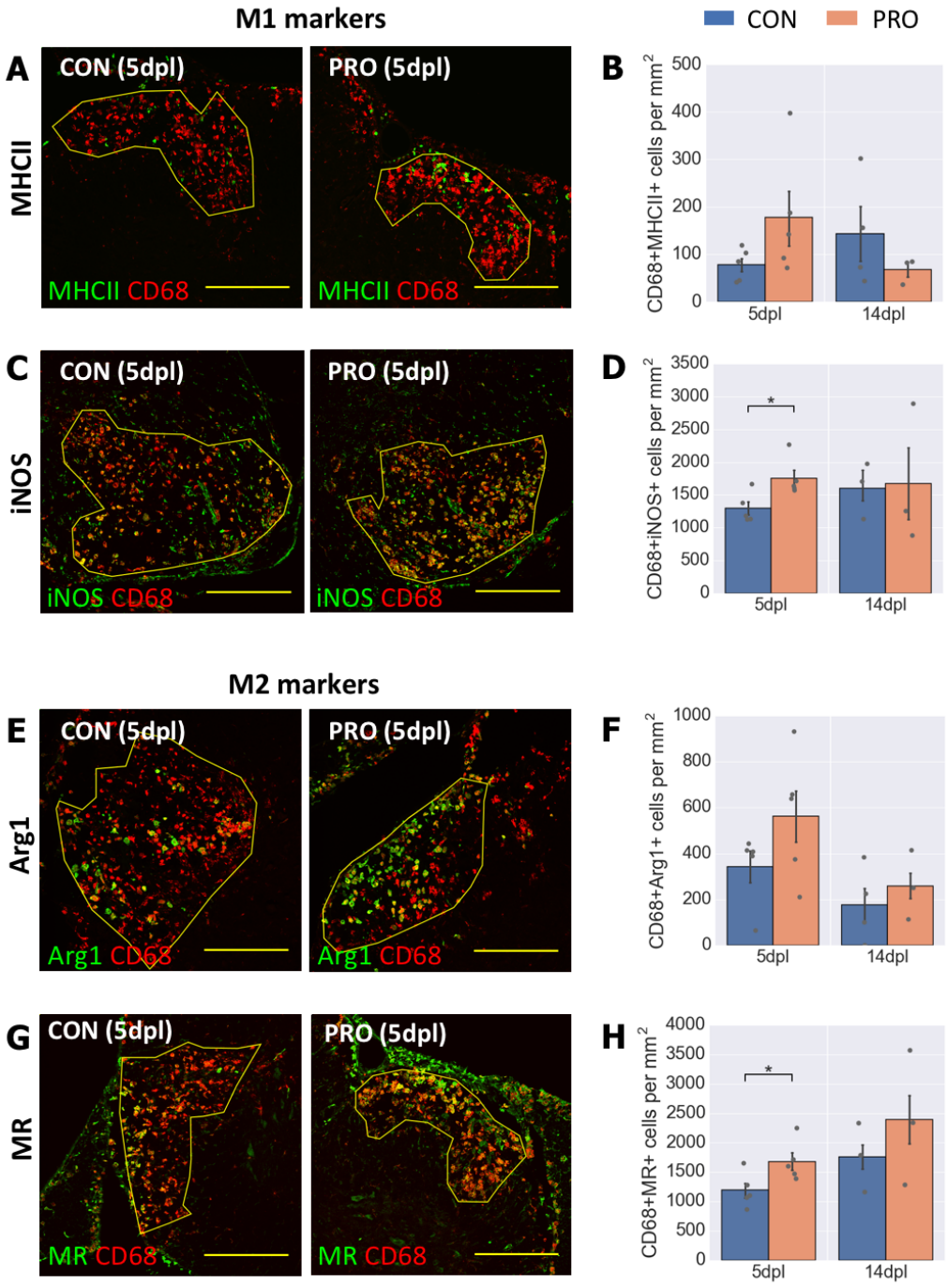

Fig. 5.5 **Probiotic treatment affects expression of different inflammatory markers following demyelination.** Lesion tissue from 5 and 14dpl was co-stained with CD68 and different M1 (A-D) and M2 (E-H) markers. At 5dpl, both iNOS+CD68+ cells (C,D) and MR+CD68+ cells (G,H) were increased in number following probiotic treatment. Bars show mean ± SEM; scale bar (A,C,E,G) = 250 µm. CON, control; PRO, probiotic. *p<0.05, Student's *t*-test.

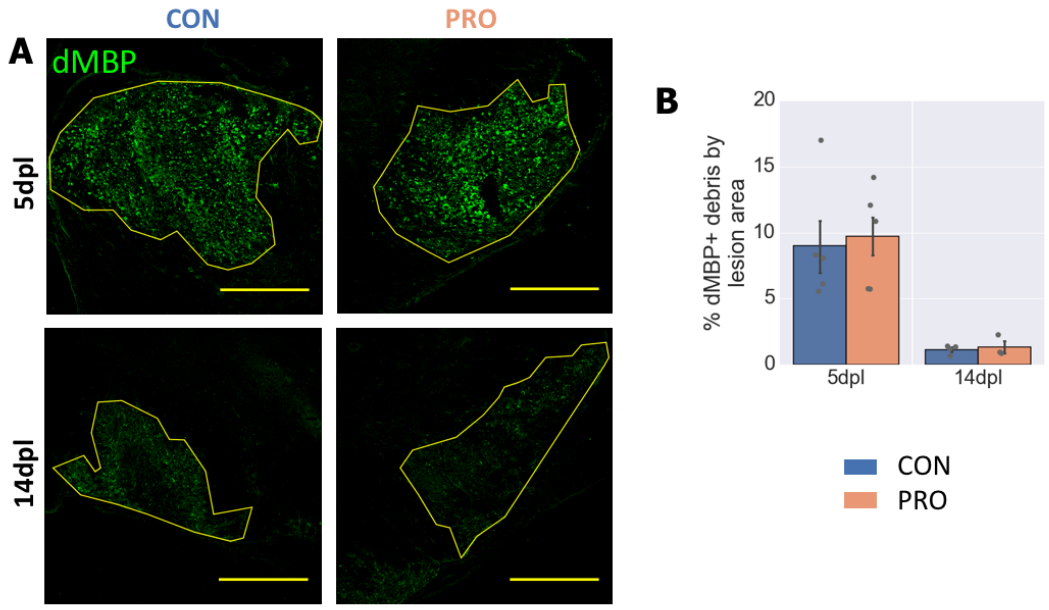

Fig. 5.6 **Myelin debris clearance following demyelination in probiotic-treated mice.** Tissue from 5 and 14dpl was stained for dMBP to visualise myelin debris. The area of positive staining for each marker is expressed as a percentage of the total lesion area for each group at each timepoint (B). There was no significant difference between the two groups at either timepoint. Bars show mean ± SEM; scale bar (A) = 250 µm. CON, control; PRO, probiotic. Student's *t*-test.

5.2.3 VSL#3 does not alter OPC differentiation or remyelination

I next assessed whether probiotic treatment could alter the OPC response to demyelination. For this study, I also included a later timepoint at 21dpl, from which I quantified remyelination from 0.75 µm resin sections.

Cells of the oligodendrocyte lineage were again identified by positivity for Sox10, with Ki67 used to mark proliferating cells and CC1 to label differentiated oligodendrocytes. There were no differences in OPC proliferation at either 5 or 14dpl (Fig. 5.7A,B), nor in the total density of Sox10+CC1- OPCs within the lesion (Fig. 5.7C,D). At 5dpl, there were more Sox10+CC1+ oligodendrocytes in the lesions of probiotic-treated mice than controls (p=0.043, Fig. 5.7C,E). As this timepoint is considered too early for significant OPC differentiation to occur, even in young adults (Keough et al., 2015), this may well reflect a reduction in oligodendrocyte death, rather than an enhancement in differentiation. At 14dpl, there was no significant difference between control and probiotic oligodendrocyte numbers (p=0.34).

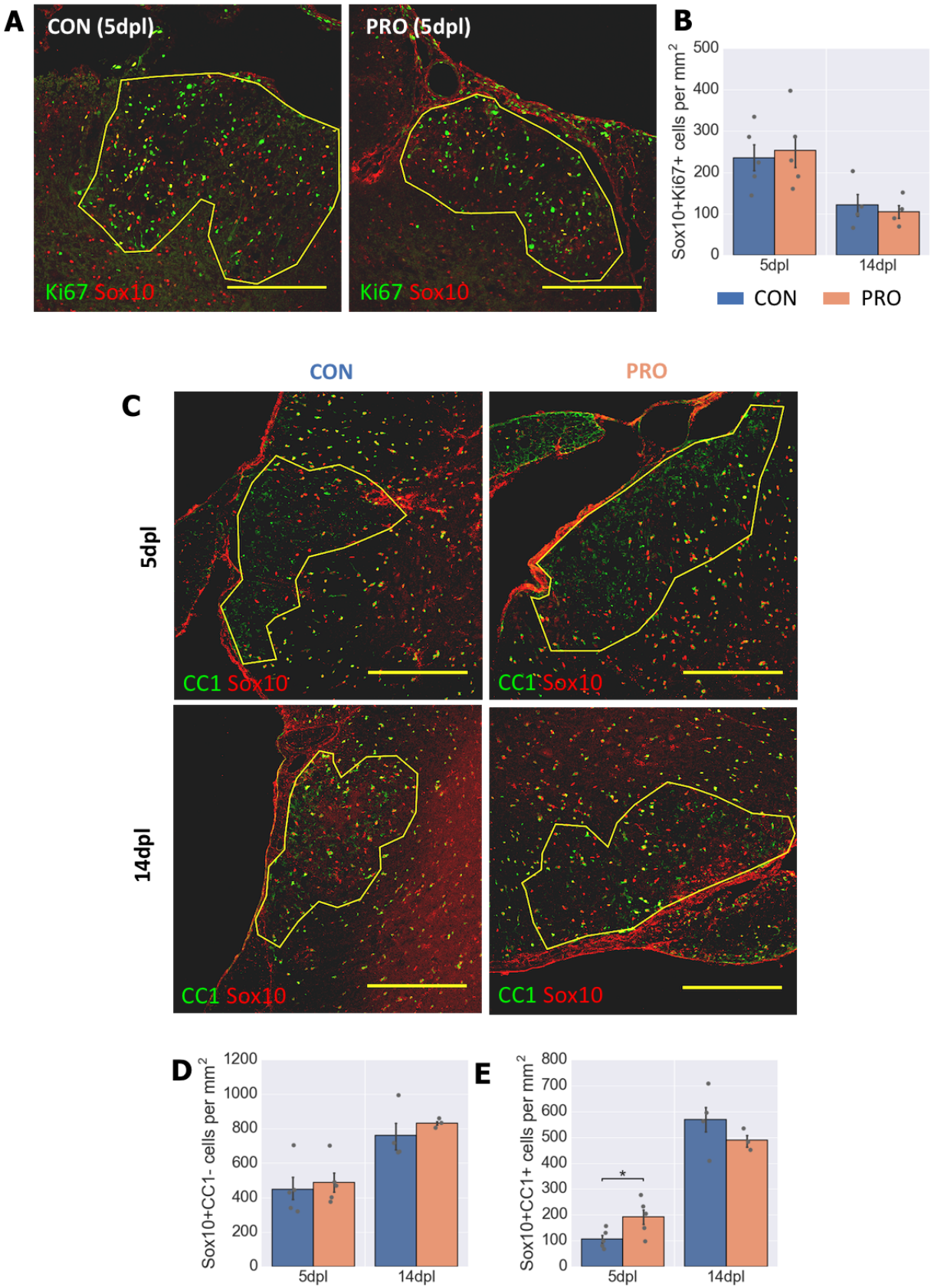
A
CON (5dpl)
Ki67 Sox10
PRO (5dpl)
Ki67 Sox10
B
Sox10+Ki67+ cells per mm2
500
400
300
200
100
0
5dpl
14dpl
CON
PRO
C
CON
PRO
5dpl
14dpl
CC1 Sox10
CC1 Sox10
CC1 Sox10
CC1 Sox10
D
Sox10+CC1- cells per mm2
1200
1000
800
600
400
200
0
5dpl
14dpl
E
Sox10+CC1+ cells per mm2
800
700
600
500
400
300
200
100
0
*
5dpl
14dpl

Fig. 5.7 **OPC responses to demyelination in probiotic-treated mice.** Tissue from 5 and 14dpl was stained for Sox10 to mark cells of the oligodendrocyte lineage. This was co-stained with Ki67 (A) to visualise proliferating OPCs or CC1 (C) to distinguish Sox10+CC1- OPCs from Sox10+CC1+ oligodendrocytes. There was no difference between the groups in the density of Sox10+Ki67+ proliferating OPCs (B) or of total Sox10+CC1- OPCs (D) at either timepoint. The probiotics-treated group had more Sox10+CC1+ oligodendrocytes at 5dpl, but there was no difference between the groups at 14dpl (E). Bars show mean ± SEM; scale bar (A,B) = 250 µm. CON, control; PRO, probiotic. *p<0.05, Student's *t*-test.

Finally, I analysed remyelination in probiotic-treated mice using 0.75 µm resin sections obtained at 21dpl. These were stained with toluidine blue to visualise myelin sheaths (Fig. 5.8A,B) and the extent of remyelination was ranked independently by two blinded assessors. Consistent with the similar numbers of oligodendrocytes at 14dpl, there was no difference in ranked remyelination at 21dpl (assessor 1, p=0.40; assessor 2, p=0.83; Fig. 5.8C).

5.2.4 A higher dose of VSL#3 is associated with mortality in aged mice

Previous studies of VSL#3 in mice have used a wide range of doses to ellicit systemic effects (Calcinaro et al. (2005): 9×10^8 CFU three times/week; Li et al. (2016): 1×10^9 CFU twice/week; Kigerl et al. (2016): 4.5×10^9 CFU/day). However, there is little data available on VSL#3 administration in aged mice. To determine whether the efficacy of our probiotic intervention was limited by the dose, I trialled some mice with a higher daily dose of VSL#3. This consisted of 4.5×10^9 CFU per day: approximately three time higher than my original dose of 1.35×10^9 CFU.

However, within the first few days there was significant mortality within the probiotic-treated group (p=0.017, Fig. 5.9). Post-mortem analysis of these mice revealed diffuse inflammation involving the lungs, spleen, abdominal lymph nodes, kidneys and pancreas, which was characterised by infiltrates of neutrophils, macrophages and lymphocytes. This was accompanied by the presence of Gram-positive rods and cocci in the alveolar spaces and walls. These changes suggest that at this higher dose, a significant bacterial load reached the lungs during gavage, causing a pneumonia with a systemic immune response. The toxicity observed prevented us from determining whether 4.5×10^9 CFU per day of VSL#3 would influence remyelination more effectively.

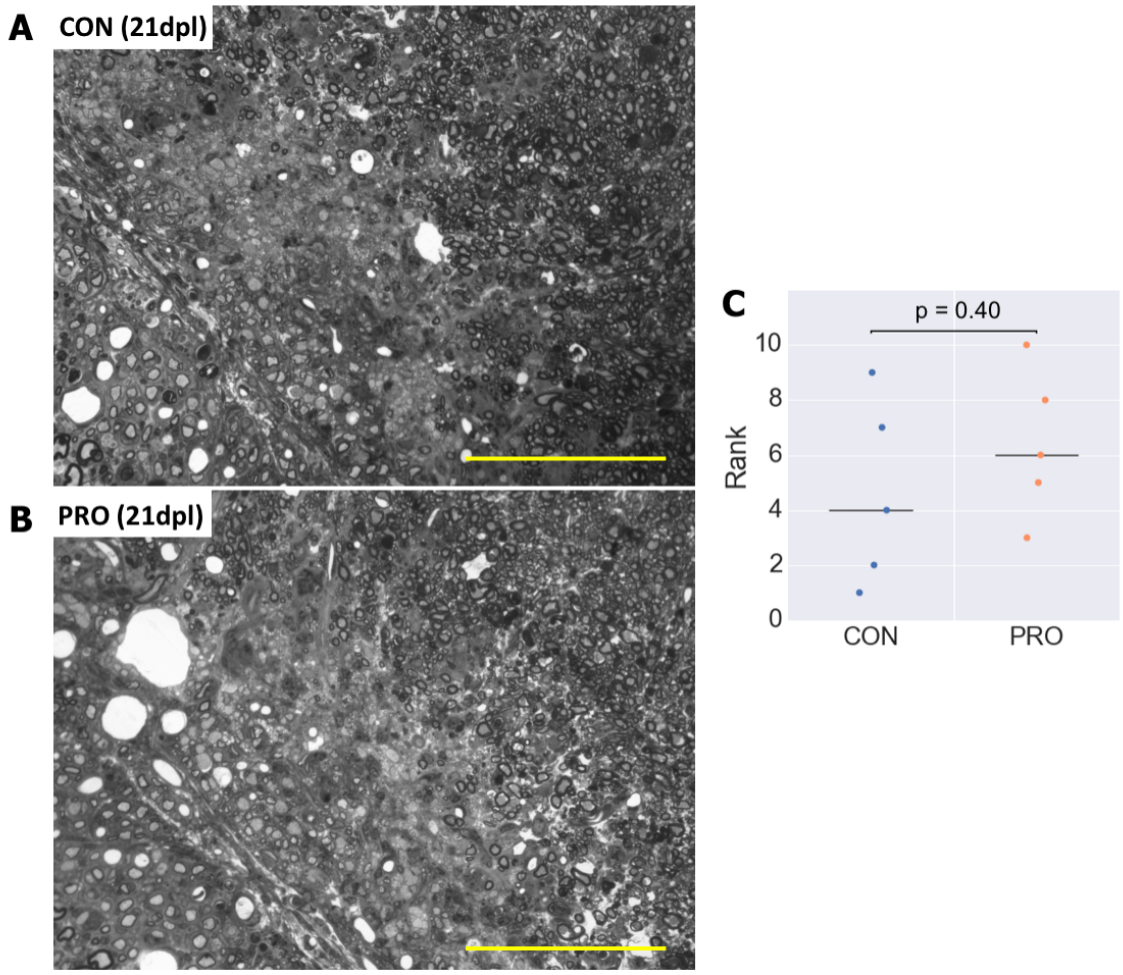

Fig. 5.8 **Remyelination in probiotic-treated mice.** Tissue from 21dpl was embedded in resin and semithin sections stained with toluidine blue. Lesions were ranked by blinded assessors based on the extent of remyelination, with 10 being the most complete. (A) Representative image of a lesion from the control group (rank = 7). (B) Representative image of a lesion from the probiotic group (rank = 8). (C) Ranks assigned by assessor 1. Neither assessor observed a difference in remyelination between the probiotic and control groups. Horizontal lines show median for each group. Images are displayed in grayscale; scale bar (A,B) = 100 µm. CON, control; PRO, probiotic. Mann–Whitney *U* test.

5.3 Discussion

I undertook this study to explore whether the insights obtained from studying remyelination in antibiotics-treated and GF mice could be applied to improve the outcome of remyelination. As an intervention, I selected the probiotic VSL#3, a combination of 8 strains of Gram-positive bacteria with known effects on the CNS (Distrutti et al., 2014; Kigerl et al., 2016).

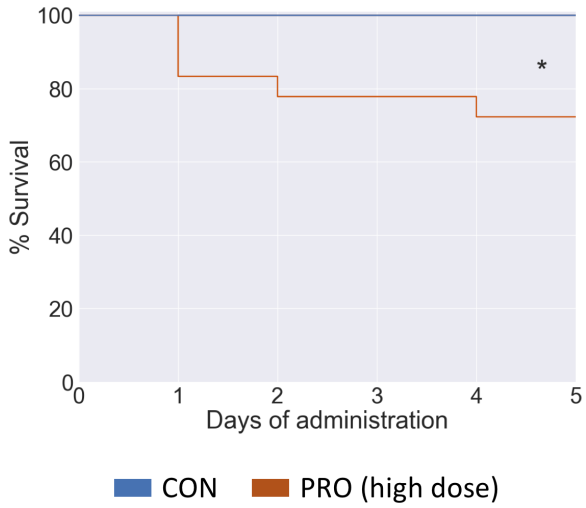

Fig. 5.9 **Survival of mice administered a higher dose of VSL#3.** Mice were gavaged with 4.5×10^9 CFU of VSL#3 probiotic per day, suspended in 100 µl autoclaved water. The treated group suffered significant mortality within the first few days of administration. CON, control; PRO, probiotic. *p<0.05, log-rank test.

By analysing the peripheral tissues of VSL#3-treated mice, I observed several changes that could be of relevance to inflammation in the CNS. Firstly, there were elevated levels of SCFAs in the serum of probiotic-treated mice (Fig. 5.2), contrasting the reduction of SCFAs in GF mice (Fig. 4.8). Specifically, all three SCFAs were present at higher concentrations in faeces, whilst acetate and propionate were also increased in the serum. A previous study suggested that increased butyrate production was important for systemic effects of VSL#3 on metabolism, but that this was acting indirectly via a local target in the gut (Yadav et al., 2013).

I investigated two types of GALT as a site at which signals from the microbiota may be integrated and communicated to distant sites in the body (Benakis et al., 2016; Fung et al., 2017). Following probiotic treatment, I observed an increase in CD11c+ dendritic cells in Peyer's patches (PPs), whilst CD4+ T cells were elevated in mesenteric lymph nodes (MLNs) (Fig. 5.3). The increase in PP dendritic cells is consistent with another study in which GALT was administered following VSL#3 administration (Mariman et al., 2015). As PPs are solely associated with the small intestine, which has substantially lower microbial colonisation than the colon (Donaldson et al., 2015), this may reflect a local innate immune response to increased dietary antigenic load (Lelouard et al., 2012).

In contrast, the MLNs drain lymphatics from the entire intestine, including the caecum and colon, where most of the microbiota are located and fermentation-derived metabolites such as SCFAs are produced in the highest concentrations (Houston et al., 2016). They are also a site to which dendritic cells from PPs and the the intestinal lamina propria can migrate to present their sampled antigens (Worbs et al., 2017). Analysis of MLN tissue revealed increased numbers of CD4+ T cells following VSL#3 treatment (Fig. 5.3). It has recently

been shown that altered trafficking of lymphocytes between the GALT and the CNS is a means by which changes in the microbiota can alter outcome in a model of ischaemic stroke (Benakis et al., 2016). In this study, beneficial effects on stroke outcome were associated with elevated GALT numbers of CD4+Foxp3+ T_{reg} cells, a population with a newly-appreciated role in promoting remyelination (Dombrowski et al., 2017). Other studies have reported that VSL#3 can specifically enhance populations of T_{reg} cells in GALT (Kigerl et al., 2016; Mariman et al., 2015). However, here I did not detect a difference in the proportion of CD4+ cells expressing Foxp3 ($p=0.51$) or in the CD4+Foxp3+ proportion of total CD45+ leukocytes ($p=0.45$), suggesting that differences in the precise regimen, the age of the mice or other factors may shape the host immune response to this probiotic.

I next studied how probiotic administration would alter the response to lysolecithin-induced demyelination in the CNS. Lesions from the probiotic-treated group had a higher density of CD68+ activated microglia/macrophages than controls at 5dpl (Fig. 5.4). This was in contrast to antibiotics-treated mice, which had a higher peak of CD68+ at 14dpl but no difference at an earlier 7dpl timepoint. The germ-free mice, whilst undergoing demyelination by a different mechanism, also had a late peak of CD68+ cells, which were present at lower densities than in SPF controls at the earlier timepoint. Taken together, these results might suggest that signals derived from the microbiome encourage a swifter response by the innate immune system following demyelination.

The elevated CD68+ activated microglia/macrophages at 5dpl in probiotic-treated mice encompassed increases in iNOS+ and MR+ subpopulations (Fig. 5.5). These are different markers to those highlighted by the antibiotics study (in which MHCII and Arg1 were both reduced) and the GF study (in which MHCII was reduced). Here, no differences were detected in MHCII+ or Arg1+ populations, though both were present in relatively small numbers with high variability between mice, hence sample size might have limited the sensitivity. It is notable that in both this and in the antibiotics study, individual M1 or M2 markers were not necessarily modulated together, emphasising how it is important not to enforce the label of M1 or M2 on activated macrophage/microglia subpopulations *in vivo* (Murray et al., 2014).

As for the outcome of remyelination, probiotic treatment did not influence OPC proliferation or differentiation (Fig. 5.7), nor the ranked extent of remyelination at 21dpl (Fig. 5.8). Whilst in antibiotics-treated mice, the impaired OPC differentiation was associated with reduced myelin debris clearance, here no difference in myelin debris clearance was seen (Fig. 5.6). Thus it might be that, whilst the probiotic did enhance inflammation at 5dpl, this was the wrong type of inflammation or otherwise insufficient to promote more rapid removal of myelin. In a heterochronic parabiosis model in which remyelination was successfully

rejuvenated in aged mice, a similar increase in MR+ microglia/macrophages was seen, but this was also accompanied by increased Arg1+ cells and more rapid myelin debris clearance (Miron et al., 2013; Ruckh et al., 2012).

However, a 3x higher dose of VSL#3 was seen to have associated mortality, most likely caused by opportunistic infection in the lungs (Fig. 5.9). Thus, even if VSL#3 were to have a beneficial effect on remyelination, this may require doses that are not feasible in patients. Whilst a higher dose of this probiotic has been used previously in mice without reported toxicity (Kigerl et al., 2016; Kumar et al., 2017), it may be that the older mice used in my study had a reduced immune capacity to defend against such an infection (Dorshkind et al., 2009). The doses of probiotic administered in my study and others are scaled to be similar to the recommended human dose of VSL#3 (Nair and Jacob, 2016). It is clear that humans would be self-administering a probiotic voluntarily, thus the probability of aspirating bacteria would be much lower compared to mice receiving oral gavage. However, there are recent efforts to increase the stringency of probiotic safety assessment (Sanders et al., 2010), and this may be particularly relevant in neurological diseases such as MS, where dysphagia and aspiration can become significant risks (Poorjavad et al., 2010).

One difference that was observed when quantifying OPC responses was a small increase in Sox10+CC1+ oligodendrocytes at 5dpl (Fig. 5.7E). As OPC differentiation in the lysolecithin model is considered minimal before 7dpl even in young adults (Keough et al., 2015), this is unlikely to reflect an early increase in production of new oligodendrocytes. VSL#3 was shown to spare white matter and limit lesion size in a model of spinal cord contusion injury (Kigerl et al., 2016). Thus it may be that here we are seeing a similar protective effect of VSL#3 administration on oligodendrocytes in response to lysolecithin injection, though the nature of this remains to be determined. Preliminary results claim that VSL#3 administration can also improve outcome in EAE, an immune-mediated model of demyelination, and this is associated with reduced circulating pro-inflammatory cytokines and increased numbers of splenic T reg cells (Tankou et al., 2016).

In summary, our regime of VSL#3 treatment elevated levels of circulating SCFAs, and increased populations of GALT dendritic cells and CD4+ T cells. It also caused an enhancement in the onset of inflammation in the CNS following lysolecithin-induced demyelination, involving iNOS+ and MR+ microglia/macrophages. This was associated with reduced oligodendrocyte loss at 5dpl, but no change in oligodendrocyte differentiation at 14dpl, or in remyelination at 21dpl. A trial of a higher dose of VSL#3 caused mortality in aged mice, suggesting that the changes observed were near the top of the therapeutic window for this probiotic.

Chapter 6

General discussion and conclusions

The aim of this project was to test the hypothesis that the gut microbiota can influence remyelination in the CNS. To do so, I have investigated how interventions that alter the microbiota change the inflammatory response accompanying toxin-induced demyelination, and whether this influences the behaviour of OPCs and eventual outcome of remyelination. I have also explored probiotic therapy as a therapeutic strategy to enhance remyelination in a mouse model.

6.1 The microbiota influence inflammation during remyelination

6.1.1 The microglia/macrophage response

As the activity of microglia/macrophages are a key determinant of the outcome of remyelination (Kotter et al., 2001; Miron et al., 2013; Ruckh et al., 2012), and are themselves tuned by the microbiota (Erny et al., 2015; Möhle et al., 2016), this is a likely mediator of any microbiota-remyelination effect. Consolidating results from across my three studies, I observed that signals from the microbiota are indeed important for the microglia/macrophage response that follows toxin-mediated demyelination.

In GF mice, following cuprizone administration, there was a delay in the inflammatory response. At the end of cuprizone treatment (5 weeks) there were fewer CD68+ activated microglia/macrophages, which then peaked two weeks later as the inflammation was resolving in control and ex-GF mice. Similarly in mice receiving oral antibiotics, the number of CD68+ cells had a late peak at the 14dpl timepoint, which was not seen in the control group. In contrast, when the microbiome of aged mice was supplemented with the probiotic

VSL#3, there was an enhanced onset of inflammation, with a higher density of CD68+ microglia/macrophages at the earlier 5dpl timepoint. Inflammation is most vital in the earlier stages of remyelination (Kotter et al., 2001) and a slow-resolving, prolonged inflammatory response is typical of situations in which remyelination outcome is poor, for example in aged mice and rats (Hinks and Franklin, 2000; Miron et al., 2013). The pattern might therefore suggest that the microbiota encourage a prompt response by the innate immune system, with appropriate resolution. With only snapshots of lesions at discrete timepoints, this is difficult to say conclusively. For example, it would be helpful to have a 5dpl timepoint for the antibiotics study, to interrogate whether there is a delayed onset of inflammation here, consistent with the findings from GF and probiotic-treated mice.

However, further weight is given to this idea by drawing parallels from other models that feature CNS inflammation. Microglia require the presence of a microbiome to acquire their adult phenotype (Matcovitch-Natan et al., 2016), and without continuous microbial input they do not respond appropriately in models of bacterial or viral infection (Erny et al., 2015). In addition, GF mice have lower numbers of peripheral monocytes (Khosravi et al., 2014), and mice treated with an antibiotic regime similar to my study had reduced entry of monocytes into the CNS under homeostatic conditions (Möhle et al., 2016). Thus, the concept that the microbiome helps to drive a timely microglial/macrophage response following demyelination is seen throughout my results and supported by existing literature.

6.1.2 Induction of specific inflammatory markers

To further explore the effect of the microbiota on inflammation, I investigated expression of M1 and M2 markers by CD68+ microglia/macrophages. The use of M1/M2 terminology is contentious *in vivo* (Murray et al., 2014), and across my results neither classical M1 markers (iNOS, MHCII) nor M2 markers (Arg1, MR) were necessarily regulated together. However, it has been clearly demonstrated that microglia/macrophages that express markers in common with the M2 phenotype (which results from IL-4/IL-13 exposure *in vitro*) are vital for successful regeneration following spinal cord contusion or demyelination (Kigerl et al., 2009; Miron et al., 2013), whilst the expression of M1 markers (which are induced by LPS and IFNγ *in vitro*) are more associated with the earlier phases of remyelination in which OPCs are recruited and proliferate (Miron et al., 2013).

MHCII is one such marker that is upregulated by M1 conditions *in vitro* (Sicher et al., 1995). This surface protein complex is expressed by macrophages and dendritic cells to present antigens to CD4+ T cells, and MHCII-deficient mice have delayed remyelination following cuprizone exposure (Arnett et al., 2003). In my work, I observed that MHCII upregulation was consistently impaired following demyelination in both antibiotics-treated

and germ-free mice. The differences only became apparent in the aftermath of demyelination, consistent with a previous comparison showing similar MHCII expression by microglia of unlesioned GF and SPF mice (Erny et al., 2015). MHCII+ immune cells within the gut help to shape the composition of the microbiota (Kubinak et al., 2015), and it is intuitive that this complex, which functions primarily to present non-host antigens to the adaptive immune system, is positively regulated by the microbiota. In fact, MHCII is likely to promote remyelination via mechanisms independent of antigen presentation, as demyelination/remyelination in the cuprizone model occur in the absence of CD4+ T cells (Hiremath et al., 2008), though specific CD4+Foxp3+ T_{reg} depletion has been shown to impair remyelination following cuprizone (Dombrowski et al., 2017).

Antibiotics-treated mice also had reduced expression of Arg1 (an M2 marker) following demyelination. Arg1 is another marker associated with efficient remyelination (Miron et al., 2013), as well as regeneration in other tissues (Rath et al., 2014). Arg1 expression is not a feature of cuprizone-mediated demyelination/remyelination, so this could not be verified in the GF system (Le Blon et al., 2016; Olah et al., 2012).

As both MHCII and Arg1, two molecules with pro-remyelination effects, were reduced following microbial depletion, I investigated whether the reverse might be true following probiotic supplementation. Whilst a positive trend was noted, neither marker was significantly upregulated in the VSL#3-treated group, suggesting that any difference was not sufficiently large to be detected above the within-group variation. However, I did observe an increased density of microglia/macrophages expressing iNOS (an M1 marker) and MR (an M2 marker) following VSL#3 treatment. These two markers were expressed by a greater proportion of the CD68+ population than MHCII or Arg1, so this might simply reflect the increased total number of CD68+ microglia/macrophages, rather than specific upregulation of the relevant pathways.

A limitation of my studies has been the inability to distinguish activated microglia from infiltrating monocyte-dervied macrophages, both of which are CD68+. Whilst there is much overlap in their function (Lampron et al., 2015; Miron et al., 2013; Natrajan et al., 2015), the two populations can in some cases have different and even opposing effects on remyelination (Lampron et al., 2015; Yamasaki et al., 2014). The most reliable techniques to distinguish microglia and monocyte-derived macrophages involve transgenic lines or BBB-impermeable toxins, whereas more straightforward tools, such as immunohistochemistry for Tmem119 (Bennett et al., 2016), are not yet fully characterised in the lysolecithin and cuprizone models. It would be interesting to see whether the differences in inflammatory marker induction after modulating the microbiome were due primarily to endogenous microglia,

infiltrating peripheral monocytes or a combination of both, and if this were consistent between interventions.

	Antibiotic treatment	Germ-free mice	Probiotic treatment
Model	Lysolecithin	Cuprizone	Lysolecithin
Timepoints	7dpl, 14dpl	Naive, 5w, 5+2w	5dpl, 14dpl, 21dpl
n	4-6	5	3-4
SCFAs	-	↓	↑
Activated microglia /macrophages (CD68+)	7dpl: ND (p=0.73) 14dpl: ↑ (p=0.043)	5w: ↓ (p=0.048) 5+2w: ↑ (p=0.043)	5dpl: ↑ (p=0.041) 14dpl: ND (p=0.24)
M1 markers	7dpl: MHCII ↓ (p=0.007) iNOS ND (p=0.9)	5w: MHCII ↓ (p=0.043)	MHCII ND (p=0.14) 5dpl: iNOS ↑ (p=0.024)
M2 markers	7dpl: Arg1 ↓ (p=0.013) MR ND (p=0.9)	-	Arg1 ND (p=0.24) 5dpl: MR ↑ (p=0.041)
Myelin debris clearance	↓ (p=0.012)	-	ND (p=0.65)
OPC proliferation	ND (p=0.9)	(p=0.76)	ND (p=0.76)
OPC differentiation	↓ (p=0.020)	ND (p=0.9)	ND (p=0.34)
Remyelination	-	-	ND (p=0.40)

Table 6.1 **Summary of results from different model systems.** Increases relative to SPF controls are shown in blue, with decreases in red. ND, no difference detected; *n*, number of biological replicates per group; dashes indicate values not measured.

6.1.3 Functional outcomes of inflammation

Associated with the impaired inflammatory response in antibiotics-treated mice there was a deficit in myelin debris clearance. Lesions of mice receiving antibiotics had more residual myelin debris at 14dpl than SPF controls. This is consistent with other studies in which

myelin debris clearance is slowed following an attenuated inflammatory response (Kotter et al., 2005; Natrajan et al., 2015). Whilst I focused here on phagocytosis of myelin debris, another important function of microglia/macrophages is the direct production of positive regulators of OPC function (Miron and Franklin, 2014; Setzu et al., 2006), which might also be perturbed following interventions that alter the microbiome.

In contrast, probiotic administration did not result in a concurrent promotion of myelin debris clearance. This may reflect the fact that the enhancement of inflammation by VSL#3 was generally subtler than the impairment seen following antibiotic treatment, or that specific functional molecules, such as MHCII or Arg1 were not sufficiently upregulated by this probiotic (Cash et al., 1993; Cherry et al., 2015).

The effects of each of my three microbiome interventions on inflammation, as well as OPC responses are summarised in Table 6.1.

6.1.4 Gut-brain communication

The microbiota have previously been shown to influence processes in the CNS through production of bioactive molecules (Erny et al., 2015; Rothhammer et al., 2016), direct vagus nerve stimulation (Bravo et al., 2011) and indirectly by interaction with the immune system in the gut (Benakis et al., 2016; Fung et al., 2017). Here, I focused on SCFAs, as oral delivery of these bacterial metabolites can recapitulate many microbiome-dependent features of microglia (Erny et al., 2015; Sampson et al., 2016).

I quantified concentrations of SCFAs in two of my models, demonstrating that these were systemically reduced in GF mice and enhanced by the probiotic VSL#3. SCFAs have long been known to be diminished in GF mice (Høverstad and Midtvedt, 1986), though the concentrations I measured here by GC-MS, consistent with other measurements from the literature (Perry et al., 2016), could not ellicit direct effects on microglial phagocytosis (or OPC responses) *in vitro*. Indeed, microglia do not express the FFAR2 receptor, which is present on splenic Iba1+ cells and is vital for the effect of the microbiota on microglial function (Erny et al., 2015). Thus any effect of microbiota-derived SCFAs is likely to be transmitted to the CNS via effects on peripheral immune tissues. It would be interesting to examine whether myelin phagocytosis by peripherally-derived macrophages is more sensitive to SCFAs than microglia, as FFAR2 is expressed by monocytes but downregulated upon differentiation into macrophages (Ang et al., 2016).

In my probiotic model, I also measured changes in GALT by flow cytometry, observing that VSL#3 treatment increased CD11c+ dendritic cells in PPs and enhanced CD4+ T cells in the MLNs. Variations of this regime in younger mice have led to increases in B cells and T_{reg} cells after VSL#3 administration (Kigerl et al., 2016; Mariman et al., 2015), though

neither were raised here, highlighting how host factors and specifics of administration will also determine the immune response.

As CD4 T cells, which tune macrophage responses, play an important role in remyelination (Bieber et al., 2003), and GF mice are deficient in CD4 T cells (Dobber et al., 1992), it may be that the larger GALT CD4 population I observed in aged VSL#3-treated mice contributes to the faster onset of inflammation following demyelination. In another study, the protective effect of amoxicillin-clavulanic acid in a stroke model, whereby macrophage infiltration and ischaemic damage are reduced, was thought to be mediated by GALT CD4 lymphocytes (Benakis et al., 2016). GALT may also be an alternative site of action for SCFAs - indeed administration of SCFAs to GF mice partially reversed their deficits in colonic CD4 lymphocytes relative to SPF mice (Smith et al., 2013). However, as the poor remyelination observed in the absence of CD4 T cells was not associated with a reduction in the total number of microglia/macrophages (Bieber et al., 2003), a microbiome - CD4 lymphocyte - microglia/macrophage axis is unlikely to be the full story.

6.2 The microbiota and OPC responses to demyelination

An influence of the microbiota on CNS inflammation was evident from all three of my studies, but it was less conclusive how this translates to changes in OPC responses and remyelination. In the antibiotics model, where immune deficits were associated with impaired myelin debris clearance, OPC differentiation into CC1+ oligodendrocytes was reduced at 14dpl, consistent with an inhibitory effect of myelin debris (Kotter et al., 2006; Robinson and Miller, 1999). However, this finding was challenging to reproduce in the GF model of microbiome depletion, as the cuprizone treatment only caused partial loss of oligodendrocytes and demyelination. In contrast, following VSL#3 treatment there was no change in myelin debris clearance and no difference in OPC differentiation. Thus, the enhancement in microglia/macrophage accumulation was not functionally relevant to the OPC response here.

The gold standard measure of remyelination is analysis of myelin sheaths at high resolution in semi-thin resin sections (Blakemore and Franklin, 2008). I used this technique at a late timepoint in the probiotic study (21dpl), in which blind ranking of remyelination showed no difference from control animals. This was consistent with the similar rates of OPC differentiation. In the antibiotics experiment, reduced OPC differentiation in the treated group may have led to a delay in remyelination, as differentiation is commonly the rate limiting step (Wolswijk, 1998; Woodruff et al., 2004). However, other studies have reported cases where slower OPC differentiation is not necessarily indicative of impaired remyelination

(Ahrendsen et al., 2017; De La Fuente et al., 2017). A later timepoint with resin sections would therefore be informative as to the eventual effect on remyelination.

6.3 The microbiota as a target in demyelinating disease

The long-term goal of doing these experiments would be to identify ways to alter the microbiota therapeutically for patients with myelin diseases such as MS. My results offer some support towards this, but important questions still remain. Perhaps most relevant, I observed deficits in the immune response following microbial depletion, with impaired OPC differentiation subsequent to antibiotic use. If future work confirms that the production of new myelin sheath is similarly delayed, this could be of relevance to patients with MS receiving high doses of antibiotics. Antibiotic use can indeed cause substantial and long-lasting changes in a patient's microbiome (Becattini et al., 2016; Jernberg et al., 2007) and the doses used in this study were scaled from human values (see Materials and Methods). Needless to say, antibiotic therapy is generally given for good reason, particularly amongst patients with MS who may be immunosuppressed by other drugs (Winkelmann et al., 2016). However, the combination of antibiotics with a probiotic supplement might be able to limit effects on the immune system and CNS secondary to dysbiosis. A similar antibiotic/probiotic combination has been useful in preventing antibiotic-associated diarrhoea (Hempel et al., 2012) and for treating complications of ulcerative colitis (Gionchetti et al., 2012), although my observation that not all deficits (including OPC differentiation) were reversed following FMT treatment suggests some limitations to this approach for remyelination.

Whether probiotics could be beneficial in the absence of antibiotic-induced dysbiosis is less clear. My "gain-of-function" study using the VSL#3 probiotic showed little effect on OPC behaviour, despite a small enhancement in the onset of inflammation. Having trialled only a single probiotic (albeit a combination of 8 strains), it may be that other formulations could be more beneficial. However, VSL#3 is certainly amongst the probiotics with the strongest characterised effects on the CNS (Distrutti et al., 2014; Kigerl et al., 2016), and was being used here at a dose close to its threshold for toxicity. It may simply be that, whilst the microbiota are necessary for the correct response by microglia/macrophages, this is not a limiting factor for the rate of remyelination in aged mice, which is likely constrained by other determinants of the immune response (Ruckh et al., 2012), besides epigenetic changes intrinsic to OPCs (Shen et al., 2008). The dysbiosis reported amongst patients with MS (Berer et al., 2017; Chen et al., 2016; Jhangi et al., 2014; Mowry et al., 2012) is a feature of the disease not represented in this model system.

Any therapy that aims to improve remyelination by modulating inflammation will need to reconcile the fact that diseases such as MS are also driven by the immune system, and enhancing the accumulation of microglia/macrophages inappropriately may in fact worsen the demyelinating insult. For example, lesions from our two microbiome depletion studies both displayed reduced expression of MHCII, an important pro-remyelination factor (Arnett et al., 2003), but MHCII haplotype in humans is also a strong risk factor for developing MS (Ramagopalan et al., 2009) and its expression facilitates demyelination in the cuprizone and EAE models (Hiremath et al., 2008; Nikodemova et al., 2007). As we learn more about inflammation in demyelinating diseases, we begin to see ways by which the same interventions could both prevent demyelination and promote remyelination. For example, the presence of M2 microglia/macrophages is vital for remyelination (Miron et al., 2013), and administration of M2 monocytes can also prevent relapses in an EAE model (Mikita et al., 2011). Thus if a probiotic therapy could succesfully bias the CNS immune response towards M2 activation, this could have a compounded benefit for patients with MS.

There is indeed a growing evidence base that the microbiota can be targeted as a means to reduce demyelination where this is driven by inflammatory processes. The observations that antibiotics-treated or GF mice are resistant to EAE (Berer et al., 2011; Lee et al., 2011; Ochoa-Reparaz et al., 2009), and that the transplanted microbiota of MS patients can provoke development of EAE (Berer et al., 2017) point towards the microbiota first initiating an autoimmune response by molecular mimicry, and then sustaining ongoing CNS inflammation. An encouraging result from my probiotic experiment was the increased number of oligodendrocytes at 5dpl following VSL#3 treatment, which likely represents reduced oligodendrocyte death. Consistent with this finding, another study reported sparing of white matter following VSL#3 treatment in a spinal cord contusion model (Kigerl et al., 2016) and mice receiving VSL#3 also develop less severe EAE (Tankou et al., 2016). This could reflect a tempering of the immune response, which also contributes to demyelination in the lysolecithin model (Ghasemlou et al., 2007; Ousman and David, 2001).

Limiting immune-mediated demyelination has been the rationale for several clinical trials of probiotic therapy in MS. In a small pilot study, patients receiving VSL#3 had a reduction in "pro-inflammatory monocytes" which reversed upon treatment cessation, though with no data currently available on neurological effects (Weiner, 2017). A double-blind placebo-controlled trial reported that 12 weeks administration of another probiotic containing *Lactobacilli* and *Bifidobacteria* caused a small reduction in disability associated with metabolic and immunological changes (Kouchaki et al., 2017). As myelin-imaging techniques like the magnetisation transfer ratio (MTR) and myelin-specific positron emission tomography (PET) ligands become more widespread in such studies, it will also be possible

to probe for effects on remyelination. Finally, it should be said that a probiotic therapy would not necessarily need to inhibit demyelination or facilitate remyelination to benefit patients living with demyelinating diseases. Bowel symptoms such as constipation can have a substantial impact on quality of life in MS (Wiesel et al., 2001) and may be independently amenable to probiotic intervention (Dimidi et al., 2014).

In conclusion, my results highlight the gut microbiota as a previously unconsidered influence on the activity of microglia/macrophages during remyelination, following three separate interventions. When antibiotics were used to deplete the microbiota, this impaired myelin debris clearance and the ability of OPCs to differentiate. Mice reared in a germ-free environment had similar deficits in their inflammatory response to demyelination. Further work will confirm whether this will affect the eventual outcome of remyelination, which might have implications for patients with MS, particularly in the context of antibiotic therapy. When a probiotic was used to supplement the microbiota, the onset of inflammation was enhanced but without without improvements in debris clearance or OPC differentiation. Taken together, these results suggest that the microbiota are necessary for, but not a limiting factor of, the appropriate innate immune response during CNS remyelination.

References

Aas, J., Gessert, C. E., and Bakken, J. S. (2003). Recurrent Clostridium difficile Colitis: Case Series Involving 18 Patients Treated with Donor Stool Administered via a Nasogastric Tube. *Clinical Infectious Diseases*, 36(5):580–585.

Aboobaker, A. A. (2011). Planarian stem cells: A simple paradigm for regeneration. *Trends in Cell Biology*, 21(5):304–311.

Ahrendsen, J. T., Harlow, D. E., Finseth, L. T., Bourne, J. N., Hickey, S. P., Gould, E. A., Culp, C. M., and Macklin, W. B. (2017). The protein tyrosine phosphatase Shp2 regulates oligodendrocyte differentiation and early myelination and contributes to timely remyelination. *The Journal of Neuroscience*, (303):2864–16.

Ajami, B., Bennett, J. L., Krieger, C., McNagny, K. M., and Rossi, F. M. V. (2011). Infiltrating monocytes trigger EAE progression, but do not contribute to the resident microglia pool. *Nature neuroscience*, 14(9):1142–1149.

Al-Dabagh, I. I. and Mohammad, F. K. (2008). Pharmacokinetics and Distribution of Metronidazole Administered Intraperitoneally in Mice. 863:858–863.

Alonso, A., Jick, S. S., Olek, M. J., and Hernán, M. A. (2007). Incidence of multiple sclerosis in the United Kingdom: Findings from a population-based cohort. *Journal of Neurology*, 254(12):1736–1741.

Aminov, R. I. (2010). A brief history of the antibiotic era: Lessons learned and challenges for the future. *Frontiers in Microbiology*, 1(DEC):1–7.

Anderson, M. A., Burda, J. E., Ren, Y., Ao, Y., O'Shea, T. M., Kawaguchi, R., Coppola, G., Khakh, B. S., Deming, T. J., and Sofroniew, M. V. (2016). Astrocyte scar formation aids central nervous system axon regeneration. *Nature*, 532(7598):195–200.

Ang, Z., Er, J. Z., Tan, N. S., Lu, J., Liou, Y.-C., Grosse, J., and Ding, J. L. (2016). Human and mouse monocytes display distinct signalling and cytokine profiles upon stimulation with FFAR2/FFAR3 short-chain fatty acid receptor agonists. *Scientific Reports*, 6(1):34145.

Arandjelovic, S. and Ravichandran, K. S. (2015). Phagocytosis of apoptotic cells in homeostasis. *Nature immunology*, 16(9):907–17.

Arentsen, T., Qian, Y., Gkotzis, S., Femenia, T., Wang, T., Udekwu, K., Forssberg, H., and Diaz Heijtz, R. (2017). The bacterial peptidoglycan-sensing molecule Pglyrp2 modulates brain development and behavior. *Molecular Psychiatry*, 22(2):257–266.

Arnett, H. A., Mason, J., Marino, M., Suzuki, K., Matsushima, G. K., and Ting, J. P.-Y. (2001). TNFα promotes proliferation of oligodendrocyte progenitors and remyelination. *Nature Neuroscience*, 4(11):1116–1122.

Arnett, H. A., Wang, Y., Matsushima, G. K., Suzuki, K., and Ting, J. P.-Y. (2003). Functional genomic analysis of remyelination reveals importance of inflammation in oligodendrocyte regeneration. *Journal of Neuroscience*, 23(30):9824–32.

Bakker, D. A. and Ludwin, S. K. (1987). Blood-brain barrier permeability during Cuprizone-induced demyelination. Implications for the pathogenesis of immune-mediated demyelinating diseases. *Journal of the Neurological Sciences*, 78(2):125–137.

Barker, N., van Es, J. H., Kuipers, J., Kujala, P., van den Born, M., Cozijnsen, M., Haegebarth, A., Korving, J., Begthel, H., Peters, P. J., and Clevers, H. (2007). Identification of stem cells in small intestine and colon by marker gene Lgr5. *Nature*, 449(7165):1003–1007.

Becattini, S., Taur, Y., and Pamer, E. G. (2016). Antibiotic-Induced Changes in the Intestinal Microbiota and Disease. *Trends in Molecular Medicine*, 22(6):458–478.

Becker, A. J., McCulloch, E. A., and Till, J. E. (1963). Cytological demonstration of the clonal nature of spleen colonies derived from transplanted mouse marrow cells. *Nature*, 197(4897):452–4.

Beecham, A. H., Patsopoulos, N. A., Xifara, D. K., Davis, M. F., Kemppinen, A., Cotsapas, C., Shah, T. S., Spencer, C., Booth, D., Goris, A., Oturai, A., Saarela, J., Fontaine, B., Hemmer, B., Martin, C., Zipp, F., D'Alfonso, S., Martinelli-Boneschi, F., Taylor, B., Harbo, H. F., Kockum, I., Hillert, J., Olsson, T., Ban, M., Oksenberg, J. R., Hintzen, R., Barcellos, L. F., Agliardi, C., Alfredsson, L., Alizadeh, M., Anderson, C., Andrews, R., Søndergaard, H. B., Baker, A., Band, G., Baranzini, S. E., Barizzone, N., Barrett, J., Bellenguez, C., Bergamaschi, L., Bernardinelli, L., Berthele, A., Biberacher, V., Binder, T. M., Blackburn, H., Bomfim, I. L., Brambilla, P., Broadley, S., Brochet, B., Brundin, L., Buck, D., Butzkueven, H., Caillier, S. J., Camu, W., Carpentier, W., Cavalla, P., Celius, E. G., Coman, I., Comi, G., Corrado, L., Cosemans, L., Cournu-Rebeix, I., Cree, B. A., Cusi, D., Damotte, V., Defer, G., Delgado, S. R., Deloukas, P., Di Sapio, A., Dilthey, A. T., Donnelly, P., Dubois, B., Duddy, M., Edkins, S., Elovaara, I., Esposito, F., Evangelou, N., Fiddes, B., Field, J., Franke, A., Freeman, C., Frohlich, I. Y., Galimberti, D., Gieger, C., Gourraud, P. A., Graetz, C., Graham, A., Grummel, V., Guaschino, C., Hadjixenofontos, A., Hakonarson, H., Halfpenny, C., Hall, G., Hall, P., Hamsten, A., Harley, J., Harrower, T., Hawkins, C., Hellenthal, G., Hillier, C., Hobart, J., Hoshi, M., Hunt, S. E., Jagodic, M., Jelcic, I., Jochim, A., Kendall, B., Kermode, A., Kilpatrick, T., Koivisto, K., Konidari, I., Korn, T., Kronsbein, H., Langford, C., Larsson, M., Lathrop, M., Lebrun-Frenay, C., Lechner-Scott, J., Lee, M. H., Leone, M. A., Leppä, V., Liberatore, G., Lie, B. A., Lill, C. M., Lindén, M., Link, J., Luessi, F., Lycke, J., Macciardi, F., Männistö, S., Manrique, C. P., Martin, R., Martinelli, V., Mason, D., Mazibrada, G., McCabe, C., Mero, I. L., Mescheriakova, J., Moutsianas, L., Myhr, K. M., Nagels, G., Nicholas, R., Nilsson, P., Piehl, F., Pirinen, M., Price, S. E., Quach, H., Reunanen, M., Robberecht, W., Robertson, N. P., Rodegher, M., Rog, D., Salvetti, M., Schnetz-Boutaud, N. C., Sellebjerg, F., Selter, R. C., Schaefer, C., Shaunak, S., Shen, L., Shields, S., Siffrin, V., Slee, M., Sorensen, P. S., Sorosina, M., Sospedra, M., Spurkland, A., Strange, A., Sundqvist, E., Thijs, V., Thorpe, J., Ticca, A., Tienari, P., Van Duijn, C., Visser, E. M., Vucic, S., Westerlind, H., Wiley,

J. S., Wilkins, A., Wilson, J. F., Winkelmann, J., Zajicek, J., Zindler, E., Haines, J. L., Pericak-Vance, M. A., Ivinson, A. J., Stewart, G., Hafler, D., Hauser, S. L., Compston, A., McVean, G., De Jager, P., Sawcer, S. J., and McCauley, J. L. (2013). Analysis of immune-related loci identifies 48 new susceptibility variants for multiple sclerosis. *Nature Genetics*, 45(11):1353–1362.

Belkaid, Y. and Hand, T. W. (2014). Review Role of the Microbiota in Immunity and Inflammation. *Cell*, 157(1):121–141.

Benakis, C., Brea, D., Caballero, S., Faraco, G., Moore, J., Murphy, M., Sita, G., Racchumi, G., Ling, L., Pamer, E. G., Iadecola, C., and Anrather, J. (2016). Commensal microbiota affects ischemic stroke outcome by regulating intestinal $\gamma\delta$ T cells. *Nature Medicine*, 22(5):516–523.

Bennett, M. L., Bennett, F. C., Liddelow, S. A., Ajami, B., Zamanian, J. L., Fernhoff, N. B., Mulinyawe, S. B., Bohlen, C. J., Adil, A., Tucker, A., Weissman, I. L., Chang, E. F., Li, G., Grant, G. A., Hayden Gephart, M. G., and Barres, B. A. (2016). New tools for studying microglia in the mouse and human CNS. *Proceedings of the National Academy of Sciences*, 113(12):E1738–E1746.

Berer, K., Gerdes, L. A., Cekanaviciute, E., Jia, X., Xiao, L., Xia, Z., Liu, C., Klotz, L., Stauffer, U., Baranzini, S. E., Kümpfel, T., Hohlfeld, R., Krishnamoorthy, G., and Wekerle, H. (2017). Gut microbiota from multiple sclerosis patients enables spontaneous autoimmune encephalomyelitis in mice. *Proceedings of the National Academy of Sciences*, 114(40):10719–10724.

Berer, K., Mues, M., Koutrolos, M., Rasbi, Z. A., Boziki, M., Johner, C., Wekerle, H., and Krishnamoorthy, G. (2011). Commensal microbiota and myelin autoantigen cooperate to trigger autoimmune demyelination. *Nature*, 479(7374):538–41.

Bibiloni, R. (2012). Rodent models to study the relationships between mammals and their bacterial inhabitants. *Gut Microbes*, 3(6):536–543.

Bieber, A. J., Kerr, S., and Rodriguez, M. (2003). Efficient central nervous system remyelination requires T cells. *Annals of Neurology*, 53(5):680–684.

Blakemore, W. F. and Franklin, R. J. M. (2008). Remyelination in experimental models of toxin-induced demyelination. *Current topics in microbiology and immunology*, 318:193–212.

Bodea, L.-G., Wang, Y., Linnartz-Gerlach, B., Kopatz, J., Sinkkonen, L., Musgrove, R., Kaoma, T., Muller, A., Vallar, L., Di Monte, D. A., Balling, R., and Neumann, H. (2014). Neurodegeneration by Activation of the Microglial Complement-Phagosome Pathway. *Journal of Neuroscience*, 34(25):8546–8556.

Boffa, L. C., Vidali, G., Mann, R. S., and Allfrey, V. G. (1978). Suppression of Histone Deacetylation in Viuo and in Vitro by Sodium Butyrate. *Journal of Biological Chemistry*, 253(10):3364–3366.

Boulangé, C. L., Neves, A. L., Chilloux, J., Nicholson, J. K., and Dumas, M.-E. (2016). Impact of the gut microbiota on inflammation, obesity, and metabolic disease. *Genome Medicine*, 8(1):42.

Bourassa, M. W., Alim, I., Bultman, S. J., and Ratan, R. R. (2016). Butyrate, neuroepigenetics and the gut microbiome: Can a high fiber diet improve brain health? *Neuroscience Letters*, 625:56–63.

Bravo, J. A., Forsythe, P., Chew, M. V., Escaravage, E., Savignac, H. M., Dinan, T. G., Bienenstock, J., and Cryan, J. F. (2011). Ingestion of Lactobacillus strain regulates emotional behavior and central GABA receptor expression in a mouse via the vagus nerve. *Proceedings of the National Academy of Sciences*, 108(38):16050–16055.

Brown, A. J., Goldsworthy, S. M., Barnes, A. A., Eilert, M. M., Tcheang, L., Daniels, D., Muir, A. I., Wigglesworth, M. J., Kinghorn, I., Fraser, N. J., Pike, N. B., Strum, J. C., Steplewski, K. M., Murdock, P. R., Holder, J. C., Marshall, F. H., Szekeres, P. G., Wilson, S., Ignar, D. M., Foord, S. M., Wise, A., and Dowell, S. J. (2003). The orphan G protein-coupled receptors GPR41 and GPR43 are activated by propionate and other short chain carboxylic acids. *Journal of Biological Chemistry*, 278(13):11312–11319.

Brown, J. W. L., Coles, A., Horakova, D., and al, E. (2017). The effect of disease-modifying treatments on conversion to secondary progressive multiple sclerosis. In *ECTRIMS*.

Butovsky, O., Jedrychowski, M. P., Moore, C. S., Cialic, R., Lanser, A. J., Gabriely, G., Koeglsperger, T., Dake, B., Wu, P. M., Doykan, C. E., Fanek, Z., Liu, L., Chen, Z., Rothstein, J. D., Ransohoff, R. M., Gygi, S. P., Antel, J. P., and Weiner, H. L. (2014). Identification of a unique TGF-β–dependent molecular and functional signature in microglia. *Nature Neuroscience*, 17(1):131–143.

Butovsky, O., Landa, G., Kunis, G., Ziv, Y., Avidan, H., Greenberg, N., Schwartz, A., Smirnov, I., Pollack, A., Jung, S., and Schwartz, M. (2006). Induction and blockage of oligodendrogenesis by differently activated microglia in an animal model of multiple sclerosis. *Journal of Clinical Investigation*, 116(4):905–915.

Calcinaro, F., Dionisi, S., Marinaro, M., Candeloro, P., Bonato, V., Marzotti, S., Corneli, R. B., Ferretti, E., Gulino, A., Grasso, F., De Simone, C., Di Mario, U., Falorni, A., Boirivant, M., and Dotta, F. (2005). Oral probiotic administration induces interleukin-10 production and prevents spontaneous autoimmune diabetes in the non-obese diabetic mouse. *Diabetologia*, 48(8):1565–1575.

Cammer, W., Rose, A. L., and Norton, W. T. (1975). Biochemical and pathological studies of myelin in hexachlorophene intoxication. *Brain Research*, 98(3):547–559.

Canesso, M. C. C., Vieira, A. T., Castro, T. B. R., Schirmer, B. G. A., Cisalpino, D., Martins, F. S., Rachid, M. A., Nicoli, J. R., Teixeira, M. M., and Barcelos, L. S. (2014). Skin Wound Healing Is Accelerated and Scarless in the Absence of Commensal Microbiota. *The Journal of Immunology*, 193(10):5171–5180.

Cash, E., Zhang, Y., and Rott, O. (1993). Microglia Present Myelin Antigens to T Cells after Phagocytosis of Oligodendrocytes. *Cellular Immunology*, 147(1):129–138.

Chang, A., Nishiyama, A., Peterson, J., Prineas, J., and Trapp, B. D. (2000). NG2-positive oligodendrocyte progenitor cells in adult human brain and multiple sclerosis lesions. *The Journal of neuroscience : the official journal of the Society for Neuroscience*, 20(17):6404–12.

Charcot, J. (1868). *Histologie de la sclerose en plaques.* Gazette des hopitaux, Paris.

Chen, J., Chia, N., Kalari, K. R., Yao, J. Z., Novotna, M., Soldan, M. M. P., Luckey, D. H., Marietta, E. V., Jeraldo, P. R., Chen, X., Weinshenker, B. G., Rodriguez, M., Kantarci, O. H., Nelson, H., Murray, J. A., and Mangalam, A. K. (2016). Multiple sclerosis patients have a distinct gut microbiota compared to healthy controls. *Scientific Reports*, 6:28484.

Cherry, J. D., Olschowka, J. A., and O'Banion, M. K. (2015). Arginase 1+ microglia reduce Aβ plaque deposition during IL-1β-dependent neuroinflammation. *Journal of Neuroinflammation*, 12(1):203.

Chrast, R., Saher, G., Nave, K.-A., and Verheijen, M. H. G. (2011). Lipid metabolism in myelinating glial cells: lessons from human inherited disorders and mouse models. *Journal of lipid research*, 52(3):419–434.

Ciorba, M. A. (2012). A Gastroenterologist's Guide to Probiotics. *Clinical Gastroenterology and Hepatology*, 10(9):960–968.

Claesson, M. J., Jeffery, I. B., Conde, S., Power, S. E., O'Connor, E. M., Cusack, S., Harris, H. M. B., Coakley, M., Lakshminarayanan, B., O'Sullivan, O., Fitzgerald, G. F., Deane, J., O'Connor, M., Harnedy, N., O'Connor, K., O'Mahony, D., van Sinderen, D., Wallace, M., Brennan, L., Stanton, C., Marchesi, J. R., Fitzgerald, A. P., Shanahan, F., Hill, C., Ross, R. P., and O'Toole, P. W. (2012). Gut microbiota composition correlates with diet and health in the elderly. *Nature*, 488(7410):178–84.

Clarner, T., Janssen, K., Nellessen, L., Stangel, M., Skripuletz, T., Krauspe, B., Hess, F.-M., Denecke, B., Beutner, C., Linnartz-Gerlach, B., Neumann, H., Vallières, L., Amor, S., Ohl, K., Tenbrock, K., Beyer, C., and Kipp, M. (2015). CXCL10 Triggers Early Microglial Activation in the Cuprizone Model. *The Journal of Immunology*, 194(7):3400–3413.

Clemente, D., Ortega, M. C., Melero-Jerez, C., and de Castro, F. (2013). The effect of glia-glia interactions on oligodendrocyte precursor cell biology during development and in demyelinating diseases. *Frontiers in Cellular Neuroscience*, 7:268.

Coles, A. J., Twyman, C. L., Arnold, D. L., Cohen, J. a., Confavreux, C., Fox, E. J., Hartung, H.-P., Havrdova, E., Selmaj, K. W., Weiner, H. L., Miller, T., Fisher, E., Sandbrink, R., Lake, S. L., Margolin, D. H., Oyuela, P., Panzara, M. a., and Compston, D. A. S. (2012). Alemtuzumab for patients with relapsing multiple sclerosis after disease-modifying therapy: a randomised controlled phase 3 trial. *The Lancet*, 380(9856):1829–1839.

Collins, S. M., Kassam, Z., and Bercik, P. (2013). The adoptive transfer of behavioral phenotype via the intestinal microbiota: Experimental evidence and clinical implications. *Current Opinion in Microbiology*, 16(3):240–245.

Comi, G., Filippi, M., and Wolinsky, J. S. (2001). European/Canadian multicenter, double-blind, randomized, placebo-controlled study of the effects of glatiramer acetate on magnetic resonance imaging-measured disease activity and burden in patients with relapsing multiple sclerosis. *Annals of Neurology*, 49(3):290–297.

Confavreux, C. and Vukusic, S. (2006). Age at disability milestones in multiple sclerosis. *Brain*, 129(3):595–605.

Conway, G. D., O'Bara, M. A., Vedia, B. H., Pol, S. U., and Sim, F. J. (2012). Histone deacetylase activity is required for human oligodendrocyte progenitor differentiation. *Glia*, 60(12):1944–1953.

Cornell, R. P., Liljequist, B. L., and Bartizal, K. F. (1990). Depressed liver regeneration after partial hepatectomy of germ-free, athymic and lipopolysaccharide-resistant mice. *Hepatology*, 11(6):916–922.

Craner, M. J., Newcombe, J., Black, J. A., Hartle, C., Cuzner, M. L., and Waxman, S. G. (2004). Molecular changes in neurons in multiple sclerosis: altered axonal expression of Nav1.2 and Nav1.6 sodium channels and Na+/Ca2+ exchanger. *Proceedings of the National Academy of Sciences of the United States of America*, 101(21):8168–8173.

Crawford, A. H., Stockley, J. H., Tripathi, R. B., Richardson, W. D., and Franklin, R. J. M. (2014). Oligodendrocyte progenitors: Adult stem cells of the central nervous system? *Experimental Neurology*, 260:50–55.

Dai, X., Ryan, G. R., Hapel, A. J., Dominguez, M. G., Russell, R. G., Kapp, S., Sylvestre, V., and Stanley, E. R. (2002). Targeted disruption of the mouse CSF-1 receptor gene results in osteopetrosis, mononuclear phagocyte deficiency, increased primititive progenitor cell frequencies and reproductive defects. *Blood*, 99(1):111–120.

David, S. and Aguayo, A. J. (1981). Axonal Elongation into Peripheral Nervous System "Bridges" after Central Nervous System Injury in Adult Rats. *Science*, 214(4523):931–933.

De La Fuente, A. G., Lange, S., Silva, M. E., Gonzalez, G. A., Tempfer, H., van Wijngaarden, P., Zhao, C., Di Canio, L., Trost, A., Bieler, L., Zaunmair, P., Rotheneichner, P., O'Sullivan, A., Couillard-Despres, S., Errea, O., Mäe, M. A., Andrae, J., He, L., Keller, A., Bátiz, L. F., Betsholtz, C., Aigner, L., Franklin, R. J., and Rivera, F. J. (2017). Pericytes Stimulate Oligodendrocyte Progenitor Cell Differentiation during CNS Remyelination. *Cell Reports*, 20(8):1755–1764.

den Besten, G., van Eunen, K., Groen, A. K., Venema, K., Reijngoud, D.-J., and Bakker, B. M. (2013). The role of short-chain fatty acids in the interplay between diet, gut microbiota, and host energy metabolism. *Journal of lipid research*, 54(9):2325–40.

Dendrou, C. A., Fugger, L., and Friese, M. A. (2015). Immunopathology of multiple sclerosis. *Nature Reviews Immunology*, 15(9):545–558.

Di Bello, I. C., Dawson, M. R., Levine, J. M., and Reynolds, R. (1999). Generation of oligodendroglial progenitors in acute inflammatory demyelinating lesions of the rat brain stem is associated with demyelination rather than inflammation. *Journal of neurocytology*, 28(4-5):365–381.

Dimidi, E., Christodoulides, S., Fragkos, K. C., Scott, S. M., and Whelan, K. (2014). The effect of probiotics on functional constipation in adults: a systematic review and meta-analysis of randomized controlled trials. *American Journal of Clinical Nutrition*, 100(4):1075–1084.

Distrutti, E., O'Reilly, J. A., McDonald, C., Cipriani, S., Renga, B., Lynch, M. A., and Fiorucci, S. (2014). Modulation of intestinal microbiota by the probiotic VSL#3 resets brain gene expression and ameliorates the age-related deficit in LTP. *PLoS ONE*, 9(9).

Dobber, R., Hertogh-Huijbregts, A., Rozing, J., Bottomly, K., and Nagelkerken, L. (1992). The Involvement of the Intestinal Microflora in the Expansion of CD4+ T Cells with a Naive Phenotype in the Periphery. *Developmental Immunology*, 2(2):141–150.

Dombrowski, Y., O'Hagan, T., Dittmer, M., Penalva, R., Mayoral, S. R., Bankhead, P., Fleville, S., Eleftheriadis, G., Zhao, C., Naughton, M., Hassan, R., Moffat, J., Falconer, J., Boyd, A., Hamilton, P., Allen, I. V., Kissenpfennig, A., Moynagh, P. N., Evergren, E., Perbal, B., Williams, A. C., Ingram, R. J., Chan, J. R., Franklin, R. J. M., and Fitzgerald, D. C. (2017). Regulatory T cells promote myelin regeneration in the central nervous system. *Nature Neuroscience*, 20(5):674–680.

Domingues, H. S., Portugal, C. C., Socodato, R., and Relvas, J. B. (2016). Oligodendrocyte, Astrocyte, and Microglia Crosstalk in Myelin Development, Damage, and Repair. *Frontiers in Cell and Developmental Biology*, 4(June):71.

Donaldson, G. P., Lee, S. M., and Mazmanian, S. K. (2015). Gut biogeography of the bacterial microbiota. *Nature Reviews Microbiology*, 14(1):20–32.

Doring, A., Sloka, S., Lau, L., Mishra, M., van Minnen, J., Zhang, X., Kinniburgh, D., Rivest, S., and Yong, V. W. (2015). Stimulation of Monocytes, Macrophages, and Microglia by Amphotericin B and Macrophage Colony-Stimulating Factor Promotes Remyelination. *Journal of Neuroscience*, 35(3):1136–1148.

Dorshkind, K., Montecino-Rodriguez, E., and Signer, R. A. J. (2009). The ageing immune system: is it ever too old to become young again? *Nature Reviews Immunology*, 9(1):57–62.

Drusano, G. L., Standiford, H. C., Plaisance, K., Forrest, A., Leslie, J., and Caldwell, J. (1986). Absolute oral bioavailability of ciprofloxacin. *Antimicrobial Agents and Chemotherapy*, 30(3):444–446.

Duffield, J. S., Forbes, S. J., Constandinou, C. M., Clay, S., Partolina, M., Vuthoori, S., Wu, S., Lang, R., and Iredale, J. P. (2005). Selective depletion of macrophages reveals distinct, opposing roles during liver injury and repair. *Journal of Clinical Investigation*, 115(1):56–65.

Duncan, I. D., Brower, A., Kondo, Y., Curlee, J. F., and Schultz, R. D. (2009). Extensive remyelination of the CNS leads to functional recovery. *Proceedings of the National Academy of Sciences*, 106(16):6832–6836.

Eckburg, P., Bik, E., Bernstein, C., Purdom, E., Dethlefsen, L., Sargent, M., Gill, S., Nelson, K., and Relman, D. (2005). Diversity of the human intestinal microbial flora. *Science*, 308(June):1635–1638.

Edwards, J. P., Zhang, X., Frauwirth, K. A., and Mosser, D. M. (2006). Biochemical and functional characterization of three activated macrophage populations Abstract : We generated three populations of macrophages (M) in vitro and characterized. *Journal of Leukocyte Biology*, 80(6):1298–307.

English, A. R., Girard, D., and Haskell, S. L. (1984). Pharmacokinetics of sultamicillin in mice, rats, and dogs. *Antimicrobial Agents and Chemotherapy*, 25(5):599–602.

Erny, D., Hrabě de Angelis, A. L., Jaitin, D., Wieghofer, P., Staszewski, O., David, E., Keren-Shaul, H., Mahlakoiv, T., Jakobshagen, K., Buch, T., Schwierzeck, V., Utermöhlen, O., Chun, E., Garrett, W. S., McCoy, K. D., Diefenbach, A., Staeheli, P., Stecher, B., Amit, I., and Prinz, M. (2015). Host microbiota constantly control maturation and function of microglia in the CNS. *Nature Neuroscience*, 18(7):965–977.

Fawcett, J. W. (2009). Recovery from spinal cord injury: Regeneration, plasticity and rehabilitation. *Brain*, 132(6):1417–1418.

Ferenczy, M. W., Marshall, L. J., Nelson, C. D. S., Atwood, W. J., Nath, A., Khalili, K., and Majora, E. O. (2012). Molecular biology, epidemiology, and pathogenesis of progressive multifocal leukoencephalopathy, the JC virus-induced demyelinating disease of the human brain. *Clinical Microbiology Reviews*, 25(3):471–506.

Ferrer, I., Bernet, E., Soriano, E., Del Rio, T., and Fonseca, M. (1990). Naturally occurring cell death in the cerebral cortex of the rat and removal of dead cells by transitory phagocytes. *Neuroscience*, 39(2):451–458.

Fife, B. T., Huffnagle, G. B., Kuziel, W. A., and Karpus, W. J. (2000). CC chemokine receptor 2 is critical for induction of experimental autoimmune encephalomyelitis. *The Journal of experimental medicine*, 192(6):899–905.

Fontaine, C. A., Skorupski, A. M., Vowles, C. J., Anderson, N. E., Poe, S. A., and Eaton, K. A. (2015). How free of germs is germ-free? Detection of bacterial contamination in a germ free mouse unit. *Gut Microbes*, 6(4):225–233.

Foulds, G., McBride, T. J., Knirsch, A. K., Rodriguez, W. J., and Khan, W. N. (1987). Penetration of sulbactam and ampicillin into cerebrospinal fluid of infants and young children with meningitis. *Antimicrobial Agents and Chemotherapy*, 31(11):1703–1705.

Franklin, R. J. and Goldman, S. A. (2015). Glia Disease and Repair—Remyelination. *Cold Spring Harbor Perspectives in Biology*, 7(7):a020594.

Franklin, R. J. M. (2002). Why does remyelination fail in multiple sclerosis? *Nature reviews. Neuroscience*, 3(9):705–14.

Franklin, R. J. M., Crang, A. J., and Blakemore, W. F. (1991). Transplanted type-1 astrocytes facilitate repair of demyelinating lesions by host oligodendrocytes in adult rat spinal cord. *Journal of Neurocytology*, 20(5):420–430.

Franklin, R. J. M. and Ffrench-Constant, C. (2008). Remyelination in the CNS: from biology to therapy. *Nature Reviews Neuroscience*, 9(11):839–855.

Franklin, R. J. M. and Ffrench-Constant, C. (2017). Regenerating CNS myelin — from mechanisms to experimental medicines. *Nature Reviews Neuroscience*, 18(12):753–769.

Fredua-Agyeman, M. and Gaisford, S. (2015). Comparative survival of commercial probiotic formulations: Tests in biorelevant gastric fluids and real-time measurements using microcalorimetry. *Beneficial Microbes*, 6(1):141–151.

Fuller, Z., Louis, P., Mihajlovski, A., Rungapamestry, V., Ratcliffe, B., and Duncan, A. J. (2007). Influence of cabbage processing methods and prebiotic manipulation of colonic microflora on glucosinolate breakdown in man. *The British journal of nutrition*, 98(2):364–72.

Fünfschilling, U., Supplie, L. M., Mahad, D., Boretius, S., Saab, A. S., Edgar, J., Brinkmann, B. G., Kassmann, C. M., Tzvetanova, I. D., Möbius, W., Diaz, F., Meijer, D., Suter, U., Hamprecht, B., Sereda, M. W., Moraes, C. T., Frahm, J., Goebbels, S., and Nave, K.-A. (2012). Glycolytic oligodendrocytes maintain myelin and long-term axonal integrity. *Nature*, 485(7399):517–521.

Fung, T. C., Olson, C. A., and Hsiao, E. Y. (2017). Interactions between the microbiota, immune and nervous systems in health and disease. *Nature Neuroscience*, 20(2):145–155.

Gacias, M., Gaspari, S., Santos, P.-M. G., Tamburini, S., Andrade, M., Zhang, F., Shen, N., Tolstikov, V., Kiebish, M. A., Dupree, J. L., Zachariou, V., Clemente, J. C., and Casaccia, P. (2016). Microbiota-driven transcriptional changes in prefrontal cortex override genetic differences in social behavior. *eLife*, 5.

Gao, H. M., Zhang, F., Zhou, H., Kam, W., Wilson, B., and Hong, J. S. (2011). Neuroinflammation and α-synuclein dysfunction potentiate each other, driving chronic progression of neurodegeneration in a mouse model of Parkinson's disease. *Environmental Health Perspectives*, 119(6):807–814.

Garbern, J. Y., Yool, D. A., Moore, G. J., Wilds, I. B., Faulk, M. W., Klugmann, M., Nave, K.-A., Sistermans, E. A., van der Knaap, M. S., Bird, T. D., Shy, M. E., Kamholz, J. A., and Griffiths, I. R. (2002). Patients lacking the major CNS myelin protein, proteolipid protein 1, develop length-dependent axonal degeneration in the absence of demyelination and inflammation. *Brain*, 125(3):551–561.

Ghasemlou, N., Jeong, S. Y., Lacroix, S., and David, S. (2007). T cells contribute to lysophosphatidylcholine-induced macrophage activation and demyelination in the CNS. *Glia*, 55(3):294–302.

Ginhoux, F., Greter, M., Leboeuf, M., Nandi, S., See, P., Gokhan, S., Mehler, M. F., Conway, S. J., Ng, L. G., Stanley, E. R., Samokhvalov, I. M., and Merad, M. (2010). Fate Mapping Analysis Reveals That Adult Microglia Derive from Primitive Macrophages. *Science*, 330(6005):841–845.

Gionchetti, P., Calafiore, A., Riso, D., Liguori, G., Calabrese, C., Vitali, G., Laureti, S., Poggioli, G., Campieri, M., and Rizzello, F. (2012). The role of antibiotics and probiotics in pouchitis. *Annals of gastroenterology*, 25(2):100–105.

Goldschmidt, T., Antel, J., König, F. B., Brück, W., and Kuhlmann, T. (2009). Remyelination capacity of the MS brain decreases with disease chronicity. *Neurology*, 72(22):1914–1921.

Gouon-Evans, V., Rothenberg, M. E., and Pollard, J. W. (2000). Postnatal mammary gland development requires macrophages and eosinophils. *Development (Cambridge, England)*, 127(11):2269–82.

Green, A., Gelfand, J., Cree, B., Bevan, C., Boscardin, W., Mei, F., Inman, J., Arnow, S., Devereux, M., Abounasr, A., Friessen, M., Gerona, R., Von Buedingen, H. C., Henry, R., Hauser, S., and Chan, J. R. (2016). Over-the-Counter Drug May Reverse Vision Damage Caused by Multiple Sclerosis. In *American Academy of Neurology 68th Annual Meeting Abstract*.

Griffiths, I., Klugmann, M., Anderson, T., Yool, D., Thomson, C., Schwab, M. H., Schneider, A., Zimmermann, F., McCulloch, M., Nadon, N., and Nave, K. A. (1998). Axonal swellings and degeneration in mice lacking the major proteolipid of myelin. *Science*, 280(5369):1610–3.

Gudi, V., Gingele, S., Skripuletz, T., and Stangel, M. (2014). Glial response during cuprizone-induced de- and remyelination in the CNS: lessons learned. *Frontiers in cellular neuroscience*, 8(March):73.

Heimesaat, M. M., Bereswill, S., Fischer, A., Fuchs, D., Struck, D., Niebergall, J., Jahn, H.-K., Dunay, I. R., Moter, A., Gescher, D. M., Schumann, R. R., Gobel, U. B., and Liesenfeld, O. (2006). Gram-Negative Bacteria Aggravate Murine Small Intestinal Th1-Type Immunopathology following Oral Infection with Toxoplasma gondii. *The Journal of Immunology*, 177(12):8785–8795.

Heimesaat, M. M., Kupz, A., Fischer, A., Nies, D. H., Grass, G., Göbel, U. B., and Bereswill, S. (2013). Colonization resistance against genetically modified Escherichia coli K12 (W3110) strains is abrogated following broad-spectrum antibiotic treatment and acute ileitis. *European journal of microbiology & immunology*, 3(3):222–8.

Helander, H. F. and Fändriks, L. (2014). Surface area of the digestive tract - revisited. *Scandinavian journal of gastroenterology*, 49(6):681–9.

Hempel, S., Newberry, S. J., Maher, A. R., Wang, Z., Miles, J. N. V., Shanman, R., Johnsen, B., and Shekelle, P. G. (2012). Probiotics for the prevention and treatment of antibiotic-associated diarrhea: a systematic review and meta-analysis. *JAMA*, 307(18):1959–69.

Heppner, F. L., Greter, M., Marino, D., Falsig, J., Raivich, G., Hövelmeyer, N., Waisman, A., Rülicke, T., Prinz, M., Priller, J., Becher, B., and Aguzzi, A. (2005). Experimental autoimmune encephalomyelitis repressed by microglial paralysis. *Nature medicine*, 11(2):146–52.

Hill, C., Guarner, F., Reid, G., Gibson, G. R., Merenstein, D. J., Pot, B., Morelli, L., Canani, R. B., Flint, H. J., Salminen, S., Calder, P. C., and Sanders, M. E. (2014). Expert consensus document: The International Scientific Association for Probiotics and Prebiotics consensus statement on the scope and appropriate use of the term probiotic. *Nature Reviews Gastroenterology & Hepatology*, 11(8):506–514.

Hinks, G. L. and Franklin, R. J. (2000). Delayed changes in growth factor gene expression during slow remyelination in the CNS of aged rats. *Molecular and cellular neurosciences*, 16(5):542–56.

Hiremath, M. M., Chen, V. S., Suzuki, K., Ting, J. P.-Y., and Matsushima, G. K. (2008). MHC class II exacerbates demyelination in vivo independently of T cells. *Journal of Neuroimmunology*, 203(1):23–32.

Hoban, A. E., Stilling, R. M., Ryan, F. J., Shanahan, F., Dinan, T. G., Claesson, M. J., Clarke, G., and Cryan, J. F. (2016). Regulation of prefrontal cortex myelination by the microbiota. *Translational Psychiatry*, 6(4):e774.

Houston, S. A., Cerovic, V., Thomson, C., Brewer, J., Mowat, A. M., and Milling, S. (2016). The lymph nodes draining the small intestine and colon are anatomically separate and immunologically distinct. *Mucosal Immunology*, 9(2):468–478.

Høverstad, T. and Midtvedt, T. (1986). Short-chain fatty acids in germfree mice and rats. *The Journal of nutrition*, 116(9):1772–6.

Huang, J. K., Jarjour, A. A., Oumesmar, B. N., Kerninon, C., Williams, A., Krezel, W., Kagechika, H., Bauer, J., Zhao, C., Evercooren, A. B.-V., Chambon, P., Ffrench-Constant, C., and Franklin, R. J. M. (2011). Retinoid X receptor gamma signaling accelerates CNS remyelination. *Nature Neuroscience*, 14(1):45–53.

Irvine, K. A. and Blakemore, W. F. (2008). Remyelination protects axons from demyelination-associated axon degeneration. *Brain*, 131(6):1464–1477.

Ivanov, I. I., Atarashi, K., Manel, N., Brodie, E. L., Shima, T., Karaoz, U., Wei, D., Goldfarb, K. C., Santee, C. A., Lynch, S. V., Tanoue, T., Imaoka, A., Itoh, K., Takeda, K., Umesaki, Y., Honda, K., and Littman, D. R. (2009). Induction of Intestinal Th17 Cells by Segmented Filamentous Bacteria. *Cell*, 139(3):485–498.

Jernberg, C., Löfmark, S., Edlund, C., and Jansson, J. K. (2007). Long-term ecological impacts of antibiotic administration on the human intestinal microbiota. *The ISME journal*, 1(1):56–66.

Jersild, C., Svejgaard, A., and Fog, T. (1972). HL-A ANTIGENS AND MULTIPLE SCLEROSIS. *The Lancet*, 299(7762):1240–1241.

Jhangi, S., Gandhi, R., Glanz, B., Cook, S., Nejad, P., Ward, D., Li, N., Gerber, G., Bry, L., and Weiner, H. (2014). Increased Archaea species and changes with therapy in gut microbiome of multiple sclerosis subjects (S24. 001). *Neurology*, 82(10):S24.001.

Ji, J., Shu, D., Zheng, M., Wang, J., Luo, C., Wang, Y., Guo, F., Zou, X., Lv, X., Li, Y., Liu, T., and Qu, H. (2016). Microbial metabolite butyrate facilitates M2 macrophage polarization and function. *Scientific Reports*, 6:1–10.

Kannan, V., Brouwer, N., Hanisch, U. K., Regen, T., Eggen, B. J., and Boddeke, H. W. (2013). Histone deacetylase inhibitors suppress immune activation in primary mouse microglia. *Journal of Neuroscience Research*, 91(9):1133–1142.

Karni, a., Abraham, M., Monsonego, a., Cai, G., Freeman, G. J., Hafler, D., Khoury, S. J., and Weiner, H. L. (2006). Innate Immunity in Multiple Sclerosis: Myeloid Dendritic Cells in Secondary Progressive Multiple Sclerosis Are Activated and Drive a Proinflammatory Immune Response. *The Journal of Immunology*, 177(6):4196–4202.

Keough, M. B., Jensen, S. K., and Yong, V. W. (2015). Experimental demyelination and remyelination of murine spinal cord by focal injection of lysolecithin. *Journal of visualized experiments : JoVE*, (97):e52679.

Khosravi, A., Yáñez, A., Price, J. G., Chow, A., Merad, M., Goodridge, H. S., and Mazmanian, S. K. (2014). Gut microbiota promote hematopoiesis to control bacterial infection. *Cell Host and Microbe*, 15(3):374–381.

Kigerl, K. A., Gensel, J. C., Ankeny, D. P., Alexander, J. K., Donnelly, D. J., and Popovich, P. G. (2009). Identification of Two Distinct Macrophage Subsets with Divergent Effects Causing either Neurotoxicity or Regeneration in the Injured Mouse Spinal Cord. *Journal of Neuroscience*, 29(43):13435–13444.

Kigerl, K. A., Hall, J. C., Wang, L., Mo, X., Yu, Z., and Popovich, P. G. (2016). Gut dysbiosis impairs recovery after spinal cord injury. *The Journal of Experimental Medicine*, 213(12):2603–2620.

Kiryu-Seo, S., Ohno, N., Kidd, G. J., Komuro, H., and Trapp, B. D. (2010). Demyelination Increases Axonal Stationary Mitochondrial Size and the Speed of Axonal Mitochondrial Transport. *Journal of Neuroscience*, 30(19):6658–6666.

Kobayashi, K., Imagama, S., Ohgomori, T., Hirano, K., Uchimura, K., Sakamoto, K., Hirakawa, A., Takeuchi, H., Suzumura, A., Ishiguro, N., and Kadomatsu, K. (2013). Minocycline selectively inhibits M1 polarization of microglia. *Cell Death & Disease*, 4(3):e525–e525.

Koeppen, A. H., Ronca, N. A., Greenfield, E. A., and Hans, M. B. (1987). Defective biosynthesis of proteolipid protein in pelizaeus-merzbacher disease. *Annals of Neurology*, 21(2):159–170.

Kordower, J. and Tuszynski, M. (2011). *CNS Regeneration: Basic Science and Clinical Advances*. Elsevier Science.

Kornek, B., Storch, M. K., Weissert, R., Wallstroem, E., Stefferl, A., Olsson, T., Linington, C., Schmidbauer, M., and Lassmann, H. (2000). Multiple Sclerosis and Chronic Autoimmune Encephalomyelitis. *The American Journal of Pathology*, 157(1):267–276.

Korzhevskii, D. E. and Kirik, O. V. (2016). Brain Microglia and Microglial Markers. *Neuroscience and Behavioral Physiology*, 46(3):284–290.

Kotter, M. R., Li, W.-W., Zhao, C., and Franklin, R. J. M. (2006). Myelin impairs CNS remyelination by inhibiting oligodendrocyte precursor cell differentiation. *The Journal of neuroscience : the official journal of the Society for Neuroscience*, 26(1):328–32.

Kotter, M. R., Setzu, A., Sim, F. J., Van Rooijen, N., and Franklin, R. J. (2001). Macrophage depletion impairs oligodendrocyte remyelination following lysolecithin-induced demyelination. *Glia*, 35(3):204–12.

Kotter, M. R., Zhao, C., van Rooijen, N., and Franklin, R. J. M. (2005). Macrophage-depletion induced impairment of experimental CNS remyelination is associated with a reduced oligodendrocyte progenitor cell response and altered growth factor expression. *Neurobiology of disease*, 18(1):166–75.

Kouchaki, E., Tamtaji, O. R., Salami, M., Bahmani, F., Daneshvar Kakhaki, R., Akbari, E., Tajabadi-Ebrahimi, M., Jafari, P., and Asemi, Z. (2017). Clinical and metabolic response to probiotic supplementation in patients with multiple sclerosis: A randomized, double-blind, placebo-controlled trial. *Clinical Nutrition*, 36(5):1245–1249.

Kubinak, J. L., Stephens, W. Z., Soto, R., Petersen, C., Chiaro, T., Gogokhia, L., Bell, R., Ajami, N. J., Petrosino, J. F., Morrison, L., Potts, W. K., Jensen, P. E., O'Connell, R. M., and Round, J. L. (2015). MHC variation sculpts individualized microbial communities that control susceptibility to enteric infection. *Nature Communications*, 6:8642.

Kumar, M., Kissoon-Singh, V., Coria, A. L., Moreau, F., and Chadee, K. (2017). Probiotic mixture VSL#3 reduces colonic inflammation and improves intestinal barrier function in Muc2 mucin-deficient mice. *American Journal of Physiology-Gastrointestinal and Liver Physiology*, 312(1):G34–G45.

Kumar, P. and Clark, M. (2012). *Kumar and Clark's Clinical Medicine*. Elsevier, 8th edition.

Lampron, A., Larochelle, A., Laflamme, N., Préfontaine, P., Plante, M.-M., Sánchez, M. G., Yong, V. W., Stys, P. K., Tremblay, M.-È., and Rivest, S. (2015). Inefficient clearance of myelin debris by microglia impairs remyelinating processes. *The Journal of experimental medicine*, 212(4):481–95.

Lan, X., Han, X., Li, Q., Yang, Q., and Wang, J. (2017). Modulators of microglial activation and polarization after intracerebral haemorrhage. *Nature Reviews Neurology*, 13(7):420–433.

Lau, A. H., Lam, N. P., Piscitelli, S. C., Wilkes, L., and Danziger, L. H. (1992). Clinical Pharmacokinetics of Metronidazole and Other Nitroimidazole Anti-Infectives. *Clinical Pharmacokinetics*, 23(5):328–364.

Le Blon, D., Guglielmetti, C., Hoornaert, C., Quarta, A., Daans, J., Dooley, D., Lemmens, E., Praet, J., De Vocht, N., Reekmans, K., Santermans, E., Hens, N., Goossens, H., Verhoye, M., Van der Linden, A., Berneman, Z., Hendrix, S., and Ponsaerts, P. (2016). Intracerebral transplantation of interleukin 13-producing mesenchymal stem cells limits microgliosis, oligodendrocyte loss and demyelination in the cuprizone mouse model. *Journal of Neuroinflammation*, 13(1):288.

Lee, J. Y., Taghian, K., and Petratos, S. (2014). Axonal degeneration in multiple sclerosis: can we predict and prevent permanent disability? *Acta Neuropathologica Communications*, 2(1):97.

Lee, Y., Morrison, B. M., Li, Y., Lengacher, S., Farah, M. H., Hoffman, P. N., Liu, Y., Tsingalia, A., Jin, L., Zhang, P.-W., Pellerin, L., Magistretti, P. J., and Rothstein, J. D. (2012). Oligodendroglia metabolically support axons and contribute to neurodegeneration. *Nature*, 487(7408):443–448.

Lee, Y. K., Menezes, J. S., Umesaki, Y., and Mazmanian, S. K. (2011). Proinflammatory T-cell responses to gut microbiota promote experimental autoimmune encephalomyelitis. *Proceedings of the National Academy of Sciences*, 108:4615–4622.

Lelouard, H., Fallet, M., de Bovis, B., Méresse, S., and Gorvel, J. (2012). Peyer's Patch Dendritic Cells Sample Antigens by Extending Dendrites Through M Cell-Specific Transcellular Pores. *Gastroenterology*, 142(3):592–601.e3.

Letourneau, R., Rozniecki, J. J., Dimitriadou, V., and Theoharides, T. C. (2003). Ultrastructural evidence of brain mast cell activation without degranulation in monkey experimental allergic encephalomyelitis. *Journal of Neuroimmunology*, 145(1-2):18–26.

Li, J. Y., Chassaing, B., Tyagi, A. M., Vaccaro, C., Luo, T., Adams, J., Darby, T. M., Weitzmann, M. N., Mulle, J. G., Gewirtz, A. T., Jones, R. M., and Pacifici, R. (2016). Sex steroid deficiency-associated bone loss is microbiota dependent and prevented by probiotics. *Journal of Clinical Investigation*, 126(6):2049–2063.

Liu, C. X., Wang, J. R., and Lu, Y. L. (1990). Pharmacokinetics of sulbactam and ampicillin in mice and in dogs. *Acta Pharmaceutica Sinica*, 25(6):406–411.

Liu, L., Belkadi, A., Darnall, L., Hu, T., Drescher, C., Cotleur, A. C., Padovani-Claudio, D., He, T., Choi, K., Lane, T. E., Miller, R. H., and Ransohoff, R. M. (2010). CXCR2-positive neutrophils are essential for cuprizone-induced demyelination: relevance to multiple sclerosis. *Nature Neuroscience*, 13(3):319–326.

Lo, D. C., Allen, F., and Brockes, J. P. (1993). Reversal of muscle differentiation during urodele limb regeneration. *Proceedings of the National Academy of Sciences of the United States of America*, 90(15):7230–7234.

Lucchinetti, C., Brück, W., Parisi, J., Scheithauer, B., Rodriguez, M., and Lassmann, H. (2000). Heterogeneity of multiple sclerosis lesions: implications for the pathogenesis of demyelination. *Annals of neurology*, 47(6):707–17.

Luczynski, P., McVey Neufeld, K.-A., Oriach, C. S., Clarke, G., Dinan, T. G., and Cryan, J. F. (2016). Growing up in a Bubble: Using Germ-Free Animals to Assess the Influence of the Gut Microbiota on Brain and Behavior. *International Journal of Neuropsychopharmacology*, 19(8):pyw020.

Luo, Y., Chen, G. L., Hannemann, N., Ipseiz, N., Krönke, G., Bäuerle, T., Munos, L., Wirtz, S., Schett, G., and Bozec, A. (2015). Microbiota from Obese Mice Regulate Hematopoietic Stem Cell Differentiation by Altering the Bone Niche. *Cell Metabolism*, 22(5):886–894.

Maghazachi, A. A. (2012). Role of Natural Killer Cells in Multiple Sclerosis. *ISRN Immunology*, 2012:1–14.

Mariman, R., Tielen, F., Koning, F., and Nagelkerken, L. (2015). The Probiotic Mixture VSL#3 Has Differential Effects on Intestinal Immune Parameters in Healthy Female BALB/c and C57BL/6 Mice. *Journal of Nutrition*, 145(6):1354–1361.

Martin, R. J. (2004). Central pontine and extrapontine myelinolysis: the osmotic demyelination syndromes. *Journal of Neurology, Neurosurgery & Psychiatry*, 75(suppl_3):iii22–iii28.

Maslowski, K. M., Vieira, A. T., Ng, A., Kranich, J., Sierro, F., Di Yu, Schilter, H. C., Rolph, M. S., Mackay, F., Artis, D., Xavier, R. J., Teixeira, M. M., and Mackay, C. R. (2009). Regulation of inflammatory responses by gut microbiota and chemoattractant receptor GPR43. *Nature*, 461(7268):1282–1286.

Matcovitch-Natan, O., Winter, D. R., Giladi, A., Vargas Aguilar, S., Spinrad, A., Sarrazin, S., Ben-Yehuda, H., David, E., Zelada Gonzalez, F., Perrin, P., Keren-Shaul, H., Gury, M., Lara-Astaiso, D., Thaiss, C. A., Cohen, M., Bahar Halpern, K., Baruch, K., Deczkowska, A., Lorenzo-Vivas, E., Itzkovitz, S., Elinav, E., Sieweke, M. H., Schwartz, M., and Amit, I. (2016). Microglia development follows a stepwise program to regulate brain homeostasis. *Science*, 353(6301):aad8670–aad8670.

Matsuo, A., Lee, G. C., Terai, K., Takami, K., Hickey, W. F., McGeer, E. G., and McGeer, P. L. (1997). Unmasking of an unusual myelin basic protein epitope during the process of myelin degeneration in humans: a potential mechanism for the generation of autoantigens. *The American journal of pathology*, 150(4):1253–66.

Mayer, E. A., Knight, R., Mazmanian, S. K., Cryan, J. F., and Tillisch, K. (2014). Gut Microbes and the Brain: Paradigm Shift in Neuroscience. *Journal of Neuroscience*, 34(46):15490–15496.

McKinnon, R. D., Piras, G., Ida, J. A., and Dubois-Dalcq, M. (1993). A role for TGF-beta in oligodendrocyte differentiation. *The Journal of cell biology*, 121(6):1397–1407.

McMorris, F. A. and Dubois-Dalcq, M. (1988). Insulin-like growth factor I promotes cell proliferation and oligodendroglial commitment in rat glial progenitor cells developing in vitro. *Journal of neuroscience research*, 21(2-4):199–209.

McNeil, P. L. and Steinhardt, R. A. (1997). Loss, restoration, and maintenance of plasma membrane integrity. *Journal of Cell Biology*, 137(1):1–4.

Medana, I. M. and Esiri, M. M. (2003). Axonal damage: A key predictor of outcome in human CNS diseases. *Brain*, 126(3):515–530.

Mei, F., Lehmann-Horn, K., Shen, Y.-A. A., Rankin, K. A., Stebbins, K. J., Lorrain, D. S., Pekarek, K., A Sagan, S., Xiao, L., Teuscher, C., von Büdingen, H.-C., Wess, J., Lawrence, J. J., Green, A. J., Fancy, S. P., Zamvil, S. S., and Chan, J. R. (2016). Accelerated remyelination during inflammatory demyelination prevents axonal loss and improves functional recovery. *eLife*, 5:1–21.

Michalopoulos, G. K. and DeFrances, M. C. (2007). Liver regeneration. *Journal of cellular physiology*, 213(2):286–300.

Mikita, J., Dubourdieu-Cassagno, N., Deloire, M. S., Vekris, A., Biran, M., Raffard, G., Brochet, B., Canron, M.-H., Franconi, J.-M., Boiziau, C., and Petry, K. G. (2011). Altered M1/M2 activation patterns of monocytes in severe relapsing experimental rat model of multiple sclerosis. Amelioration of clinical status by M2 activated monocyte administration. *Multiple Sclerosis Journal*, 17(1):2–15.

Miller, A., Korem, M., Almog, R., and Galboiz, Y. (2005). Vitamin B12, demyelination, remyelination and repair in multiple sclerosis. *Journal of the neurological sciences*, 233(1-2):93–7.

Miron, V. E., Boyd, A., Zhao, J.-W., Yuen, T. J., Ruckh, J. M., Shadrach, J. L., van Wijngaarden, P., Wagers, A. J., Williams, A., Franklin, R. J. M., and Ffrench-Constant, C. (2013). M2 microglia and macrophages drive oligodendrocyte differentiation during CNS remyelination. *Nature Neuroscience*, 16(9):1211–1218.

Miron, V. E. and Franklin, R. J. M. (2014). Macrophages and CNS remyelination. *Journal of Neurochemistry*, 130(2):165–171.

Mitchell, R. W., On, N. H., Del Bigio, M. R., Miller, D. W., and Hatch, G. M. (2011). Fatty acid transport protein expression in human brain and potential role in fatty acid transport across human brain microvessel endothelial cells. *Journal of Neurochemistry*, 117(4):735–746.

Miyoshi, M., Sakaki, H., Usami, M., Iizuka, N., Shuno, K., Aoyama, M., and Usami, Y. (2011). Oral administration of tributyrin increases concentration of butyrate in the portal vein and prevents lipopolysaccharide-induced liver injury in rats. *Clinical Nutrition*, 30(2):252–258.

Moayyedi, P., Ford, A. C., Talley, N. J., Cremonini, F., Foxx-Orenstein, A. E., Brandt, L. J., and Quigley, E. M. M. (2010). The efficacy of probiotics in the treatment of irritable bowel syndrome: a systematic review. *Gut*, 59:325–332.

Möhle, L., Mattei, D., Heimesaat, M., Bereswill, S., Fischer, A., Alutis, M., French, T., Hambardzumyan, D., Matzinger, P., Dunay, I., and Wolf, S. (2016). Ly6Chi Monocytes Provide a Link between Antibiotic-Induced Changes in Gut Microbiota and Adult Hippocampal Neurogenesis. *Cell Reports*, pages 1945–1956.

Mowry, E., Waubant, E., Chehoud, C., DeSantis, T., Kuczynski, J., and Warrington, J. (2012). Gut Bacterial Populations in Multiple Sclerosis and in Health (P05.106). *Neurology*, 78(Meeting Abstracts 1):P05.106–P05.106.

Murray, P. J., Allen, J. E., Biswas, S. K., Fisher, E. A., Gilroy, D. W., Goerdt, S., Gordon, S., Hamilton, J. A., Ivashkiv, L. B., Lawrence, T., Locati, M., Mantovani, A., Martinez, F. O., Mege, J. L., Mosser, D. M., Natoli, G., Saeij, J. P., Schultze, J. L., Shirey, K. A., Sica, A., Suttles, J., Udalova, I., Van Ginderachter, J. A., Vogel, S. N., and Wynn, T. A. (2014). Macrophage Activation and Polarization: Nomenclature and Experimental Guidelines. *Immunity*, 41(1):14–20.

Nair, A. B. and Jacob, S. (2016). A simple practice guide for dose conversion between animals and human. *Journal of Basic and Clinical Pharmacy*, 7(2):27.

Nathan, C., Ding, A., Castellheim, A., Brekke, O. L., Espevik, T., Harboe, M., Mollnes, T. E., and Immunol, S. J. (2013). Pleiotropic Actions of Insulin. *Inflammation*, 871(January):172–177.

Natrajan, M. S., De La Fuente, A. G., Crawford, A. H., Linehan, E., Nuñez, V., Johnson, K. R., Wu, T., Fitzgerald, D. C., Ricote, M., Bielekova, B., and Franklin, R. J. M. (2015). Retinoid X receptor activation reverses age-related deficiencies in myelin debris phagocytosis and remyelination. *Brain*, 138(12):3581–3597.

Nau, R., Sorgel, F., and Eiffert, H. (2010). Penetration of Drugs through the Blood-Cerebrospinal Fluid/Blood-Brain Barrier for Treatment of Central Nervous System Infections. *Clinical Microbiology Reviews*, 23(4):858–883.

Nave, K.-A. and Werner, H. B. (2014). Myelination of the Nervous System: Mechanisms and Functions. *Annual Review of Cell and Developmental Biology*, 30(1):503–533.

Nicklas, W., Keubler, L., and Bleich, A. (2015). Maintaining and monitoring the defined microbiota status of gnotobiotic rodents. *ILAR Journal*, 56(2):241–249.

Nikodemova, M., Watters, J. J., Jackson, S. J., Yang, S. K., and Duncan, I. D. (2007). Minocycline Down-regulates MHC II Expression in Microglia and Macrophages through Inhibition of IRF-1 and Protein Kinase C (PKC) α/βII. *Journal of Biological Chemistry*, 282(20):15208–15216.

Nimmerjahn, A., Kirchhoff, F., and Helmchen, F. (2005). Resting microglial cells are highly dynamic surveillants of brain parenchyma in vivo. *Science*, 308(5726):1314–8.

Ochoa-Reparaz, J., Mielcarz, D. W., Ditrio, L. E., Burroughs, A. R., Begum-Haque, S., Dasgupta, S., Kasper, D. L., and Kasper, L. H. (2010). Central Nervous System Demyelinating Disease Protection by the Human Commensal Bacteroides fragilis Depends on Polysaccharide A Expression. *The Journal of Immunology*, 185(7):4101–4108.

Ochoa-Reparaz, J., Mielcarz, D. W., Ditrio, L. E., Burroughs, A. R., Foureau, D. M., Haque-Begum, S., and Kasper, L. H. (2009). Role of Gut Commensal Microflora in the Development of Experimental Autoimmune Encephalomyelitis. *The Journal of Immunology*, 183(10):6041–6050.

Ogbonnaya, E. S., Clarke, G., Shanahan, F., Dinan, T. G., Cryan, J. F., and O'Leary, O. F. (2015). Adult Hippocampal Neurogenesis Is Regulated by the Microbiome. *Biological Psychiatry*, 78(4):e7–e9.

Olah, M., Amor, S., Brouwer, N., Vinet, J., Eggen, B., Biber, K., and Boddeke, H. W. (2012). Identification of a microglia phenotype supportive of remyelination. *Glia*, 60(2):306–321.

Ousman, S. S. and David, S. (2001). MIP-1alpha, MCP-1, GM-CSF, and TNF-alpha control the immune cell response that mediates rapid phagocytosis of myelin from the adult mouse spinal cord. *The Journal of Neuroscience*, 21(13):4649–56.

Packey, C. D., Shanahan, M. T., Manick, S., Bower, M. A., Ellermann, M., Tonkonogy, S. L., Carroll, I. M., and Sartor, R. B. (2013). Molecular detection of bacterial contamination in gnotobiotic rodent units. *Gut Microbes*, 4(5):361–370.

Paolicelli, R. C., Bolasco, G., Pagani, F., Maggi, L., Scianni, M., Panzanelli, P., Giustetto, M., Ferreira, T. A., Guiducci, E., Dumas, L., Ragozzino, D., and Gross, C. T. (2011). Synaptic Pruning by Microglia Is Necessary for Normal Brain Development. *Science*, 333(6048):1456–1458.

Parkinson, R. B., Hopkins, R. O., Cleavinger, H. B., Weaver, L. K., Victoroff, J., Foley, J. F., and Bigler, E. D. (2002). White matter hyperintensities and neuropsychological outcome following carbon monoxide poisoning. *Neurology*, 58(10):1525–1532.

Patrikios, P., Stadelmann, C., Kutzelnigg, A., Rauschka, H., Schmidbauer, M., Laursen, H., Sorensen, P. S., Brück, W., Lucchinetti, C., and Lassmann, H. (2006). Remyelination is extensive in a subset of multiple sclerosis patients. *Brain*, 129(12):3165–3172.

Perry, R. J., Peng, L., Barry, N. A., Cline, G. W., Zhang, D., Cardone, R. L., Petersen, K. F., Kibbey, R. G., Goodman, A. L., and Shulman, G. I. (2016). Acetate mediates a microbiome–brain–β-cell axis to promote metabolic syndrome. *Nature*, 534(7606):213–217.

Perry, V. H. (1998). A revised view of the central nervous system microenvironment and major histocompatibility complex class II antigen presentation. *Journal of Neuroimmunology*, 90(2):113–121.

Phatnani, H. and Maniatis, T. (2015). Astrocytes in Neurodegenerative Disease. *Cold Spring Harbor Perspectives in Biology*, 7(6):a020628.

Pohl, H. B. F., Porcheri, C., Mueggler, T., Bachmann, L. C., Martino, G., Riethmacher, D., Franklin, R. J. M., Rudin, M., and Suter, U. (2011). Genetically Induced Adult Oligodendrocyte Cell Death Is Associated with Poor Myelin Clearance, Reduced Remyelination, and Axonal Damage. *Journal of Neuroscience*, 31(3):1069–1080.

Polman, C. H., O'Connor, P. W., Havrdova, E., Hutchinson, M., Kappos, L., Miller, D. H., Phillips, J. T., Lublin, F. D., Giovannoni, G., Wajgt, A., Toal, M., Lynn, F., Panzara, M. A., and Sandrock, A. W. (2006). A Randomized, Placebo-Controlled Trial of Natalizumab for Relapsing Multiple Sclerosis. *New England Journal of Medicine*, 354(9):899–910.

Poorjavad, M., Derakhshandeh, F., Etemadifar, M., Soleymani, B., Minagar, A., and Maghzi, A.-H. (2010). Oropharyngeal dysphagia in multiple sclerosis. *Multiple Sclerosis Journal*, 16(3):362–365.

Popescu, B. F. G., Pirko, I., and Lucchinetti, C. F. (2013). Pathology of multiple sclerosis: Where do we stand? *CONTINUUM Lifelong Learning in Neurology*, 19(4):901–921.

Potente, M., Gerhardt, H., and Carmeliet, P. (2011). Basic and therapeutic aspects of angiogenesis. *Cell*, 146(6):873–887.

Pouteau, E., Nguyen, P., Ballevre, O., and Krempf, M. (2003). Production rates and metabolism of short-chain fatty acids in the colon and whole body using stable isotopes. *Proceedings of the Nutrition Society*, 62(1):87–93.

Praet, J., Guglielmetti, C., Berneman, Z., Van der Linden, A., and Ponsaerts, P. (2014). Cellular and molecular neuropathology of the cuprizone mouse model: Clinical relevance for multiple sclerosis. *Neuroscience and Biobehavioral Reviews*, 47:485–505.

PRISMS Study Group (1998). Randomised double-blind placebo-controlled study of interferon β-1a in relapsing/remitting multiple sclerosis. *The Lancet*, 352(9139):1498–1504.

Qin, J., Li, R., Raes, J., Arumugam, M., Burgdorf, K. S., Manichanh, C., Nielsen, T., Pons, N., Levenez, F., Yamada, T., Mende, D. R., Li, J., Xu, J., Li, S., Li, D., Cao, J., Wang, B., Liang, H., Zheng, H., Xie, Y., Tap, J., Lepage, P., Bertalan, M., Batto, J.-M., Hansen, T., Le Paslier, D., Linneberg, A., Nielsen, H. B., Pelletier, E., Renault, P., Sicheritz-Ponten,

T., Turner, K., Zhu, H., Yu, C., Li, S., Jian, M., Zhou, Y., Li, Y., Zhang, X., Li, S., Qin, N., Yang, H., Wang, J., Brunak, S., Doré, J., Guarner, F., Kristiansen, K., Pedersen, O., Parkhill, J., Weissenbach, J., Antolin, M., Artiguenave, F., Blottiere, H., Borruel, N., Bruls, T., Casellas, F., Chervaux, C., Cultrone, A., Delorme, C., Denariaz, G., Dervyn, R., Forte, M., Friss, C., van de Guchte, M., Guedon, E., Haimet, F., Jamet, A., Juste, C., Kaci, G., Kleerebezem, M., Knol, J., Kristensen, M., Layec, S., Le Roux, K., Leclerc, M., Maguin, E., Melo Minardi, R., Oozeer, R., Rescigno, M., Sanchez, N., Tims, S., Torrejon, T., Varela, E., de Vos, W., Winogradsky, Y., Zoetendal, E., Bork, P., Ehrlich, S. D., and Wang, J. (2010). A human gut microbial gene catalogue established by metagenomic sequencing. *Nature*, 464(7285):59–65.

Ramagopalan, S. V., Knight, J. C., and Ebers, G. C. (2009). Multiple sclerosis and the major histocompatibility complex. *Current Opinion in Neurology*, 22(3):219–225.

Rath, M., Müller, I., Kropf, P., Closs, E. I., and Munder, M. (2014). Metabolism via arginase or nitric oxide synthase: Two competing arginine pathways in macrophages. *Frontiers in Immunology*, 5(OCT):1–10.

Redford, E. J., Kapoor, R., and Smith, K. J. (1997). Nitric oxide donors reversibly block axonal conduction: Demyelinated axons are especially susceptible. *Brain*, 120(12):2149–2157.

Ridaura, V. K., Faith, J. J., Rey, F. E., Cheng, J., Duncan, A. E., Kau, A. L., Griffin, N. W., Lombard, V., Henrissat, B., Bain, J. R., Muehlbauer, M. J., Ilkayeva, O., Semenkovich, C. F., Funai, K., Hayashi, D. K., Lyle, B. J., Martini, M. C., Ursell, L. K., Clemente, J. C., Van Treuren, W., Walters, W. A., Knight, R., Newgard, C. B., Heath, A. C., and Gordon, J. I. (2013). Gut microbiota from twins discordant for obesity modulate metabolism in mice. *Science*, 341(6150):1241214.

Robinson, A. P., Harp, C. T., Noronha, A., and Miller, S. D. (2014). The experimental autoimmune encephalomyelitis (EAE) model of MS. pages 173–189.

Robinson, S. and Miller, R. H. (1999). Contact with central nervous system myelin inhibits oligodendrocyte progenitor maturation. *Developmental biology*, 216(1):359–368.

Rothhammer, V., Mascanfroni, I., Bunse, L., Takenaka, M., Kenison, J., and Mayo, L. (2016). Type I interferons and micorbial metabolites of tryptophan modulate astrocyte activity and central nervous system inflammation via the aryl hydrocarbon receptor. *Inflammatory Bowel Disease Monitor*, 22(6):586–597.

Ruckh, J. M., Zhao, J.-W., Shadrach, J. L., van Wijngaarden, P., Rao, T. N., Wagers, A. J., and Franklin, R. J. (2012). Rejuvenation of Regeneration in the Aging Central Nervous System. *Cell Stem Cell*, 10(1):96–103.

Sampson, T. R., Debelius, J. W., Thron, T., Janssen, S., Shastri, G. G., Ilhan, Z. E., Challis, C., Schretter, C. E., Rocha, S., Gradinaru, V., Chesselet, M.-f., Keshavarzian, A., Shannon, K. M., Krajmalnik-Brown, R., Wittung-Stafshede, P., Knight, R., and Mazmanian, S. K. (2016). Gut Microbiota Regulate Motor Deficits and Neuroinflammation in a Model of Parkinson's Disease. *Cell*, 167(6):1469–1480.e12.

Sanders, M. E., Akkermans, L. M. A., Haller, D., Hammerman, C., Heimbach, J., Hörmannsperger, G., Huys, G., Levy, D. D., Lutgendorff, F., Mack, D., Phothirath, P., Solano-Aguilar, G., and Vaughan, E. (2010). Safety assessment of probiotics for human use. *Gut microbes*, 1(3):164–185.

Schuijt, T. J., Lankelma, J. M., Scicluna, B. P., de Sousa e Melo, F., Roelofs, J. J. T. H., de Boer, J. D., Hoogendijk, A. J., de Beer, R., de Vos, A., Belzer, C., de Vos, W. M., van der Poll, T., and Wiersinga, W. J. (2016). The gut microbiota plays a protective role in the host defence against pneumococcal pneumonia. *Gut*, 65(4):575–583.

Scott, K. P., Antoine, J.-m., Midtvedt, T., and Hemert, S. V. (2015). Manipulating the gut microbiota to maintain health and treat disease. *Microbial Ecology in Health & Disease*, 26:1–10.

Sealy, L. (1978). The effect of sodium butyrate on histone modification. *Cell*, 14(1):115–121.

Sears, C. L. (2005). A dynamic partnership: Celebrating our gut flora. *Anaerobe*, 11(5):247–251.

Sender, R., Fuchs, S., and Milo, R. (2016). Are We Really Vastly Outnumbered ? Revisiting the Ratio of Bacterial to Host Cells in Humans. *Cell*, 164(3):337–340.

Setzu, A., Lathia, J. D., Zhao, C., Wells, K., Rao, M. S., Ffrench-Constant, C., and Franklin, R. J. M. (2006). Inflammation stimulates myelination by transplanted oligodendrocyte precursor cells. *Glia*, 54(4):297–303.

Shafritz, D. A. and Dabeva, M. D. (2002). Liver stem cells and model systems for liver repopulation. *Journal of Hepatology*, 36(4):552–564.

Shen, S., Sandoval, J., Swiss, V. a., Li, J., Dupree, J., Franklin, R. J. M., and Casaccia-Bonnefil, P. (2008). Age-dependent epigenetic control of differentiation inhibitors is critical for remyelination efficiency. *Nature Neuroscience*, 11(9):1024–1034.

Shi, C., Jia, T., Mendez-Ferrer, S., Hohl, T. M., Serbina, N. V., Lipuma, L., Leiner, I., Li, M. O., Frenette, P. S., and Pamer, E. G. (2011). Bone Marrow Mesenchymal Stem and Progenitor Cells Induce Monocyte Emigration in Response to Circulating Toll-like Receptor Ligands. *Immunity*, 34(4):590–601.

Sicher, S. C., Chung, G. W., Vazquez, M. A., and Lu, C. Y. (1995). Augmentation or inhibition of IFN-gamma-induced MHC class II expression by lipopolysaccharides. The roles of TNF-alpha and nitric oxide, and the importance of the sequence of signaling. *Journal of Immunology*, 155(12):5826–34.

Silver, J. and Miller, J. H. (2004). Regeneration beyond the glial scar. *Nature Reviews Neuroscience*, 5(2):146–156.

Simon, J. H. and Kleinschmidt-DeMasters, B. K. (2005). *MR Imaging in White Matter Diseases of the Brain and Spinal Cord*. Medical Radiology Diagnostic Imaging. Springer-Verlag, Berlin/Heidelberg.

Smith, K., McCoy, K. D., and Macpherson, A. J. (2007). Use of axenic animals in studying the adaptation of mammals to their commensal intestinal microbiota. *Seminars in Immunology*, 19(2):59–69.

Smith, K. J., Blakemore, W. F., and McDonald, W. I. (1979). Central remyelination restores secure conduction. *Nature*, 280(5721):395–396.

Smith, P. M., Howitt, M. R., Panikov, N., Michaud, M., Gallini, C. A., Bohlooly-Y, M., Glickman, J. N., and Garrett, W. S. (2013). The Microbial Metabolites, Short-Chain Fatty Acids, Regulate Colonic Treg Cell Homeostasis. *Science*, 341(6145):569–573.

Steelman, A. J. (2015). Infection as an Environmental Trigger of Multiple Sclerosis Disease Exacerbation. *Frontiers in Immunology*, 6(OCT).

Steelman, A. J., Thompson, J. P., and Li, J. (2012). Demyelination and remyelination in anatomically distinct regions of the corpus callosum following cuprizone intoxication. *Neuroscience Research*, 72(1):32–42.

Stocum, D. L. (2012). *Regenerative Biology and Medicine (Second Edition)*. Elsevier.

Tankou, S., Bailey, K., Regev, K., Kivisakk, P., Ghandi, R., Kirlis, A., Cook, S., Stuart, F., Glanz, B., Stankiewicz, J., and Weiner, H. (2016). Treatment of EAE and MS Subjects with Probiotic VSL#3 (P5.320). *Neurology*, 86(16 Supplement).

Tasaki, I. (1939). The electro-saltatory transmission of the nerve impulse and the effect of narcosis upon the nerve fiber. *Am. J. Physiol.*, 127:211–227.

Till, J. E. and McCulloch, E. A. (1961). A Direct Measurement of the Radiation Sensitivity of Normal Mouse Bone Marrow Cells. *Radiation Research*, 14(2):213.

Trapp, B. D. and Nave, K.-A. (2008). Multiple sclerosis: an immune or neurodegenerative disorder? *Annual review of neuroscience*, 31(1):247–69.

Trebst, C., Jarius, S., Berthele, A., Paul, F., Schippling, S., Wildemann, B., Borisow, N., Kleiter, I., Aktas, O., and Kümpfel, T. (2014). Update on the diagnosis and treatment of neuromyelitis optica: Recommendations of the Neuromyelitis Optica Study Group (NEMOS). *Journal of Neurology*, 261(1):1–16.

Vallee, E., Azoulay-Dupuis, E., Bauchet, J., and Pocidalo, J. J. (1992). Kinetic disposition of temafloxacin and ciprofloxacin in a murine model of pneumococcal pneumonia. Relevance for drug efficacy. *J Pharmacol Exp Ther*, 262(3):1203–1208.

van Baarlen, P., Kleerebezem, M., and Wells, J. M. (2013). Omics approaches to study host-microbiota interactions. *Current Opinion in Microbiology*, 16(3):270–277.

Vinolo, M. a. R., Rodrigues, H. G., Nachbar, R. T., and Curi, R. (2011). Regulation of inflammation by short chain fatty acids. *Nutrients*, 3(10):858–876.

Wang, H., Lee, I.-S., Braun, C., and Enck, P. (2016). Effect of Probiotics on Central Nervous System Functions in Animals and Humans: A Systematic Review. *Journal of Neurogastroenterology and Motility*, 22(4):589–605.

Waxman, S. G. (2006). Axonal conduction and injury in multiple sclerosis: the role of sodium channels. *Nature Reviews Neuroscience*, 7(12):932–941.

Weiner, H. (2017). Probiotics as a Therapy for MS. In *ACTRIMS*.

Wiesel, P. H., Norton, C., Glickman, S., and Kamm, M. A. (2001). Pathophysiology and management of bowel dysfunction in multiple sclerosis. *European journal of gastroenterology & hepatology*, 13(4):441–8.

Winek, K., Engel, O., Koduah, P., Heimesaat, M. M., Fischer, A., Bereswill, S., Dames, C., Kershaw, O., Gruber, A. D., Curato, C., Oyama, N., Meisel, C., Meisel, A., and Dirnagl, U. (2016). Depletion of Cultivatable Gut Microbiota by Broad-Spectrum Antibiotic Pretreatment Worsens Outcome After Murine Stroke. *Stroke*, 47(5):1354–1363.

Winkelmann, A., Loebermann, M., Reisinger, E. C., Hartung, H.-P., and Zettl, U. K. (2016). Disease-modifying therapies and infectious risks in multiple sclerosis. *Nature Reviews Neurology*, 12(4):217–233.

Wolswijk, G. (1998). Chronic stage multiple sclerosis lesions contain a relatively quiescent population of oligodendrocyte precursor cells. *The Journal of Neuroscience*, 18(2):601–9.

Wolswijk, G. (2002). Oligodendrocyte precursor cells in the demyelinated multiple sclerosis spinal cord. *Brain*, 125:338–349.

Woodruff, R. H., Fruttiger, M., Richardson, W. D., and Franklin, R. J. (2004). Platelet-derived growth factor regulates oligodendrocyte progenitor numbers in adult CNS and their response following CNS demyelination. *Molecular and Cellular Neuroscience*, 25(2):252–262.

Worbs, T., Hammerschmidt, S. I., and Förster, R. (2017). Dendritic cell migration in health and disease. *Nature Reviews Immunology*, 17(1):30–48.

Wynn, T. A. and Vannella, K. M. (2016). Macrophages in Tissue Repair, Regeneration, and Fibrosis. *Immunity*, 44(3):450–462.

Yadav, H., Lee, J. H., Lloyd, J., Walter, P., and Rane, S. G. (2013). Beneficial metabolic effects of a probiotic via butyrate-induced GLP-1 hormone secretion. *Journal of Biological Chemistry*, 288(35):25088–25097.

Yamasaki, R., Lu, H., Butovsky, O., Ohno, N., Rietsch, A. M., Cialic, R., Wu, P. M., Doykan, C. E., Lin, J., Cotleur, A. C., Kidd, G., Zorlu, M. M., Sun, N., Hu, W., Liu, L., Lee, J.-C., Taylor, S. E., Uehlein, L., Dixon, D., Gu, J., Floruta, C. M., Zhu, M., Charo, I. F., Weiner, H. L., and Ransohoff, R. M. (2014). Differential roles of microglia and monocytes in the inflamed central nervous system. *The Journal of experimental medicine*, 211(8):1533–1549.

Young, K. M., Psachoulia, K., Tripathi, R. B., Dunn, S.-J., Cossell, L., Attwell, D., Tohyama, K., and Richardson, W. D. (2013). Oligodendrocyte Dynamics in the Healthy Adult CNS: Evidence for Myelin Remodeling. *Neuron*, 77(5):873–885.

Yu, Y.-R. A., O'Koren, E. G., Hotten, D. F., Kan, M. J., Kopin, D., Nelson, E. R., Que, L., and Gunn, M. D. (2016). A Protocol for the Comprehensive Flow Cytometric Analysis of Immune Cells in Normal and Inflamed Murine Non-Lymphoid Tissues. *PLOS ONE*, 11(3):e0150606.

Yuen, T. J., Johnson, K. R., Miron, V. E., Zhao, C., Quandt, J., Harrisingh, M. C., Swire, M., Williams, A., McFarland, H. F., Franklin, R. J. M., and Ffrench-Constant, C. (2013). Identification of endothelin 2 as an inflammatory factor that promotes central nervous system remyelination. *Brain*, 136(4):1035–1047.

Zhang, C., Li, S., Yang, L., Huang, P., Li, W., Wang, S., Zhao, G., Zhang, M., Pang, X., Yan, Z., Liu, Y., and Zhao, L. (2013). Structural modulation of gut microbiota in life-long calorie-restricted mice. *Nature communications*, 4:2163.

Zhao, C., Li, W.-W., and Franklin, R. J. M. (2006). Differences in the early inflammatory responses to toxin-induced demyelination are associated with the age-related decline in CNS remyelination. *Neurobiology of aging*, 27(9):1298–307.

Appendix A

Media formulations

A.1 Microglia media

Component	Concentration	Supplier
DMEM/F12	87%	Gibco
FBS	10%	Biosera
Penicillin-streptomycin	100 U/ml	Sigma
B27	2%	Thermo Fisher
NAC	500 µM	Sigma

A.2 OPC media

Component	Concentration	Supplier
DMEM/F12	95.3%	Gibco
NAC	60 µg ml^{-1}	Sigma
D-glucose	25 mM	Sigma
Insulin	10 µg ml^{-1}	Gibco
Sodium pyruvate	4.5 mM	Gibco
Apo-transferrin	50 µg ml^{-1}	Sigma
Putrescine	16.1 µg ml^{-1}	Sigma
Sodium selenite	40 ng ml^{-1}	Sigma
Progesterone	60 ng ml^{-1}	Sigma
Penicillin-streptomycin	100 U/ml	Sigma

A.3 Hibernate A Low Fluorescence (HALF)

Component	Concentration
Amino acids	
Glycine	400 µM
L-alanine	22 µM
L-arginine hydrochloride	483 µM
L-asparagine-H_2O	5.5 µM
L-cysteine hydrochloride-H_2O	7.7 µM
L-histidine hydrochloride-H_2O	200 µM
L-isoleucine	802 µM
L-leucine	802 µM
L-lysine hydrochloride	798 µM
L-methionine	201 µM
L-phenylalanine	400 µM
L-proline	67 µM
L-serine	400 µM
L-threonine	798 µM
L-tryptophan	78 µM
L-tyrosine disodium salt dihydrate	398 µM
L-valine	803 µM
Vitamins	
Choline chloride	28 µM
D-calcium pantothenate	8 µM
Niacinamide	30 µM
Pyridoxine hydrochloride	20 µM
Thiamine hydrochloride	10 µM
i-inositol	40 µM
Inorganic salts	
Ferric nitrate ($Fe(NO_3)_3.9H_2O$)	250 nM
Potassium chloride (KCl)	5.36 mM
Sodium bicarbonate ($NaHCO_3$)	880 µM
Sodium chloride (NaCl)	89 mM
Sodium phosphate dibasic (Na_2HPO_4) anhydrous	906 µM
Zinc sulfate ($ZnSO_4.7H_2O$)	670 nM
Other components	
D-glucose (dextrose)	25 mM
Sodium pyruvate	227 µM
3-(*N*-morpholino)propanesulfonic acid (MOPS)	10 mM

All chemicals were purchased from Sigma.

A.4 Modified Miltenyi Wash Buffer (MWB)

Component	Concentration	Supplier
PBS, pH7.3	1x%	Lifetech
EDTA	2 mM	Gibco
Sodium pyruvate	3 mM	Gibco
Bovine serum albumin	0.5%	Gibco
NAC	500 µM	Sigma
B27	2%	Thermo Fisher
Insulin	10 µg ml^{-1}	Gibco

Appendix B

Microbiome profile of antibiotics study

Fig. B.1 **Full quantification of faecal bacteria following antibiotic and FMT treatments (Chapter 3).** DNA was extracted from faecal pellets was quantified by quantitative PCR using primers for group-specific 16S rRNA amplicons. Gene copy numbers per ng total DNA were determined for *Enterobacteria* (A), *Enterococci* (B), *Lactobacilli* (C), *Bifidobacteria* (D), *Bacteroides / Prevotella spp.* (E), *Clostridium coccoides* group (F), *Clostridium leptum* group (G) and mouse intestinal *Bacteroides* (H). Points represent individual mice, with horizontal lines showing the median value for each group. SPF, specific-pathogen-free controls; ABX, antibiotics-treated; AFT, antibiotics and human (H) or murine (M) faecal transplant. Mann–Whitney *U* test. *Figures produced by Markus Heimesaat.*

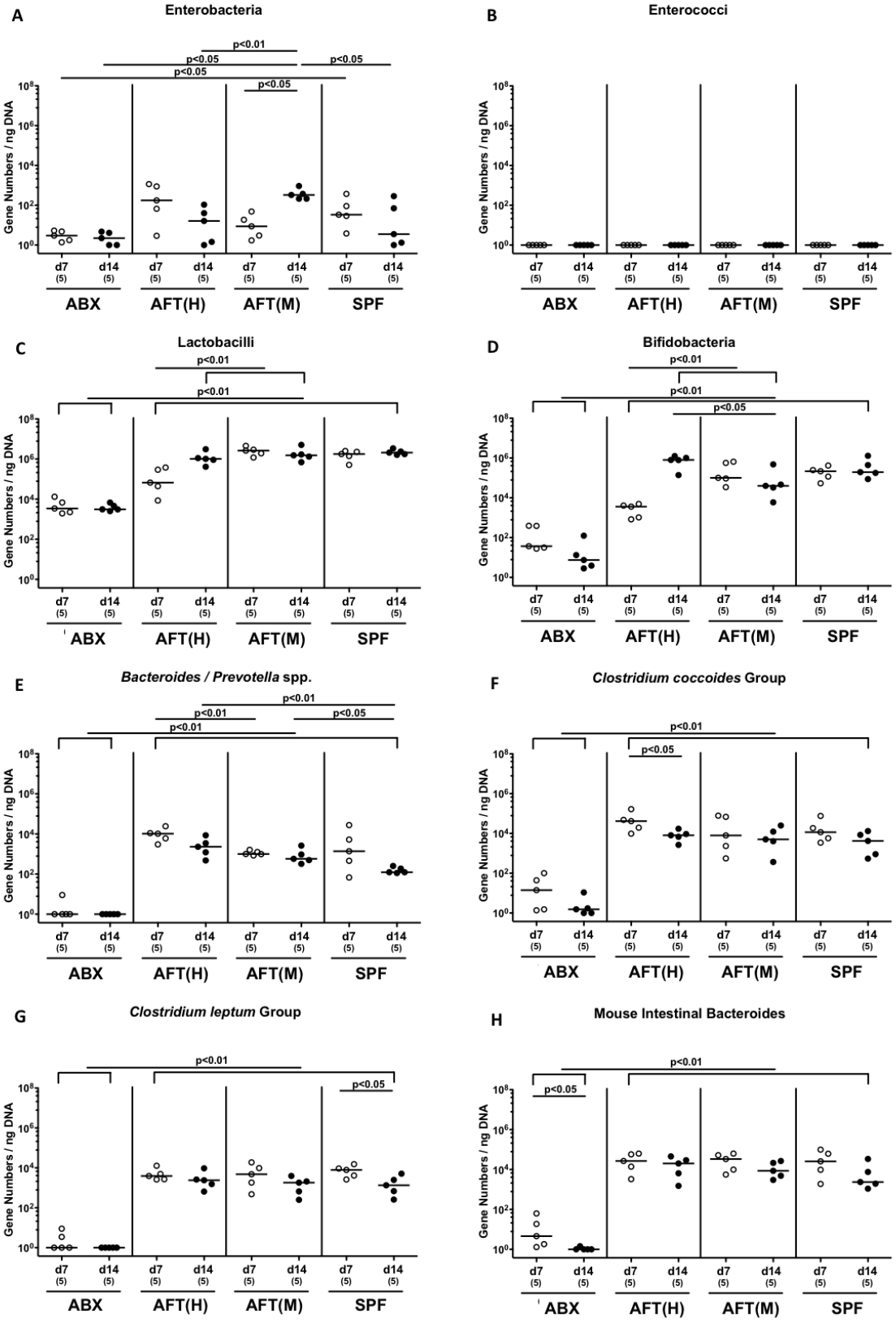
A
Enterobacteria
B
Enterococci
C
Lactobacilli
D
Bifidobacteria
E
Bacteroides / Prevotella spp.
F
Clostridium coccoides Group
G
Clostridium leptum Group
H
Mouse Intestinal Bacteroides
Gene Numbers / ng DNA
p<0.01
p<0.05
d7 (5)
d14 (5)
ABX
AFT(H)
AFT(M)
SPF